1-1-2015

Silicone Elastomer-Based Combinatorial Biomaterial Gradients for High Throughput Screening of Cell-Substrate Interactions

Greeshma Mohan
University of South Florida, mohan.greeshma@gmail.com

Silicone Elastomer-Based Combinatorial Biomaterial Gradients for High Throughput Screening of Cell-Substrate Interactions

by

Greeshma Mohan

A dissertation submitted in partial fulfillment
of the requirements for the degree of
Doctor of Philosophy
Department of Chemical and Biomedical Engineering
College of Engineering
University of South Florida

Major Professor: Nathan Gallant, Ph.D.
Robert Frisina, Jr., Ph.D.
Piyush Koria, Ph.D.
Ryan Toomey, Ph.D.
Marzenna Wiranowska, Ph.D.

Date of Approval:
March 30, 2015

Keywords: polydimethyl siloxane (PDMS), surface chemistry, mechanotransduction, hydrophobicity, stiffness, fibronectin

For my Amma (mother) & Achcha (father):

Well, a *femtogram* more for my Achcha ☺

ACKNOWLEDGMENTS

This journey here at USF has been a very enriching and life altering experience for me and I wish to express my heartfelt gratitude to the people who have been a part of it. To my mentor, Dr. Nathan Gallant, thank you for giving me this incredible opportunity and for allowing me to explore, learn, gain confidence and evolve at my own pace. As I move on, I will carry with me not only your lessons in scientific and engineering problem solving skills but also the unique compassionate way you treat everyone around you. Thank you for helping me to become a better researcher and a better person. I also convey my appreciation to my committee members, Dr. Robert Frisina Jr., Dr. Piyush Koria, Dr. Ryan Toomey and Dr. Marzenna Wiranowska for extending their support and help whenever I have needed it. I would like to thank all current and former members of our lab. Thank you for the wonderful, easy working environment, your help and all the happy memories. I also wish to thank the staff of the Mechanical Engineering for help with the academic process, CHBME department for the TA appointments and staff of the machine shop for making material parts needed for research. I also express my thanks to Leigh West at the CDDI to avail the facilities at Research Park.

I acknowledge what I have taken for granted for the most part of my life: My family, my prayer, my strength including my Amma & Achcha (parents: Geetha & Mohandas Pisharody), my late grandparents, Amma & Appa (parents-in-law: Rani & Das Mankidy) and entire extended family. Finally, my favorite two people in this world, they are my biggest critics and they are my most loyal fans: My loving sister Swathy Mohan and my soulmate and better half Bijith Das Mankidy.

TABLE OF CONTENTS

LIST OF FIGURES

ABSTRACT

Biomaterials have evolved over the years from the passive role of mere biocompatibility to an increasingly active role of presenting instructive cues to elicit precise responses at the molecular and cellular levels. Various characteristics common to synthetic biomaterials *in vitro* and extracellular matrices *in vivo*, such as immobilized functional or peptide groups, mechanical stiffness, bulk physical properties and topographical features, are key players that regulate cell response. The dynamics in the cell microenvironment and at the cell adhesive interface trigger a web of cell-material and cell-cell information exchanges that have a profound impact in directing the ultimate cell fate decision. Therefore, comprehension of cell substrate interactions is crucial to propel forward the evolution of new instructive biomaterials. Combinatorial biomaterials that encompass a wide range of properties can help to recapitulate the complexity of a cell microenvironment**.** The objective of this research was to fabricate combinatorial biomaterials with properties that span wide ranges in both surface chemistries and mechanical moduli. These materials were based on polydimethyl siloxane (PDMS), an elastomeric silicone biomaterial with physiologically relevant stiffness. After developing these mechano-chemical gradient biomaterials, we conducted high throughput screening of cell responses on them to elucidate cell substrate interactions and material directed behaviors.

Our central hypothesis was that materials encompassing monotonic gradients in mechanical elastic modulus and orthogonal surface chemistry gradients could be engineered using the soft biomaterial, polydimethyl siloxane (PDMS) and that these gradient biomaterials would evoke a

varied cell response. Furthermore, we expected high throughput screening of cell-material interactions using these materials would elucidate patterns and thresholds of synergy or antagonism in the overall cell response to the increased complexity presented by combinatorial materials. First, reproducible gradients in surface chemistry were generated on PDMS through surface modification techniques. Cell response to PDMS surface chemistry gradients was then screened in a rapid high throughput manner. Additionally, characteristics of the adhesive interface were probed to understand its role in cell response. Finally, a 2D combinatorial gradient with a gradient in mechanical elastic modulus and an orthogonal gradient in surface chemistry was fabricated with PDMS. High throughput screening of the synergistic influence of the varied mechanical and biochemical extracellular signals presented by the combinatorial biomaterial on cell response was conducted in a systematic manner. This research demonstrates the fabrication of combinatorial biomaterials with a wide range of mechanochemical properties for rapid screening of cell response; a technique that will facilitate the development of biomaterial design criteria for numerous biomedical engineering applications including in vitro cell culture platforms and tissue engineering.

CHAPTER 1

INTRODUCTION

1.1 Project Significance

Commercial scale production of tissue engineered constructs depends on, among many other aspects, optimization of biomaterials that can persuade cells to perform desired functions. The process that ensues from the time a product is conceptualized to the preliminary testing period and latter stages of detailed, rigorous testing followed by clinical trials is a complex procedure that may extend to years before the product finally reaches market. This is because cell response is a multifaceted and very complex phenomenon. Cell fate decision is the end result of an orchestrated and inter connected network of events that involves cell-cell and cell-cell communications. Furthermore, multiple elements comprising the cell microenvironment ranging from mechanical stiffness, biochemical properties, physical or topographical attributes, soluble and immobilized factors contribute to the dynamic interactions in the interfacial cell adhesive layer and cell mechanotransduction events.

Biomaterials are also increasingly expected to have more functionality. Next generation biomaterials are expected to be instructive biomimetic substrates that can precisely control specific cellular functions by mimicking the extracellular environment. Therefore, information regarding how multiple stimuli both independently and synergistically evoke cellular response is imperative to understanding and controlling cell-material interactions. In this regard, a combinatorial high throughput platform that allows rapid broad spectrum analysis of the effect of single and multiple

factors either independently or in combination provides several advantages: (i) Rapid screening of variables in a systematic manner leads to faster acquisition of data; (ii) Potential for large volume of data acquisition from a single experiment compared to traditional method of conducting manifold individual experiments; (iii) Trends and patterns in cell responses to continuous gradients emerge as positive hit zones that may be pursued further (with greater resolution) to test potential for developing new design criteria for greater therapeutic value. Furthermore, the synergistic effect of two variables may be different from an outcome from independent influence of each variable, similar to the complex interplay of variables in native cell microenvironments.

Although some of the previous studies have highlighted the prospective of different gradient materials to screen cell response, a significant portion of the reported work used either very rigid or very soft materials. In this research, we use polydimethyl siloxane (PDMS), a soft biomaterial having physiologically relevant stiffness to produce gradient materials.

1.2 Project Objective and Specific Aims

The overall objective of this dissertation research was to fabricate combinatorial biomaterials which exhibit properties that span wide ranges in surface chemistries and mechanical moduli in monotonically varying gradient formats for the high throughput screening of cell response to matrix properties.

The central hypothesis was that materials encompassing monotonic gradient properties in both mechanical elastic modulus and surface chemistry could be engineered on a single substrate using polydimethyl siloxane (PDMS), an elastomeric silicone biomaterial with physiologically relevant

stiffness. Additionally, it was expected that using these combinatorial biomaterials for high throughput screening of cell-material interactions would yield patterns of synergy or antagonism. The overall objective was accomplished by testing this central hypothesis through the following specific aims.

- Aim 1 was to fabricate a gradient material with continuous and monotonically changing surface chemistry on a soft biomaterial for the purpose of screening cell-material interactions.

Gradients in surface chemistry have been created previously on conventional rigid surfaces like glass and silicon wafers. The surface of PDMS was modified through the deposition of an alkylsilane monolayer followed by ultraviolet ozone oxidation (UVO) of the monolayer in a spatiotemporally controlled manner.

The hypothesis was that a gradient in monotonically varying surface chemistries can be generated on PDMS, a soft biomaterial with physiologically relevant stiffness, for high throughput screening of cell response. This can be achieved through tightly controlled procedures involved in modification of the PDMS surface through alkylsilanization and its subsequent spatiotemporal UVO treatment.

- Aim 2 was to screen cell morphological response to surface chemistry gradients upon the soft biomaterial in a systematic high throughput manner and investigate the contributory role of protein interfacial layer to specific cell response.

Two different cell types, NIH3T3 fibroblasts and Human Umbilical Vein Endothelial Cells (HUVEC), were cultured on fibronectin coated PDMS surface chemistry gradients. The cells were fluorescently stained to determine the effect of varying surface chemistry on cell spreading and adhesion. High throughput and automated data extraction procedures were developed to control a Nikon fluorescent microscope with a computer controlled stage and analyze large volumes of acquired image data. This high content data analysis approach enabled the identification of predominant patterns or tendencies in cell response on the gradient material. Additionally, the adhesive interface was analyzed through the fluorescent labeling of adsorbed fibronectin. Furthermore, the molecular conformational aspects of fibronectin were examined through a modified ELISA procedure. In this manner, the effect of surface chemistry on both the macroscopic cell response and the intermediary events of cell substrate interactions were thoroughly investigated.

The hypothesis was that a monotonically varying surface chemistry gradient fabricated on PDMS will modulate adhesive protein adsorption and thereby regulate cell response.

- Aim 3: To fabricate a two dimensional (2D) combinatorial gradient platform that encompasses a gradient in physiologically relevant mechanical stiffness on one axis and a gradient in surface chemistry on the orthogonal axis for screening synergistic cell response to the mechano-biochemical cues in a high throughput manner.

The material PDMS was modified through manipulating its crosslinker concentrations to obtain PDMS with varying stiffness to fabricate a gradient in elastic modulus. This was achieved using a pair of programmable syringe pumps with inverse ramping profiles each carrying a different

composition of PDMS with a different crosslinker concentration that were joined and mixed downstream and deposited on a substrate placed on a translational moving stage. Gradients in mechanical stiffness obtained upon curing were later subjected to surface modification through alkylsilane deposition and subsequent controlled UVO treatment in the orthogonal direction to obtain surface chemistry gradient. The resulting 2D combinatorial gradient was then cultured with fibroblast NIH3T3 cells to screen cell response. High throughput data acquisition using a custom made macro with NISE software on Nikon fluoroscope enabled high content data extraction. A vast variation of combined stiffness and surface chemistry gradients were screened and regions of interest or 'hot spots' were identified. This demonstrated the potential of the fabricated 2D combinatorial substrates to elucidate cell response to multiple microenvironmental parameters as an important step in moving toward developing complete combinatorial biomaterials.

The hypothesis was that a 2D combinatorial gradient biomaterial can be fabricated using the same soft material PDMS through manipulation of its bulk mechanical properties by varying the crosslinker concentration in a linear manner to obtain the stiffness gradient, followed by modification of surface properties via silane deposition and spatiotemporal UVO treatment atop the mechanical gradient to obtain the orthogonal surface chemistry gradient. Combinatorial high throughput screening has the potential to recognize 'hot spots' or 'thresholds of positive hit zone' regions of synergistic cell response to multiple stimuli on the 2D gradient platform.

The tasks undertaken to achieve these specific aims are detailed in following chapters of this doctoral thesis. Background information and a detailed review of literature are presented in Chapter 2. Preliminary investigations of PDMS involving modification of its surface and bulk

physical properties are discussed in Chapter 3. The principal work to accomplish the objectives addressed in Aim1, Aim2 and Aim 3 are described in Chapter 4, Chapter 5 and Chapter 6, respectively. Finally the major conclusions from this dissertation and possible future considerations are detailed in Chapter 7.

CHAPTER 2

BACKGROUND AND SIGNIFICANCE

The structures, interactions, organizations and functions from the lowest molecular and cellular level all the way to the highest organism level are awe inspiring in their elegance and complexity and represent an unparalleled architectural wonder. Therefore, when a loss of tissue/organ function due to pathological conditions occurs in higher order animals that have limited capacity for regeneration, scientists and engineers face the uphill task of designing, building and optimizing bioengineered implant replacements to restore that lost function. This is an emerging process that involves deciphering the intercellular and cell interfacial interactions *in vitro* based on events that take place *in vivo*, connecting the dots and simultaneously translating that knowledge to manufacture biomedical products with enhanced biocompatibility and improved functionality.

2.1 Factors that Determine Cell Fate

It is widely appreciated that a multitude of factors contribute to determination of cell fate or cell response. Several elements in the environment of a cell such the physical, mechanical and chemical properties of the resting/supportive substrate/basement membrane, topographical features, and soluble factors trigger a web of events both between individual cells and in combination with the basement membrane, that ultimately results in events such as cell growth, cell differentiation, proliferation, division etc (Oliveira and Mano 2014; Wong, Leach, and Brown 2004).

The role of biochemical signals such as chemokines and hormones to initiate both short range and long range signaling events in cells with significant response *in vivo* (example: wound healing process, angiogenesis) and cues in the form of soluble and immobilized factors affect cell behavior in *in vitro* have been long appreciated and recognized (Shen et al. 2015; Walters and Gentleman 2015; Kasuya and Tokura 2014). Upregulation of certain biochemical cues such as growth factors are also associated with pathological conditions such as cancer (Lössner et al. 2008; Shang, Li, and Li 2007).

It has been reported that the presence of topographical features in the form of grooves and ridges with even finer details of features such as width, aspect ratio, depth and pitch that have an impact on cell morphology and other higher functions such as proliferation, gene expression as an effect of 'contact guidance' (Saito et al. 2014; Gerecht et al. 2007; Biela et al. 2009; Martínez et al. 2009). This is when the cells align themselves and/ or exhibit changes in cell function that are attributed to presence of the features. Microfabrication is the process of patterning features with the aim of controlled cell adhesion on substrates and may be used to conduct co culture of different cell types to study cell substrate and cell-cell interactions (Brunette et al. 2005; Kaji et al. 2011; Goubko and Cao 2009).

Surface properties of biomaterials also form an integral design parameter to obtain optimum functionality and cell response. Foreign body reactions to implant biomaterials depend on numerous material properties like porosity, composition, degradation rate, surface chemistry and roughness (Onuki et al. 2008). Upon implantation of a biomaterial *in vivo*, different proteins in varied concentrations and conformations adsorb on material surface that dictate adhesion and

survival of different cell types (Anderson, Rodriguez, and Chang 2008). The effect of different surface chemistry on endothelial cell migration was investigated by Shen et al. It was found that cell migration was in the order of CH_3 > NH_2 > OH > COOH(Shen et al. 2015). Surface functionality has also shown to affect cell adhesion strength, matrix mineralization by osteoblasts and also shown to influence degree of osteogenic differentiation marked by variation in the gene expression of osteogenic markers (Keselowsky, Collard, and Garcia 2004; Keselowsky, Collard, and Garcia 2005; Keselowsky, Collard, and García 2003). Similarly, different functional surface chemistries have shown to influence skeletal myoblast proliferation and myogenic differentiation (Lan et al. 2005). Iluliano et al reported that, under serum free conditions bovine endothelial cell adhesion on preadsorbed fibronectin hydrophilic glass and hydrophobic silane surfaces were similar though focal adhesion formation was higher on hydrophilic glass (Iuliano, Saavedra, and Truskey 1993). Substrates that had wettabilities ranging from 43°-96° and different intensity of shear stresses under flow conditions on bovine pulmonary endothelial cells was studied by Lee et al which indicated surface wettability was an important regulator of preferential cell adherent fractions and also affected cell adhesion strength (Lee et al. 2000). However, how multiples signals like biomechanical cues are transduced and bring about specific cell response is largely unknown (Yeung et al. 2005). Also, there is generally no clear theory that predicts correlation between the surface chemistry of materials to cellular responses (Hook et al. 2010).

Local matrix stiffness, acting through transmembrane integrins, focal adhesion complexes, cytoskeletal forces and molecular signaling pathways, has a profound impact on determining cell fate (adhesion, spreading, survival, differentiation, pathology) (Discher, Janmey, and Wang 2005; Byfield et al. 2009; Peyton et al. 2007; Engler et al. 2004). In general, cells tend to spread more

on and migrate toward stiffer substrates over softer surfaces. This ability of cells to perceive difference in rigidity of synthetic matrix beneath, was first demonstrated by Pelham and Wang using fibroblasts on collagen coated soft and stiff polyacrylamide gels (Pelham and Wang 1997). NIH3T3 fibroblasts exhibit durotaxis from softer to stiffer polyacrylamide gels with corresponding increase in cell spreading area (Lo et al. 2000). Engler et al showed that matrix stiffness determined mesenchymal stem cell differentiation to different cell types with substrates with least stiffness giving rise to neurogenic, intermediate to myogenic and stiffest to osteogenic lineage respectively (Engler et al. 2006). Recently, studies of EC stiffness in single, group and monolayers demonstrated that cell stiffness is a function of cell spreading area and that the stiffness of cells in a monolayer approaches the stiffness of a single cell. Interestingly, the density of fibroblasts and EC is an important player in ability of cells to sense the underlying substrate stiffness. Detectable differences in fibroblast and EC spreading on soft versus stiff substrates in the absence of cell-cell contacts disappear when a confluent cell layer is attained (Yeung et al. 2005). Therefore, cell-cell and cell–matrix interactions are suggested to be important for maintaining cell tension homeostasis (Stroka and Aranda-Espinoza 2011). Most studies reported on stiffnesses that are not in the physiologically relevant range. For example, studies with EC response to stiffness is in the range of 0.2kPa-75kPa mostly using polyacrylamide gels. However, human saphenous vein and arterial wall have tissues whose rigidity lie in the range of 25 kPa-1.25 MPa and 10 kPa- 7 MPa respectively (Nemir and West 2010). The range of stiffness reported by using polydimethylsiloxane, (PDMS), a silicone elastomer, to tune the crosslinking density lies between 50 kPa to 1.78 MPa which is within the physiological range of stiffness.(Brown, Ookawa, and Wong 2005) The research presented in this dissertation is focused on the influence of surface chemistry and matrix stiffness on cell functions.

2.2 Cell-Substrate Interactions

Cells interact with biomaterial surfaces through the intermediate adhesive layer that comprises of a network of adsorbed proteins including adhesion proteins and growth factors. In tissues, a highly organized but similar protein matrix supports cell adhesion, stores and presents growth factors to cells, and interacts with cells to transduce signaling events (Rozario and DeSimone 2010). There are many different proteins found in the basement membrane, the ECM supporting epithelial tissues, include fibronectin, fibrinogen, collagen I, collagen IV, vitronectin etc (Alberts B et al. 2002). For instance, the endothelial cell basement membrane contains several ECM proteins like Laminin, Collagen IV, Fibronectin (Herbst et al. 1988). Integrins, a class of mechanosensory proteins, recognize and bind specifically to certain motifs with a specific sequence of aminco acids like the arginine-glycine-aspartic acid (RGD) tripeptide in ECM proteins like fibronectin, laminin, and vitronectin (Hernandez et al. 2007) Among these, fibronectin is a protein found in both soluble form in body fluids like blood plasma and insoluble form in stromal connective tissue like the basement membrane (Mosher and Furcht 1981). The structure and functional aspects of fibronectin has been extensively studied and characterized (Bradshaw and Smith 2014; Hynes 2009; Pankov and Yamada 2002; Potts and Campbell 1996). This makes it advantageous to study cell response on engineered biomaterials since modifications in fibronectin may be tracked down more efficiently. It has been reported that protein adsorption favors hydrophobic surfaces in comparison with hydrophilic surfaces (Elwing 1998; Elwing et al. 1987; Ma, Mao, and Gao 2007; Gugutkov et al. 2010). Surface chemistry has been shown to impact fibronectin adsorption, induce unfolding and molecular level conformational changes causing downstream regulation integrin function, recruitment of mechanosensory complexes and higher order functions of cells (Keselowsky,

Collard, and Garcia 2004; Keselowsky, Collard, and Garcia 2005; Keselowsky, Collard, and García 2003; Michael et al. 2003; Gugutkov et al. 2010; Ma, Mao, and Gao 2007).

Apart from the molecular changes in the protein, properties of the bulk protein such as the stiffness of the fibronectin fibers both at the more 'individual' fiber level and the 'population' matrix level may be sensed by attachment receptors on cells (Bradshaw and Smith 2014). Also, fibronectin can withstand remarkable extension, a strain greater than 700% before failure occurs in about one-half of the fibers tested. The extension has effects on the rigidity or modulus of the fibers which increases to the MPa range and also cause conformational changes at the molecular level with increased exposure of buried binding sites on FNIII modules that are acknowledged to affect cellular functions (Klotzsch et al. 2009). Consequently, different properties of the basement membrane or substrate are a source of stimuli that effect dynamics of protein turnover and positioning/presentation for cell interaction. Eventually, the manner in which cells perceive this protein interface affects cell functionality (Bradshaw and Smith 2014; Hynes 2009).

2.3 Cell Mechanobiology

Specific proteins found in the cell membrane called integrins and cadherins mediate cell-substrate and cell-cell communications respectively (Weber, Bjerke, and DeSimone 2011). Integrins are a major class of adhesion proteins with heterodimeric α and β subunits which are involved in both outside-in and inside-out cell signaling events. They are transmembrane proteins and have domains in the outer region of the cell membrane, extending through the membrane and into the cytoplasm. These integrins tether cells to the adhesive extracellular matrix discussed in the previous section. There are about 24 dimers of integrins (Hynes 2002; Humphries, Byron, and Humphries 2006;

Chen et al. 2003). Integrins associated with cell-fibronectin connectivity include the $\alpha_5\beta_1$,$\alpha_v\beta_3$ and $\alpha_v\beta_6$ (Lee and Gotlieb 2003; Scatena et al. 1998; Garcia and Garcia 2014). Integrin adhesion of cell on a substrate evolved from the initial weaker attachment to a more strengthened grip (Garcia and Gallant 2003). This is concurrent with clustering together of multiple integrins and positioning of different protein subsets such as paxillin, vinculin, talin, α actinin and enzyme kinases connected to deeper cell architectural elements such as the cytoskeleton. Such an arrangement/formation is called a focal adhesion complex and information is signaled to and fro between the cell and substrate through a series of short lived phophorylations, signal amplifications and modifications. Collectively, these events are called mechanotransduction (Gallant, Michael, and Garcia 2005; Geiger et al. 2001). The cytoplasmic region of integrins induce intracellular signal transduction, cell cytoskelatal organization and also modulate gene expression (Shyy and Chien 2002).

Cell-cell connections, on the other hand are sustained by cadherins, occludins and connexins. Among these, cadherins are of prime importance for mechanotransduction between cells linked through adherent junctions. Cadherins are hemophilic cell-cell adhesive proteins that require divalent cations like Ca^{+2} for their homotypic activity and are connected to the cell cytoskeleton (Chen, Tan, and Tien 2004).

Both integrins and cadherins are wired to the the actin filaments of the cytoskeleton. The signaling events have the capacity to switch on/off genetic materials within the cell nucleus. Existence of cross-talk between integrins and cadherins/ cell-cell and cell-matrix adhesions has been reported and this once again highlights the interconnected and interdependent nature in the different levels of cell communications (Weber, Bjerke, and DeSimone 2011). For instance, it has been shown that

while vascular smooth muscle cells are affected by substrate stiffness through integrin mediated adhesion, an increase in cell to cell contacts make them less sensitive to the stiffness (Sazonova et al. 2011). Endothelial cells (EC) are anchorage dependent cells, require integrin mediated attachment to ECM for their survival and display several integrins on their surfaces that bind to different proteins in ECM like fibronectin, laminin, Collagen I and IV (Stromblad and Cheresh 1996). At the same time, EC make cell-cell connections through Vascular Endothelial (VE)-cadherins junctions. An EC monolayer forms the protective inner lining of every blood vessel in the body exposed to continuous blood flow or shear stress, cyclic strain and hydrostatic from the luminal side and is also anchored to the basal lamina on the other side. The forces these cells experience are transduced by both cadherins and integrins (Califano and Reinhart-King 2010; Weber, Bjerke, and DeSimone 2011). And overall, endothelial mechanobiology is characterized by both chemical and mechanical aspects like matrix stiffness, substrate ligands, shear forces and soluble biochemical factors (Stroka and Aranda-Espinoza 2010). This example truly highlights the need for engineering scaffolds and biomaterials for biomedical engineering applications to factor in the structural, mechanical and biochemical aspects of a cell microenvironment along with the dynamic interplay between cells and with the substrate in order to provide instructive cues to elicit specific response for optimum functionality (Edalat et al. 2012).

2.4 High Throughput Techniques to Screen Cell Response

The numerous aspects that affect cell behavior have been discussed in earlier sections. The design, production and testing of new biomaterials have to consider all these elements related to cell functionality and biocompatibility. The expectations from a biomaterial have also increased over the years to now requiring very specific functions in addition to a prolonged shelf life, more

bioactivity, specific interactions at the molecular level, easy implantation and continuous monitoring (Hench and Polak 2002). Checking all the boxes individually of such a very long list would mean a very large investment in terms of money, time and resources. Instead of individual parameter testing, a more time efficient approach is the implementation of high throughput platforms with discrete arrays, or spatially controlled gradient properties to screen cell response. (Peters, Brey, and A. 2009; Simon and Lin-Gibson 2011). Such a screening technique is more efficient and effective than individual testing of parameters (Yliperttula et al. 2008; Moraes et al. 2010; Mei, Goldberg, and Anderson 2007; Kim, Khang, and Lee 2008). In this manner detailed studies can be focused on positive hits identified from a large screening field of variables and an optimal blend of different variables for a certain biomedical application can be identified (Hook et al. 2010; Neuss et al. 2008; Rasi Ghaemi et al. 2013). Based on the experimental conditions used in a particular study, combinatorial gradient materials could have the potential to pave the way for optimization of design parameters for a new generation of biomaterials. For example, unraveling facets of angiogenesis, more specifically endothelial cell behavior in blood vessel formation, will directly impact vascularization of complex tissue engineered constructs which still poses a big challenge in all tissue engineering applications. Along the same lines, optimizing design parameters in cardiovascular implants that support complete re-endothelialization of implant materials is essential for enhanced performance, durability and biocompatibility (Lv et al. 2008). Another prospect of working with gradient materials includes comprehending factors or events that contribute to specific pathological conditions (example cancer, cardiovascular disease) through screening for possible variations in the form of upregulation or downregulation of specific cell markers.

In a landmark study, Anderson et al demonstrated the power of high throughput screening of cell-material interaction through creating nanoscale array of polymeric biomaterials to screen approximately 1700 human embryonic stem cell-biomaterial interface reactions (Anderson, Levenberg, and Langer 2004). Some of the studies conducted using high throughput gradients; to investigate different factors of cell behavior are described in the next two sections. These include gradients in physical aspects such as biomaterial stiffness, topography and biochemical features such as surface chemistry and bioactive agents (Oliveira and Mano 2014).

2.5 1D Gradient Materials

A single gradient material in which one property is varied can be used to study how the variations in that parameter affect cell response. Gradients in physical parameters have been investigated for their effect on cell response (Obregón et al. 2015; Bailey, Nail, and Grunlan 2013). Physical gradients are engineered with variations in topographical attributes such as porosity gradients where pore size variation could range from micro to nano scale. Porosity gradients have been utilized to study the effect of osteoblast related functions for application in bone tissue engineering (Tampieri et al. 2001; Collart Dutilleul et al. 2014). Porosity gradients in nanometer scale have been studied to understand neuroblastoma cell growth (Khung, Barritt, and Voelcker 2008). Similarly gradients in surface roughness, crystallinity, and swelling have been employed to study cell functions (Washburn et al. 2004; Kunzler et al. 2007; Faia-Torres et al. 2014; Han et al. 2013, 2013). A spatial stepwise gradient with PDMS microchannels that are wide on one side and tapered on the other side has been used to study cell invasion where it was found that 87% metastatic breast cancer cells were invasively migrated to the narrower zone compared to the lower 25% of the normal breast epithelial cells (Mak, Reinhart-King, and Erickson 2011).

The effect of a gradient in applied mechanical shear forces in the form of hydrodynamic shear assay to quantify strength of cellular adhesion has been reported. It is a high throughput cell adhesion assay that applies a range of shear stresses on cells population under uniform chemical conditions using a spinning disk device. A cell population on circular substrates is mounted on a spinning shaft and is subjected to a well characterized linear range of hydrodynamic forces using a solution of known viscosity and density (Elineni and Gallant 2011; Garcia and Gallant 2003; Garcia, Ducheyne, and Boettiger 1997). The magnitude of applied shear stress increases linearly with the radial position (Gallant and García 2007) from the center of disc to its rim. After spinning, the ratio of the number of cells at a specific radial position r to the number of cells in the center that experience least shear forces represents the fraction of adhered cells. The cell detachment profile of adhered cell fraction vs. shear stresses is fit using a sigmoid curve in which the inflection point of the curve gives the shear stress required to detach 50% of cells and represents the mean cell adhesion strength of the population.

Gradients in mechanical property such elastic modulus gradients have shown to be a significant player in directing cell response. Polymers with a 'step gradient' containing stiffer regions through contact printing was demonstrated using two polymers, poly acrylamide (PA) and polydimethyl siloxane (PDMS) which were then fibronectin coated for fibroblast NIH3t3 and bovine endothelial cell culture. Both cell types showed preferential migration and accumulation toward the stiffer regions of the polymers (PA 34 kPa, PDMS 2.5 MPa) than the softer regions (PA 1.8kPa, PDMS12kPa) (Gray, Tien, and Chen 2003). Lo et al created a polyacrylamide sheet with a soft and stiff end through manipulation of crosslinker concentration and discovered that while NIH3t3 cells readily migrated from the soft to the stiff end, cells that were migrating in the direction toward

soft side stopped short at the transition boundary and 'turned' around (Lo et al. 2000). Similarly, microelasticity gradients having soft and stiff regions have been produced through photolithography using photocurable gelatin and it was concluded that mechanotaxis was more favorable when the elasticity ratio of hard and soft regions were higher (Karageorgiou and Kaplan 2005). Isenberg et al made stiffness gradients using polyacrylamide hydrogels surface modified with collagen and ranging from 1 to 80kPa in modulus of elasticity. The gradient substrate itself was made using a microfluidic device with a three channel inlet carrying monomer, crosslinker and initiator with several dividing and converging channels downstream for mixing. It was concluded that vascular smooth muscle cell orientation and durotaxis was affected by the presence of a stiffness gradient and that cell spreading and polarization was correlated with higher stiffness (Isenberg et al. 2009). A mechanical gradient (~12-28 kPa) in polyacrylamide hydrogels in a circular geometry was generated through controlled photopolymerization with the use of a radially patterned mask that either transitioned from light to dark grey scale from center to periphery or an inverse mask with gradient in the opposite direction. It was found that vascular smooth muscle cells exhibited durotaxis and later increased cell accumulation on the stiffer regions (Wong et al. 2003). A cylindrical hydrogel with a stiffness gradient with a 1 kPa to 24 kPa range produced through a freeze thaw procedure has also been to study stem cell differentiation (Kim et al. 2015). While several mechanical elasticity moduli materials and results have been obtained, the number of studies that used materials with physiologically relevant stiffnesses (~MPa range) and especially a continuous mechanical stiffness gradient was rare. Recently, Wang et al made a stiffness gradient using PDMS generated through controlling the directionality of heating during the curing process of PDMS to study mesenchymal cell response. This study is discussed in more detail in section 2.7 (Wang, Tsai, and Voelcker 2012).

Material surfaces are also altered in a controlled manner to obtain gradients biochemical aspects to screen cells. Polymeric gradients, plasma polymerized polymer brush gradients and gradients obtained through corona discharge have been reported to obtain gradients different chemical functional groups (Zelzer et al. 2008; Lee et al. 1998; Lee et al. 2000; Coad, Bilgic, and Klok 2014; Neuhaus, Padeste, and Spencer 2011; Ekblad et al. 2009; Zelzer, Alexander, and Russell 2011). Gradients in immobilized peptide density groups such as RGD, ligands, and proteins like fibronectin, collagen and laminin have also been demonstrated to impact cell functions (Wu et al. 2014; Mimura et al. 2008; Li, Wu, and Gao 2011; Herman et al. 2011; Maheshwari et al. 2000). In an interesting study that looked at the influence of a chemotactic gradient in the form of VEGF oriented perpendicular to the presence of electrospun hyaluronic fibers on HUVEC motility, and it was found that the topographical cues was the more potent regulating factor (Sundararaghavan et al. 2013).

The availability of plentiful types of self-assembled monolayer (SAM) molecules and their deposition and further modifications upon different types of substrates offers more options of making gradient materials. Microfluidic lithography techniques have been used to prepare dynamic hydroquinone-terminated SAM gradients that supports an RGD peptide density gradient which guided cell migration to the end higher peptide density (Lamb, Westcott, and Yousaf 2008).

Roberson et al demonstrated the creation of surface energy gradients with water contact angle ranging from ~5° to 95° by chemically modifying the chlorodimethyl octylsilane deposited on Si wafers using controlled UV ozone radiation through varying density mask filter. In the presence of oxygen, the UV ozone treatment generates atomic oxygen by dissociating ozone with the 257

nm and molecular oxygen with the 185 nm wavelength of the lamp. The atomic oxygen in turn oxidizes the silane monolayer and generates oxygenated species. Analysis of the chemistry through time-of-flight secondary ion mass spectroscopy (ToF SIMS) was also investigated and found changes in $SiCH3^{+}$, $SiOH^{+}$ and $COOH^{-}$ (Roberson et al. 2002). This method was later adopted by Kennedy et al to study osteoblast cell response to a gradient in surface chemistry coated with fibronectin protein. They found that maximum cell proliferation occurred at hydrophobic end of gradient (Kennedy et al. 2006). Gallant et al observed that smooth muscle adhesion correlated with increases in hydophobicity on a surface chemistry gradient and with increase in RGD concentration on a peptide density gradient (Gallant et al. 2007). A similar gradient approach was adopted by Acharya et al who performed a systematic characterization of dendritic cell adhesion on RGD peptide density gradients fabricated through biofunctionalization of peptides on glass slides with linear surface energy gradients. Dendritic cell activation of cytokines and integrin α_V subunit binding as a function of peptide density gradient were also assessed using these universal gradient substrates (Acharya et al. 2010). We chose a similar UVO treatment of ODMS discussed in the above mentioned studies to create gradients on PDMS surface due to the inherent similarity of the siloxane backbone in PDMS to the structure of glass.

2.6 2D Gradient Materials

Combinatorial and high throughput methods have the potential to screen cell responses to multiple parameters (Smith Callahan et al. 2013; Peters, Brey, and A. 2009). A combinatorial high throughput platform that allows screening of different combinations of various physical, biological, chemical and mechanical properties in a systematic manner is highly advantageous (Thasneem and Sharma 2013; Oliveira and Mano 2014). The data obtained helps illustrate the

added or synergistic effect of the factors involved on cells rather than the effect of one single parameter. And as discussed extensively in the previous sections, multiple cues provide stimuli in a cell microenvironment. Also, the use of high throughput and automated techniques to screen cell response, such as automated microscopy, supports multi parameter, rich content data collection and analysis (Liu et al. 2009; Simon Jr et al. 2005).

Following is a brief review of work done where 2D gradients were utilized for cell and protein assays. The review includes 2D chemistry gradients where both the gradients are variations in a chemical factor and 2D physic-chemical gradients where at least one among the two gradients presents a variation in a physical parameter.

2D gradient with a linear gradient in compositions of two polymers along an axis was annealed on a stage with graded temperature in the orthogonal direction that in turned induced a phase separation in polymers (Meredith et al. 2003). A region of enhanced osteogenic marker expression was identified for an intermediate polymer blend exposed to ~105°C. Two sets of dual axis polymer brush gradients with one varying molecular weight of two polymers and the other that varied molecular weight and grafting density of a polymer were generated and were used to study protein adsorption and cell adhesion (Bhat, Tomlinson, and Genzer 2005).Plasma polymerization of allylamine on polyethylene through a two-step diffusion controlled process was done to achieve a 2D amine gradient. Cell morphology was examined and found to correlate with the higher nitrogen content on the substrate (Mangindaan, Kuo, and Wang 2013). Other examples include a fibrinogen and lysozyme two protein gradients by subjecting poly ethylene glycol (PEG) to controlled surface grafting density (Vasilev et al. 2010), 2D orthogonal gradients immobilized with

peptide density gradients through ‘click’ chemistry on silane coated silicon and glass wafers to assay cell functions (Ma et al. 2013), 2D gradients in polymer brush grafting density and molecular weight to study lysozyme adsorption (Genzer et al. 2011) and orthogonal gradients with functional groups through modification of several silanes to study adsorption of proteins like albumin and fibrinogen (Beurer et al. 2012).

A 2D physico-chemical gradient having an orthogonal gradient platform varying physical cues with a micrometer roughness gradient on one axis and a nanometer scale roughness on the other axis induced higher levels of osteopontin production, a marker of osteogenesis, at highest micrometer roughness and a midway nanometer roughness region (Zink et al. 2012), a 2D physical gradient featuring groove depth and pitch gradients to study endothelial and fibroblast cell adhesion has also been demonstrated (Reynolds et al. 2012). A nanoporosity gradient combined with peptide ligand density gradient has shown mesenchymal stem cell response being stronger toward the peptide gradient (Clements et al. 2012). A strip based discrete blend gradients of two polymers were annealed on graded temperature stage that induced a gradient in increasing roughness and modulus correlating with one of the polymer concentration to study osteoblast functions (Simon Jr et al. 2005). An interesting study where the effect of the combination of low Collagen concentration with higher elastic modulus and a higher Collagen concentration with a lower modulus was conducted using polyacrylamide hydrogels to study cell migration. It was essentially a 2D ‘step’ non continuous gradient where equal volume of each of the two blends were added beside one another on glass and allowed to crosslink resulting in an interface between the two zones. Varying crosslinker concentration allowed making 2D ‘step’ gradients with different sets of moduli. It was found that the biochemical stimuli were more overpowering than the stiffness

stimuli for fibroblast migration. The stiffness was ~35 kPa for the low modulus and 55 kPa or 85 kPa represented the high modulus (Hale, Yang, and Rajagopalan 2010).

Some of the 1D and 2D gradients described in this chapter are not truly continuous in nature, rather discrete blends beside another with a clear transition boundary layer. Overall, combined gradient materials that incorporate stiffness gradients with another parameter are limited. Specifically, 2D continuous long range gradients engineered to incorporate a bulk mechanical stiffness in the physiologically relevant range along with another variable gradient on its orthogonal axis is virtually quite nonexistent.

2.7 Silicone Elastomer PDMS as a Model Biomaterial

The objective of this project is to fabricate a 2D gradient material with a continuous gradient in surface chemistry along one axis and a continuously varying modulus of elasticity along the orthogonal axis. Toward this objective, polydimethylsiloxane (PDMS), a silicone elastomer was chosen as the model biomaterial. PDMS offers a long list of beneficial properties. It is a material that is fairly inexpensive, easy to procure and manufacture since it is commercially available in two components with one being a base and the other a crosslinker that undergoes a hydrosilation reaction with Pt as a catalyst (Simpson et al. 2004). Its other characteristics include being thermally stable, having a high modulus of elasticity, chemical resistance, low toxicity, being water impermeable optically transparent (Li, Wang, and Shen 2012; Ng et al. 2002; McDonald and Whitesides 2002). Unsurprisingly therefore, PDMS is a widely used material in multiple fields of applications including microfluidics, photolithography, biomaterials and tissue engineering to name a few.(Lih et al. 2014; Ai et al. 2003; Jo and Guldiken 2014; Xia and Whitesides 1998).

However, PDMS has some inconvenient features such as poor surface energy properties that do not support cell adhesion and while the surface may be modified by plasma processing, the changes made are lost quickly due to hydrophobic recovery (Evaraert, Mei, and Busscher 1996; Everaert et al. 1995; Zhao, Lee, and Sen 2012). This is where the low molecular weight species make its way back to the surface and buries the altered surface. The shelf life of the superior plasma cleaned PDMS surface has been extended further through several days of curing the PDMS at elevated temperatures, solvent extraction for an extended time period and by immersion of substrate in water or ethanol (Mata, Fleischman, and Roy 2005; Wang et al. 2010; Vickers, Caulum, and Henry 2006; Tan et al. 2010; Almutairi, Ren, and Simon 2012).

PDMS surfaces may also be altered through silanization and UV crosslinking (Almutairi, Ren, and Simon 2012; Beltran et al. 2011; Bhagat, Jothimuthu, and Papautsky 2007; Efimenko, Wallace, and Genzer 2002; Berdichevsky et al. 2004). The elastic modulus may be tweaked with variations in time and temperature of curing, chemical interventions and also in the more typical way when the base and crosslinker concentrations are changed (Brown, Ookawa, and Wong 2005; Fuard et al. 2008; Palchesko RN et al. 2012; Wang, Tsai, and Voelcker 2012). The Dow Corning 184 Sylgard PDMS in which the base component is made of vinyl terminated dimethlysiloxane oligomers to which the curing crosslinker agent of dimethyl methylhydrogen siloxane (silicon hydride) reacts through a hydrosilylation reaction which results in a Si-C bond (Esteves et al. 2009; Oulad Hammouch, Beinert, and Herz 1996).The base also contains silica filler in the form of dimethylvinylated and trimethylated silica and the curing crosslinker agent carries tetramethyl tetravinyl cyclotetrasiloxane as an inhibitor to control the curing rate (Lee et al. 2004). PDMS

materials have also been used for cell studies which investigated the phenomena of chemotaxis and durotaxis (Isenberg et al. 2009; Gray, Tien, and Chen 2003; Sia and Whitesides 2003).

Palchesko et al made discrete blends of two commercially available PDMS, the Sylgard 184 and Sylgard 527 in varying ratios of the two to with the softest blend having a modulus of 5 kPa and the stiffest blend with a modulus of 1.72 MPa. There was no significant variation in surface roughness or wettabilities in the crosslinked networks made from mixing the two types of PDMS. Myoblast differentiation into myotubes and neurite extension length were both sensitive to the variations in the change in substrate stiffness (Palchesko RN et al. 2012). In another study where Sylgard 184 was use to modify the base to crosslinking ratios to make discrete PDMS networks varying stiffness ranging from 1.8 to 0.05 MPa followed by surface treatment using layer-by layer treatment with positively and negatively charged solutions (Ai et al. 2003) affected cell functions attachment, spreading and growth of vascular smooth muscle cells (Brown, Ookawa, and Wong 2005).

Wang et al have created stiffness gradients using PDMS to study rat mesenchymal stem cell (rMSC) response. Three separate stiffness gradients were prepared with one using PDMS in the conventional 10 to 1 ratio of base and crosslinker, the other with 20 to 1 and finally a combination of the two blends to obtain a wider range of stiffness. This last combination gradient was made by pouring PDMS, first the mixture containing 10 to 1 ratio of base and curing agent and then other with 20 to 1on top of that, into teflon spacer clamped by two glass slides and the placed vertically on a hot surface (120°C) for about 2 hours. The directional variation in the heating intensity over the 12mm length of combination PDMS obtained the widest stiffness range of 0.2 MPa to 3.1MPa

on which osteogenesis of the rMSC occurred more at the stiffer end (Wang, Tsai, and Voelcker 2012). And while this one study has been reported where the PDMS material has been used to create mechanical gradients, surface gradients on PDMS and 2D gradients with PDMS have not been attempted before. To our knowledge, it is the for the first time in the presented study that surface chemistry gradients are generated on PDMS through surface modifications to screen cell response and study the interfacial adhesive layer. Also presented in this study for the first time is a 2D gradient combinatorial biomaterial fabricated using PDMS, that encompasses an elastic modulus gradient portraying a range of physiologically relevant stiffness and an orthogonal surface chemistry gradient for the purpose of a systematic screening of synergistic cell response to the engineered mechanochemical cues.

2.8 References

Acharya, Abhinav P., Natalia V. Dolgova, Nicole M. Moore, Chang-Qing Xia, Michael J. Clare-Salzler, Matthew L. Becker, Nathan D. Gallant, and Benjamin G. Keselowsky. 2010. The modulation of dendritic cell integrin binding and activation by RGD-peptide density gradient substrates. *Biomaterials* 31 (29):7444-7454.

Ai, Hua, YuriM Lvov, DavidK Mills, Merilyn Jennings, JonathanS Alexander, and StevenA Jones. 2003. Coating and selective deposition of nanofilm on silicone rubber for cell adhesion and growth. *Cell Biochemistry and Biophysics* 38 (2):103-114.

Alberts B, Johnson A, Lewis J, M. Raff, K. Roberts, and, and P. Walter, eds. 2002. *Molecular Biology of the Cell*. Vol. 4th edition, *New York: Garland Science*.

Almutairi, Zeyad, Carolyn L. Ren, and Leonardo Simon. 2012. Evaluation of polydimethylsiloxane (PDMS) surface modification approaches for microfluidic applications. *Colloids and Surfaces A: Physicochemical and Engineering Aspects* 415 (0):406-412.

Anderson, Daniel G., Shulamit Levenberg, and Robert Langer. 2004. Nanoliter-scale synthesis of arrayed biomaterials and application to human embryonic stem cells. *Nature Biotechnology* 22 (7):863-866.

Anderson, J M., A Rodriguez, and D T. Chang. 2008. Foreign Body Reaction to Biomaterials. *Seminars in immunology* 20 (2):86-100.

Bailey, Brennan M., Lindsay N. Nail, and Melissa A. Grunlan. 2013. Continuous gradient scaffolds for rapid screening of cell–material interactions and interfacial tissue regeneration. *Acta Biomaterialia* 9 (9):8254-8261.

Beltran, Arnel B., Grace M. Nisola, Eulsaeng Cho, Erli Eros D. Lee, and Wook-Jin Chung. 2011. Organosilane modified silica/polydimethylsiloxane mixed matrix membranes for enhanced propylene/nitrogen separation. *Applied Surface Science* 258 (1):337-345.

Berdichevsky, Yevgeny, Julia Khandurina, András Guttman, and Y. H. Lo. 2004. UV/ozone modification of poly(dimethylsiloxane) microfluidic channels. *Sensors and Actuators B: Chemical* 97 (2–3):402-408.

Beurer, Eva, Nagaiyanallur V. Venkataraman, Marianne Sommer, and Nicholas D. Spencer. 2012. Protein and Nanoparticle Adsorption on Orthogonal, Charge-Density-Versus-Net-Charge Surface-Chemical Gradients. *Langmuir* 28 (6):3159-3166.

Bhagat, Ali Asgar S., Preetha Jothimuthu, and Ian Papautsky. 2007. Photodefinable polydimethylsiloxane (PDMS) for rapid lab-on-a-chip prototyping. *Lab on a Chip* 7 (9):1192-1197.

Bhat, Rajendra R., Michael R. Tomlinson, and Jan Genzer. 2005. Orthogonal surface-grafted polymer gradients: A versatile combinatorial platform. *Journal of Polymer Science Part B: Polymer Physics* 43 (23):3384-3394.

Biela, Sarah A., Yi Su, Joachim P. Spatz, and Ralf Kemkemer. 2009. Different sensitivity of human endothelial cells, smooth muscle cells and fibroblasts to topography in the nano–micro range. *Acta Biomaterialia* 5 (7):2460-2466.

Bradshaw, M. J., and M. L. Smith. 2014. Multiscale relationships between fibronectin structure and functional properties. *Acta Biomaterialia* 10 (4):1524-1531.

Brown, Xin Q, Keiko Ookawa, and Joyce Y Wong. 2005. Evaluation of polydimethylsiloxane scaffolds with physiologically-relevant elastic moduli: interplay of substrate mechanics and surface chemistry effects on vascular smooth muscle cell response. *Biomaterials* 26 (16):3123-3129.

Brunette, D. M., D. W. Hamilton, B. Chehroudi, and J. D. Waterfield. 2005. Update on improving the bio-implant interface by controlling cell behaviour using surface topography. *International Congress Series* 1284 (0):229-238.

Byfield, Fitzroy J., Rashmeet K. Reen, Tzu-Pin Shentu, Irena Levitan, and Keith J. Gooch. 2009. Endothelial actin and cell stiffness is modulated by substrate stiffness in 2D and 3D. *Journal of Biomechanics* 42 (8):1114-1119.

Califano, Joseph P., and Cynthia A. Reinhart-King. 2010. Exogenous and endogenous force regulation of endothelial cell behavior. *Journal of Biomechanics* 43 (1):79-86.

Chen, C. S., J. L. Alonso, E. Ostuni, G. M. Whitesides, and D. E. Ingber. 2003. Cell shape provides global control of focal adhesion assembly. *Biochem Biophys Res Commun* 307 (2):355-61.

Chen, Christopher S., John Tan, and Joe Tien. 2004. Mechanotransduction at cell-matrix and cell-cell contacts. *Annual Review of Biomedical Engineering* 6 (1):275-302.

Clements, Lauren R., Peng-Yuan Wang, Wei-Bor Tsai, Helmut Thissen, and Nicolas H. Voelcker. 2012. Electrochemistry-enabled fabrication of orthogonal nanotopography and surface chemistry gradients for high-throughput screening. *Lab on a Chip* 12 (8):1480-1486.

Coad, Bryan R., Tugba Bilgic, and Harm-Anton Klok. 2014. Polymer Brush Gradients Grafted from Plasma-Polymerized Surfaces. *Langmuir* 30 (28):8357-8365.

Collart Dutilleul, P. Y., D. Deville De Périère, F. J. Cuisinier, F. Cunin, and C. Gergely. 2014. 20 - Porous silicon scaffolds for stem cells growth and osteodifferentiation. In *Porous Silicon for Biomedical Applications,* edited by H. A. Santos: Woodhead Publishing.

Discher, Dennis E., Paul Janmey, and Yu-li Wang. 2005. Tissue Cells Feel and Respond to the Stiffness of Their Substrate. *Science* 310 (5751):1139-1143.

Edalat, Faramarz, Iris Sheu, Sam Manoucheri, and Ali Khademhosseini. 2012. Material strategies for creating artificial cell-instructive niches. *Current Opinion in Biotechnology* 23 (5):820-825.

Efimenko, Kirill, William E. Wallace, and Jan Genzer. 2002. Surface Modification of Sylgard-184 Poly(dimethyl siloxane) Networks by Ultraviolet and Ultraviolet/Ozone Treatment. *Journal of Colloid and Interface Science* 254 (2):306-315.

Ekblad, Tobias, Olof Andersson, Feng- I. Tai, Thomas Ederth, and Bo Liedberg. 2009. Lateral Control of Protein Adsorption on Charged Polymer Gradients. *Langmuir* 25 (6):3755-3762.

Elineni, K K , and N D Gallant. 2011. Regulation of Cell Adhesion Strength by Peripheral Focal Adhesion Distribution. *Biophysical journal* 101 (12):2903-2911.

Elwing, Hans. 1998. Protein absorption and ellipsometry in biomaterial research. *Biomaterials* 19 (4):397-406.

Elwing, Hans, Stefan Welin, Agneta Askendal, Ulf Nilsson, and Ingemar Lundstram. 1987. A wettability gradient method for studies of macromolecular interactions at the liquid/solid interface. *Journal of Colloid and Interface Science* 119 (1):203-210.

Engler, Adam, Lucie Bacakova, Cynthia Newman, Alina Hategan, Maureen Griffin, and Dennis Discher. 2004. Substrate Compliance versus Ligand Density in Cell on Gel Responses. *Biophysical Journal* 86 (1):617-628.

Engler, Adam J., Shamik Sen, H. Lee Sweeney, and Dennis E. Discher. 2006. Matrix Elasticity Directs Stem Cell Lineage Specification. *Cell* 126 (4):677-689.

Esteves, A. C. C., J. Brokken-Zijp, J. Laven, H. P. Huinink, N. J. W. Reuvers, M. P. Van, and G. de With. 2009. Influence of cross-linker concentration on the cross-linking of PDMS and the network structures formed. *Polymer* 50 (16):3955-3966.

Evaraert, Emmannuel P., Henny C. Van Der Mei, and Henk J Busscher. 1996. Hydrophobic recovery of repeatedly plasma-treated silicone rubber. Part 2 A comparison of the hydophobic recovery in air,water,or liq.N2. *J. Adhesion Sci Technol. Vol. 10, No.4, pp 351-359* 10 (4):351-359.

Everaert, E P, H C Van der Mei, J De Vries, and H J Busscher. 1995. Hydrophobic recovery of repeatedly plasma-treated silicone rubber. Part 1. Storage in air. *Journal of Adhesion Science & Technology* 9 (9):1263-1278.

Faia-Torres, Ana B., Stefanie Guimond-Lischer, Markus Rottmar, Mirren Charnley, Tolga Goren, Katharina Maniura-Weber, Nicholas D. Spencer, Rui L. Reis, Marcus Textor, and Nuno M. Neves. 2014. Differential regulation of osteogenic differentiation of stem cells on surface roughness gradients. *Biomaterials* 35 (33):9023-9032.

Fuard, D., T. Tzvetkova-Chevolleau, S. Decossas, P. Tracqui, and P. Schiavone. 2008. Optimization of poly-di-methyl-siloxane (PDMS) substrates for studying cellular adhesion and motility. *Microelectronic Engineering* 85 (5–6):1289-1293.

Gallant, N. D, K. A Lavery, E. J Amis, and M. L Becker. 2007. Universal Gradient Substrates for "Click" Biofunctionalization. *Advanced Materials* 19 (7):965-969.

Gallant, Nathan D., and Andrés J. García. 2007. Quantitative Analyses of Cell Adhesion Strength.

Gallant, Nathan D., Kristin E. Michael, and Andres J. Garcia. 2005. Cell Adhesion Strengthening: Contributions of Adhesive Area, Integrin Binding, and Focal Adhesion Assembly. *Molecular Biology of the Cell* 16 (9):4329-4340.

Garcia, Andrés, and Nathan Gallant. 2003. Stick and grip. *Cell Biochemistry and Biophysics* 39 (1):61-73.

Garcia, Andres J., Paul Ducheyne, and David Boettiger. 1997. Quantification of cell adhesion using a spinning disc device and application to surface-reactive materials. *Biomaterials* 18 (16):1091-1098.

Garcia, Jose R., and Andres J. Garcia. 2014. Cellular mechanotransduction: Sensing rigidity. *Nat Mater* 13 (6):539-540.

Geiger, Benjamin, Alexander Bershadsky, Roumen Pankov, and Kenneth M. Yamada. 2001. Transmembrane crosstalk between the extracellular matrix and the cytoskeleton. *Nat Rev Mol Cell Biol* 2 (11):793-805.

Genzer, Jan, Shafi Arifuzzaman, Rajendra R. Bhat, Kirill Efimenko, Chun-lai Ren, and Igal Szleifer. 2011. Time Dependence of Lysozyme Adsorption on End-Grafted Polymer Layers of Variable Grafting Density and Length. *Langmuir* 28 (4):2122-2130.

Gerecht, Sharon, Christopher J. Bettinger, Zhitong Zhang, Jeffrey T. Borenstein, Gordana Vunjak-Novakovic, and Robert Langer. 2007. The effect of actin disrupting agents on contact guidance of human embryonic stem cells. *Biomaterials* 28 (28):4068-4077.

Goubko, Catherine A., and Xudong Cao. 2009. Patterning multiple cell types in co-cultures: A review. *Materials Science and Engineering: C* 29 (6):1855-1868.

Gray, Darren S., Joe Tien, and Christopher S. Chen. 2003. Repositioning of cells by mechanotaxis on surfaces with micropatterned Young's modulus. *Journal of Biomedical Materials Research Part A* 66A (3):605-614.

Gugutkov, Dencho, George Altankov, José Carlos Rodríguez Hernández, Manuel Monleón Pradas, and Manuel Salmerón Sánchez. 2010. Fibronectin activity on substrates with controlled □OH density. *Journal of Biomedical Materials Research Part A* 92A (1):322-331.

Hale, N. A., Y. Yang, and P. Rajagopalan. 2010. Cell Migration at the Interface of a Dual Chemical-Mechanical Gradient. *ACS Applied Materials & Interfaces* 2 (8):2317-2324.

Han, Lulu, Zhengwei Mao, Jindan Wu, Yang Guo, Tanchen Ren, and Changyou Gao. 2013. Directional cell migration through cell–cell interaction on polyelectrolyte multilayers with swelling gradients. *Biomaterials* 34 (4):975-984.

Han, Lulu, Zhengwei Mao, Jindan Wu, Yang Guo, Tanchen Ren, and Changyou Gao. 2013. Unidirectional migration of single smooth muscle cells under the synergetic effects of gradient swelling cue and parallel groove patterns. *Colloids and Surfaces B: Biointerfaces* 111 (0):1-6.

Hench, Larry L., and Julia M. Polak. 2002. Third-Generation Biomedical Materials. *Science* 295 (5557):1014-1017.

Herbst, T. J., J. B. McCarthy, E. C. Tsilibary, and L. T. Furcht. 1988. Differential effects of laminin, intact type IV collagen, and specific domains of type IV collagen on endothelial cell adhesion and migration. *The Journal of Cell Biology* 106 (4):1365-1373.

Herman, Christine T., Gregory K. Potts, Madeline C. Michael, Nicole V. Tolan, and Ryan C. Bailey. 2011. Probing dynamic cell-substrate interactions using photochemically generated surface-immobilized gradients: application to selectin-mediated leukocyte rolling. *Integrative Biology* 3 (7):779-791.

Hernandez, Jose Carlos Rodraguez, Manuel Salmeran Sanchez, Jose Miguel Soria, Jose Luis Gamez Ribelles, and Manuel Monleon Pradas. 2007. Substrate Chemistry-Dependent Conformations of Single Laminin Molecules on Polymer Surfaces are Revealed by the Phase Signal of Atomic Force Microscopy. *Biophysical journal* 93 (1):202-207.

Hook, Andrew L., Daniel G. Anderson, Robert Langer, Paul Williams, Martyn C. Davies, and Morgan R. Alexander. 2010. High throughput methods applied in biomaterial development and discovery. *Biomaterials* 31 (2):187-198.

Humphries, Jonathan D, Adam Byron, and Martin J Humphries. 2006. Integrin ligands at a glance. *Journal of Cell Science* 119 (19):3901-3903.

Hynes, Richard O. 2002. Integrins: Bidirectional, Allosteric Signaling Machines. *Cell* 110 (6):673-687.

Hynes, Richard O. 2009. Extracellular matrix: not just pretty fibrils. *Science (New York, N.Y.)* 326 (5957):1216-1219.

Isenberg, Brett C., Paul A. DiMilla, Matthew Walker, Sooyoung Kim, and Joyce Y. Wong. 2009. Vascular Smooth Muscle Cell Durotaxis Depends on Substrate Stiffness Gradient Strength. *Biophysical Journal* 97 (5):1313-1322.

Iuliano, Denise J., Steven S. Saavedra, and George A. Truskey. 1993. Effect of the conformation and orientation of adsorbed fibronectin on endothelial cell spreading and the strength of adhesion. *Journal of Biomedical Materials Research* 27 (8):1103-1113.

Jo, Myeong Chan, and Rasim Guldiken. 2014. Effects of polydimethylsiloxane (PDMS) microchannels on surface acoustic wave-based microfluidic devices. *Microelectronic Engineering* 113 (0):98-104.

Kaji, Hirokazu, Gulden Camci-Unal, Robert Langer, and Ali Khademhosseini. 2011. Engineering systems for the generation of patterned co-cultures for controlling cell–cell interactions. *Biochimica et Biophysica Acta (BBA) - General Subjects* 1810 (3):239-250.

Karageorgiou, Vassilis, and David Kaplan. 2005. Porosity of 3D biomaterial scaffolds and osteogenesis. *Biomaterials* 26 (27):5474-5491.

Kasuya, Akira, and Yoshiki Tokura. 2014. Attempts to accelerate wound healing. *Journal of Dermatological Science* 76 (3):169-172.

Kennedy, Scott B., Newell R. Washburn, Carl George Simon Jr, and Eric J. Amis. 2006. Combinatorial screen of the effect of surface energy on fibronectin-mediated osteoblast adhesion, spreading and proliferation. *Biomaterials* 27 (20):3817-3824.

Keselowsky, B G., D M. Collard, and A J. Garcia. 2005. Integrin binding specificity regulates biomaterial surface chemistry effects on cell differentiation. *Proceedings of the National Academy of Sciences* 102 (17):5953-5957.

Keselowsky, Benjamin G., David M. Collard, and Andres J. Garcia. 2004. Surface chemistry modulates focal adhesion composition and signaling through changes in integrin binding. *Biomaterials* 25 (28):5947-5954.

Keselowsky, Benjamin G., David M. Collard, and Andrés J. García. 2003. Surface chemistry modulates fibronectin conformation and directs integrin binding and specificity to control cell adhesion. *Journal of Biomedical Materials Research Part A* 66A (2):247-259.

Khung, Y. L., G. Barritt, and N. H. Voelcker. 2008. Using continuous porous silicon gradients to study the influence of surface topography on the behaviour of neuroblastoma cells. *Experimental Cell Research* 314 (4):789-800.

Kim, Moon Suk, Gilson Khang, and Hai Bang Lee. 2008. Gradient polymer surfaces for biomedical applications. *Progress in Polymer Science* 33 (1):138-164.

Kim, Tae Ho, Dan Bi An, Se Heang Oh, Min Kwan Kang, Hyun Hoon Song, and Jin Ho Lee. 2015. Creating stiffness gradient polyvinyl alcohol hydrogel using a simple gradual freezing–thawing method to investigate stem cell differentiation behaviors. *Biomaterials* 40 (0):51-60.

Klotzsch, Enrico, Michael L. Smith, Kristopher E. Kubow, Simon Muntwyler, William C. Little, Felix Beyeler, Delphine Gourdon, Bradley J. Nelson, and Viola Vogel. 2009. Fibronectin forms the most extensible biological fibers displaying switchable force-exposed cryptic binding sites. *Proceedings of the National Academy of Sciences* 106 (43):18267-18272.

Kunzler, Tobias P., Tanja Drobek, Martin Schuler, and Nicholas D. Spencer. 2007. Systematic study of osteoblast and fibroblast response to roughness by means of surface-morphology gradients. *Biomaterials* 28 (13):2175-2182.

Lamb, Brian M., Nathan P. Westcott, and Muhammad N. Yousaf. 2008. Microfluidic Lithography to Create Dynamic Gradient SAM Surfaces for Spatio-temporal Control of Directed Cell Migration. *ChemBioChem* 9 (16):2628-2632.

Lan, Michael A., Charles A. Gersbach, Kristin E. Michael, Benjamin G. Keselowsky, and Andres J. Garcia. 2005. Myoblast proliferation and differentiation on fibronectin-coated self assembled monolayers presenting different surface chemistries. *Biomaterials* 26 (22):4523-4531.

Lee, Jessamine Ng, Xingyu Jiang, Declan Ryan, and George M. Whitesides. 2004. Compatibility of Mammalian Cells on Surfaces of Poly(dimethylsiloxane). *Langmuir* 20 (26):11684-11691.

Lee, Jin Ho, Gilson Khang, Jin Whan Lee, and Hai Bang Lee. 1998. Interaction of Different Types of Cells on Polymer Surfaces with Wettability Gradient. *Journal of Colloid and Interface Science* 205 (2):323-330.

Lee, Jin Ho, Sang Jin Lee, Gilson Khang, and Hai Bang Lee. 2000. The Effect of Fluid Shear Stress on Endothelial Cell Adhesiveness to Polymer Surfaces with Wettability Gradient. *Journal of Colloid and Interface Science* 230 (1):84-90.

Lee, Tsu-Yee Joseph, and Avrum I. Gotlieb. 2003. Microfilaments and microtubules maintain endothelial integrity. *Microscopy Research and Technique* 60 (1):115-127.

Li, Jueyu, Min Wang, and Yanbin Shen. 2012. Chemical modification on top of nanotopography to enhance surface properties of PDMS. *Surface and Coatings Technology* 206 (8–9):2161-2167.

Li, Linhui, Jindan Wu, and Changyou Gao. 2011. Gradient immobilization of a cell adhesion RGD peptide on thermal responsive surface for regulating cell adhesion and detachment. *Colloids and Surfaces B: Biointerfaces* 85 (1):12-18.

Lih, Eugene, Se Heang Oh, Yoon Ki Joung, Jin Ho Lee, and Dong Keun Han. 2014. Polymers for cell/tissue anti-adhesion. *Progress in Polymer Science* (0).

Liu, Er, Matthew D. Treiser, Hiral Patel, Hak-Joon Sung, Kristen E. Roskov, Joachim Kohn, Matthew L. Becker, and Prabhas V. Moghe. 2009. High-Content Profiling of Cell Responsiveness to Graded Substrates Based on Combinatorially Variant Polymers. *Combinatorial chemistry & high throughput screening* 12 (7):646-655.

Lo, Chun-Min, Hong-Bei Wang, Micah Dembo, and Yu-li Wang. 2000. Cell Movement Is Guided by the Rigidity of the Substrate. *Biophysical Journal* 79 (1):144-152.

Lössner, Daniela, Claudia Abou-Ajram, Anke Benge, and Ute Reuning. 2008. Integrin αvβ3 mediates upregulation of epidermal growth-factor receptor expression and activity in human ovarian cancer cells. *The International Journal of Biochemistry & Cell Biology* 40 (12):2746-2761.

Lv, Jiu-an, Jia-ni Ma, Peng-bo HuangFu, Shan Yang, and Yong-kuan Gong. 2008. Surface modification with both phosphorylcholine and stearyl groups to adjust hydrophilicity and hydrophobicity. *Applied Surface Science* 255 (2):498-501.

Ma, Yanrui, Jukuan Zheng, Emily F. Amond, Christopher M. Stafford, and Matthew L. Becker. 2013. Facile Fabrication of "Dual Click" One- and Two-Dimensional Orthogonal Peptide Concentration Gradients. *Biomacromolecules* 14 (3):665-671.

Ma, Zuwei, Zhengwei Mao, and Changyou Gao. 2007. Surface modification and property analysis of biomedical polymers used for tissue engineering. *Colloids and Surfaces B: Biointerfaces* 60 (2):137-157.

Maheshwari, G., G. Brown, D. A. Lauffenburger, A. Wells, and L. G. Griffith. 2000. Cell adhesion and motility depend on nanoscale RGD clustering. *Journal of Cell Science* 113 (10):1677-1686.

Mak, Michael, Cynthia A. Reinhart-King, and David Erickson. 2011. Microfabricated Physical Spatial Gradients for Investigating Cell Migration and Invasion Dynamics. *PLoS ONE* 6 (6):e20825.

Mangindaan, Dave, Wei-Hsuan Kuo, and Meng-Jiy Wang. 2013. Two-dimensional amine-functionality gradient by plasma polymerization. *Biochemical Engineering Journal* 78 (0):198-204.

Martínez, E., E. Engel, J. A. Planell, and J. Samitier. 2009. Effects of artificial micro- and nano-structured surfaces on cell behaviour. *Annals of Anatomy - Anatomischer Anzeiger* 191 (1):126-135.

Mata, Alvaro, Aaron Fleischman, and Shuvo Roy. 2005. Characterization of Polydimethylsiloxane (PDMS) Properties for Biomedical Micro/Nanosystems. *Biomedical Microdevices* 7 (4):281-293.

McDonald, J. Cooper, and George M. Whitesides. 2002. Poly(dimethylsiloxane) as a Material for Fabricating Microfluidic Devices. *Accounts of Chemical Research* 35 (7):491-499.

Mei, Ying, Michael Goldberg, and Daniel Anderson. 2007. The development of high-throughput screening approaches for stem cell engineering. *Current Opinion in Chemical Biology* 11 (4):388-393.

Meredith, J. Carson, Joe- L. Sormana, Benjamin G. Keselowsky, Andrés J. García, Alessandro Tona, Alamgir Karim, and Eric J. Amis. 2003. Combinatorial characterization of cell interactions with polymer surfaces. *Journal of Biomedical Materials Research Part A* 66A (3):483-490.

Michael, KE, VN Vernekar, BG Keselowsky, JC Meredith, RA Latour, and AJ Garcia. 2003. Adsorption-induced conformational changes in fibronectin due to interactions with well-defined surface chemistries. *Langmuir* 19:8033-8040.

Mimura, T., S. Imai, M. Kubo, E. Isoya, K. Ando, N. Okumura, and Y. Matsusue. 2008. A novel exogenous concentration-gradient collagen scaffold augments full-thickness articular cartilage repair. *Osteoarthritis and Cartilage* 16 (9):1083-1091.

Moraes, Christopher, GongHao Wang, Yu Sun, and Craig A. Simmons. 2010. A microfabricated platform for high-throughput unconfined compression of micropatterned biomaterial arrays. *Biomaterials* 31 (3):577-584.

Mosher, Deane F, and Leo T Furcht. 1981. Fibronectin: Review of its Structure and Possible Functions. *J Investig Dermatol* 77 (2):175-180.

Nemir, Stephanie, and Jennifer West. 2010. Synthetic Materials in the Study of Cell Response to Substrate Rigidity. *Annals of Biomedical Engineering* 38 (1):2-20.

Neuhaus, Sonja, Celestino Padeste, and Nicholas D. Spencer. 2011. Versatile Wettability Gradients Prepared by Chemical Modification of Polymer Brushes on Polymer Foils. *Langmuir* 27 (11):6855-6861.

Neuss, Sabine, Christian Apel, Patricia Buttler, Bernd Denecke, Anandhan Dhanasingh, Xiaolei Ding, Dirk Grafahrend, Andreas Groger, Karsten Hemmrich, Alexander Herr, Willi Jahnen-Dechent, Svetlana Mastitskaya, Alberto Perez-Bouza, Stephanie Rosewick, Jochen Salber, Michael Waltje, and Martin Zenke. 2008. Assessment of stem cell/biomaterial combinations for stem cell-based tissue engineering. *Biomaterials* 29 (3):302-313.

Ng, Jessamine M. K., Irina Gitlin, Abraham D. Stroock, and George M. Whitesides. 2002. Components for integrated poly(dimethylsiloxane) microfluidic systems. *Electrophoresis* 23 (20):3461-3473.

Obregón, Raquel, Javier Ramón-Azcón, Samad Ahadian, Hitoshi Shiku, Murugan Ramalingam, Ali Khademhosseini, and Tomokazu Matsue. 2015. Chapter 13 - Gradient Biomaterials as Tissue Scaffolds. In *Stem Cell Biology and Tissue Engineering in Dental Sciences*, edited by A. V. S. S. Ramalingam. Boston: Academic Press.

Oliveira, Mariana B., and João F. Mano. 2014. High-throughput screening for integrative biomaterials design: exploring advances and new trends. *Trends in Biotechnology* 32 (12):627-636.

Onuki, Yoshinori, Upkar Bhardwaj, Fotios Papadimitrakopoulos, and Diane J. Burgess. 2008. A Review of the Biocompatibity of Implantable Devices: Current Challenges to Overcome Foreign Body Response. *Journal of Diabetes Science and Technology* 2 (6):1003-1015.

Oulad Hammouch, S., G. J. Beinert, and J. E. Herz. 1996. Contribution to a better knowledge of the crosslinking reaction of polydimethylsiloxane (PDMS) by end-linking: the formation of star-branched PDMS by the hydrosilylation reaction. *Polymer* 37 (15):3353-3360.

Palchesko RN, Zhang L, Sun Y, and Feinberg AW. 2012. Development of Polydimethylsiloxane Substrates with Tunable Elastic Modulus to Study Cell Mechanobiology in Muscle and Nerve. *PLoS ONE* 7 ((12): e51499. doi:10.1371/journal.pone.0051499).

Pankov, Roumen, and Kenneth M. Yamada. 2002. Fibronectin at a glance. *Journal of Cell Science* 115 (20):3861-3863.

Pelham, Robert J, and Yu-li Wang. 1997. Cell locomotion and focal adhesions are regulated by substrate flexibility. *Proceedings of the National Academy of Sciences* 94 (25):13661-13665.

Peters, Anthony, Darren M. Brey, and and Burdick Jason A. 2009. High-Throughput and Combinatorial Technologies for Tissue Engineering Applications. *Tissue Engineering Part B* 15 (3):225-239.

Peyton, Shelly, Cyrus Ghajar, Chirag Khatiwala, and Andrew Putnam. 2007. The emergence of ECM mechanics and cytoskeletal tension as important regulators of cell function. *Cell Biochemistry and Biophysics* 47 (2):300-320.

Potts, Jennifer R., and Iain D. Campbell. 1996. Structure and function of fibronectin modules. *Matrix Biology* 15 (5):313-320.

Rasi Ghaemi, Soraya, Frances J. Harding, Bahman Delalat, Stan Gronthos, and Nicolas H. Voelcker. 2013. Exploring the mesenchymal stem cell niche using high throughput screening. *Biomaterials* 34 (31):7601-7615.

Reynolds, Paul M., Rasmus H. Pedersen, Mathis O. Riehle, and Nikolaj Gadegaard. 2012. A Dual Gradient Assay for the Parametric Analysis of Cell–Surface Interactions. *Small* 8 (16):2541-2547.

Roberson, Sonya V., Albert J. Fahey, Amit Sehgal, and Alamgir Karim. 2002. Multifunctional ToF-SIMS: combinatorial mapping of gradient energy substrates. *Applied Surface Science* 200 (1“4):150-164.

Rozario, Tania, and Douglas W. DeSimone. 2010. The extracellular matrix in development and morphogenesis: A dynamic view. *Developmental Biology* 341 (1):126-140.

Saito, Akira C., Tsubasa S. Matsui, Taiki Ohishi, Masaaki Sato, and Shinji Deguchi. 2014. Contact guidance of smooth muscle cells is associated with tension-mediated adhesion maturation. *Experimental Cell Research* 327 (1):1-11.

Sazonova, Olga V, Kristen L Lee, Brett C Isenberg, Celeste B Rich, Matthew A Nugent, and Joyce Y Wong. 2011. Cell-Cell Interactions Mediate the Response of Vascular Smooth Muscle Cells to Substrate Stiffness. *Biophysical Journal* 101 (3):622-630.

Scatena, Marta, Manuela Almeida, Michelle L. Chaisson, Nelson Fausto, Roberto F. Nicosia, and Cecilia M. Giachelli. 1998. NF-kB Mediates alphav beta3 Integrin-induced Endothelial Cell Survival. *The Journal of Cell Biology* 141 (4):1083-1093.

Shang, Zheng-Jun, Jin-Rong Li, and Zu-Bing Li. 2007. Upregulation of Serum and Tissue Vascular Endothelial Growth Factor Correlates With Angiogenesis and Prognosis of Oral Squamous Cell Carcinoma. *Journal of Oral and Maxillofacial Surgery* 65 (1):17-21.

Shen, Yang, Min Gao, Yunlong Ma, Hongchi Yu, Fu-zhai Cui, Hans Gregersen, Qingsong Yu, Guixue Wang, and Xiaoheng Liu. 2015. Effect of surface chemistry on the integrin induced pathway in regulating vascular endothelial cells migration. *Colloids and Surfaces B: Biointerfaces* 126 (0):188-197.

Shyy, John Y. J., and Shu Chien. 2002. Role of Integrins in Endothelial Mechanosensing of Shear Stress. *Circulation Research* 91 (9):769-775.

Sia, Samuel K., and George M. Whitesides. 2003. Microfluidic devices fabricated in Poly(dimethylsiloxane) for biological studies. *Electrophoresis* 24 (21):3563-3576.

Simon, Carl G., and Sheng Lin-Gibson. 2011. Combinatorial and High-Throughput Screening of Biomaterials. *Advanced Materials* 23 (3):369-387.

Simon Jr, Carl G., Naomi Eidelman, Scott B. Kennedy, Amit Sehgal, Chetan A. Khatri, and Newell R. Washburn. 2005. Combinatorial screening of cell proliferation on poly(l-lactic acid)/poly(d,l-lactic acid) blends. *Biomaterials* 26 (34):6906-6915.

Simpson, T. R. E., Z. Tabatabaian, C. Jeynes, B. Parbhoo, and J. L. Keddie. 2004. Influence of interfaces on the rates of crosslinking in poly(dimethyl siloxane) coatings. *Journal of Polymer Science Part A: Polymer Chemistry* 42 (6):1421-1431.

Smith Callahan, Laura A., Anna M. Ganios, Erin P. Childers, Scott D. Weiner, and Matthew L. Becker. 2013. Primary human chondrocyte extracellular matrix formation and phenotype maintenance using RGD-derivatized PEGDM hydrogels possessing a continuous Young’s modulus gradient. *Acta Biomaterialia* 9 (4):6095-6104.

Stroka, Kimberly, and Helim Aranda-Espinoza. 2011. Effects of Morphology vs. Cell–Cell Interactions on Endothelial Cell Stiffness. *Cellular and Molecular Bioengineering* 4 (1):9-27.

Stroka, Kimberly M., and Helim Aranda-Espinoza. 2010. A biophysical view of the interplay between mechanical forces and signaling pathways during transendothelial cell migration. *FEBS Journal* 277 (5):1145-1158.

Stromblad, Staffan, and David A. Cheresh. 1996. Cell adhesion and angiogenesis. *Trends in Cell Biology* 6 (12):462-468.

Sundararaghavan, Harini G., Randi L. Saunders, Daniel A. Hammer, and Jason A. Burdick. 2013. Fiber alignment directs cell motility over chemotactic gradients. *Biotechnology and Bioengineering* 110 (4):1249-1254.

Tampieri, A., G. Celotti, S. Sprio, A. Delcogliano, and S. Franzese. 2001. Porosity-graded hydroxyapatite ceramics to replace natural bone. *Biomaterials* 22 (11):1365-1370.

Tan, Say Hwa, Nam-Trung Nguyen, Yong Chin Chua, and Tae Goo Kang. 2010. Oxygen plasma treatment for reducing hydrophobicity of a sealed polydimethylsiloxane microchannel. *Biomicrofluidics* 4 (3):032204.

Thasneem, Y. M., and Chandra P. Sharma. 2013. Chapter 5.1 - In Vitro Characterization of Cell–Biomaterials Interactions. In *Characterization of Biomaterials*, edited by A. B. Bose. Oxford: Academic Press.

Vasilev, Krasimir, Agnieszka Mierczynska, Andrew L. Hook, Joseph Chan, Nicolas H. Voelcker, and Rob D. Short. 2010. Creating gradients of two proteins by differential passive adsorption onto a PEG-density gradient. *Biomaterials* 31 (3):392-397.

Vickers, Jonathan A., Meghan M. Caulum, and Charles S. Henry. 2006. Generation of Hydrophilic Poly(dimethylsiloxane) for High-Performance Microchip Electrophoresis. *Analytical Chemistry* 78 (21):7446-7452.

Walters, Nick J., and Eileen Gentleman. 2015. Evolving insights in cell–matrix interactions: Elucidating how non-soluble properties of the extracellular niche direct stem cell fate. *Acta Biomaterialia* 11 (0):3-16.

Wang, Lin, Bing Sun, Katherine S. Ziemer, Gilda A. Barabino, and Rebecca L. Carrier. 2010. Chemical and physical modifications to poly(dimethylsiloxane) surfaces affect adhesion of Caco-2 cells. *Journal of Biomedical Materials Research Part A* 93A (4):1260-1271.

Wang, Peng-Yuan, Wei-Bor Tsai, and Nicolas H. Voelcker. 2012. Screening of rat mesenchymal stem cell behaviour on polydimethylsiloxane stiffness gradients. *Acta Biomaterialia* 8 (2):519-530.

Washburn, Newell R., Kenneth M. Yamada, Carl G. Simon Jr, Scott B. Kennedy, and Eric J. Amis. 2004. High-throughput investigation of osteoblast response to polymer crystallinity: influence of nanometer-scale roughness on proliferation. *Biomaterials* 25 (7–8):1215-1224.

Weber, Gregory F., Maureen A. Bjerke, and Douglas W. DeSimone. 2011. Integrins and cadherins join forces to form adhesive networks. *Journal of Cell Science* 124 (8):1183-1193.

Wong, Joyce Y., Jennie B. Leach, and Xin Q. Brown. 2004. Balance of chemistry, topography, and mechanics at the cell-biomaterial interface: Issues and challenges for assessing the role of substrate mechanics on cell response. *Surface Science* 570:119-133.

Wong, Joyce Y., Alan Velasco, Padmavathy Rajagopalan, and Quynh Pham. 2003. Directed Movement of Vascular Smooth Muscle Cells on Gradient-Compliant Hydrogels†. *Langmuir* 19 (5):1908-1913.

Wu, Jindan, Zhengwei Mao, Lulu Han, Yizhi Zhao, Jiabin Xi, and Changyou Gao. 2014. A density gradient of basic fibroblast growth factor guides directional migration of vascular smooth muscle cells. *Colloids and Surfaces B: Biointerfaces* 117 (0):290-295.

Xia, Younan, and George M. Whitesides. 1998. Soft Lithography. *Angewandte Chemie International Edition* 37 (5):550-575.

Yeung, Tony, Penelope C. Georges, Lisa A. Flanagan, Beatrice Marg, Miguelina Ortiz, Makoto Funaki, Nastaran Zahir, Wenyu Ming, Valerie Weaver, and Paul A. Janmey. 2005. Effects of Substrate Stiffness on Cell Morphology, Cytoskeletal Structure,and Adhesion. *Cell Motility and the Cytoskeleton* 60:24-34.

Yliperttula, Marjo, Bong Geun Chung, Akshay Navaladi, Amir Manbachi, and Arto Urtti. 2008. High-throughput screening of cell responses to biomaterials. *European Journal of Pharmaceutical Sciences* 35 (3):151-160.

Zelzer, Mischa, Morgan R. Alexander, and Noah A. Russell. 2011. Hippocampal cell response to substrates with surface chemistry gradients. *Acta Biomaterialia* 7 (12):4120-4130.

Zelzer, Mischa, Ruby Majani, James W. Bradley, Felicity R. A. J. Rose, Martyn C. Davies, and Morgan R. Alexander. 2008. Investigation of cell–surface interactions using chemical gradients formed from plasma polymers. *Biomaterials* 29 (2):172-184.

Zhao, Li Hong, Jennifer Lee, and Pabitra N. Sen. 2012. Long-term retention of hydrophilic behavior of plasma treated polydimethylsiloxane (PDMS) surfaces stored under water and Luria-Bertani broth. *Sensors and Actuators A: Physical* 181 (0):33-42.

Zink, Christian, Heike Hall, Don M. Brunette, and Nicholas D. Spencer. 2012. Orthogonal nanometer-micrometer roughness gradients probe morphological influences on cell behavior. *Biomaterials* 33 (32):8055-8061.

CHAPTER 3

MODULATION OF SILICONE ELASTOMER PROPERTIES TO ENGINEER COMBINATORIAL MATERIALS

3.1 Introduction

Polydimethyl Siloxane (PDMS) is the material of popular choice for a variety of applications including microfluidics, Biomicroelectromechanical Systems (BioMEMS) and photolithography (Maji, Lahiri, and Das 2012; Xia and Whitesides 1998; Almutairi, Ren, and Simon 2012; Wheeler et al. 2004). PDMS is cost effective and also possesses attractive material properties such as being very easy to manufacture, chemical and biological compatibility, thermal stability over a wide range of temperatures, optical transparency and non-toxicity (Jo and Guldiken 2014; Zhou, Ellis, and Voelcker 2010). Since PDMS offered the prospective for surface modifications and tuning of its bulk elastic modulus, it was chosen for this project to fabricate combinatorial gradient materials with varying surface and mechanical properties.

In this chapter, different aspects regarding modification of PDMS material properties with a special emphasis on surface chemical and bulk mechanical characteristics of PDMS are studied. PDMS offers the prospective of relatively easy surface modifications by protein adsorption, silanization, UV radiations, plasma processing, (Bhagat, Jothimuthu, and Papautsky 2007; Efimenko, Wallace, and Genzer 2002; Almutairi, Ren, and Simon 2012; Wang et al. 2010). Silane chemistry on oxides or Self Assembled Monolayers of alkanethiols on gold is immensely popular

means for modification of functional groups and altering surface chemistry of materials (Jo, Yu, and Yang 2011; Hong and Park 2005; Hemmilä et al. 2012). Silane modification of PDMS, particularly with organosilanes such as chlorodimethyloctylsilane, has also been reported (Beltran et al. 2011). For example, silanization of PDMS has been studied for improving surface properties of self-expandable stents to reduce stent migration post implantation (Karakoy et al. 2014).

The mechanical properties of PDMS may also be altered with ease through adjusting the crosslinker concentration and curing conditions (Wang, Tsai, and Voelcker 2012; Brown, Ookawa, and Wong 2005; Fuard et al. 2008; Tzvetkova-Chevolleau et al. 2008). PDMS is an elastomer that has been demonstrated to have a physiologically relevant range of elastic moduli (Wong, Leach, and Brown 2004; Wang, Tsai, and Voelcker 2012; Brown, Ookawa, and Wong 2005). Several tissue structures in our body have high modulus of elasticity in the range of ~1 to 2 MPa such as the ECM basement membrane, the thoracic aorta, abdominal aorta, iliac and carotid arteries (Candiello et al. 2007; Wong, Leach, and Brown 2004; Wang et al. 2010).

The main objective of this project was to make combinatorial 2D gradient materials using PDMS through surface and mechanical modifications of the materials. The preliminaries of this objective have been addressed in this chapter which details surface modifications including silane deposition on PDMS substrate, Ultraviolet Oxidation (UVO) treatment of PDMS surface, and solvent extraction of PDMS using a polar solvent, as well as tuning of mechanical properties of PDMS by varying the crosslinker concentration to achieve a wide range in modulus of elasticity.

3.2 Experimental Section

- Cross-linked networks of PDMS for surface modification and mechanical testing

Cross-linked networks of PDMS were prepared using Sylgard®184 purchased from Dow Corning Corporation. The kit is provided with a base and cross-linker that is mixed in a standard 10:1 ratio as per manufacturer's recommendations. 0.9 ml of mixed PDMS was dispensed on to glass slides (Fisher brand) using a 1 ml syringe. PDMS was cured at 65°C overnight. Plain glass slides and PDMS substrates were sonicated for 15 minutes to remove physical impurities and were then dried with a stream of N_2 or under vacuum in a desiccator.

Some of the cross-linked PDMS networks were Soxhlet extracted (Figure 3.1) to study the effect extraction on surface modifications such as recovery after plasma cleaning and gradient fabrication on PDMS. Samples were refluxed in 90% ethanol for 48 hrs, followed by baking at 65°C for 2.0 hrs and then stored in ambient air till further processing.

For further surface modifications, PDMS substrates were oxidized using an oxygen plasma cleaner (Plasma Etch PE-50, 011810 1D-678, Carson City, NV) at 100 watts for 5 minutes, to render sample surfaces hydrophilic and conducible for silane deposition. Physical vapor deposition was used for assembling a hydrophobic monolayer, chlorodimethyloctylsilane (ODMS) (Sigma Aldrich) via silane chemistry on glass and PDMS substrates. Samples were placed under vacuum for 24 hours in a glass desiccator that contained ODMS and toluene mixed in a 1:1 ratio. Silane deposition time was varied to study the kinetics of ODMS coverage on PDMS. After samples were removed from the desiccator, they were rinsed with 90% proof ethanol and baked for one and half hours at 65 °C.

- Ultraviolet oxidation of alkylsilane deposited PDMS to generate surface gradients

The procedure to obtain surface chemistry gradients on PDMS was adopted from previously published work (Gallant et al. 2007, Kennedy et al. 2006 and Roberson et al. 2002). Briefly, alkylsilane coated PDMS samples were placed on an accelerating linear translation stage (Aerotech, Inc.) controlled by LabVIEW (National Instruments) for modification of the alkylsilane surface layer as shown below in Figure 3.2. Residence time of the substrates beneath a stationary UV lamp (with emission at frequencies 254nm and 185nm) directly correlated with the extent of hydrophilicity at any given position on the sample. The stage advanced in 0.1 mm steps and was accelerated by decreasing the dwell time at each step. The result was a linear variation in exposure time over the length of the sample. A 1 cm zone with no UVO treatment acted as the internal control for each sample. The surface modified PDMS was characterized by contact angle analysis of water drops using the Young-La Place fit algorithm.

- Effect of curing time and temperature on PDMS elastic modulus

Two combinations of PDMS base and cross-linker (10% and 2% mass fraction cross-linker) were mixed, degassed and cured for varying times at either 65°C or 90°C. Cured polymeric samples were first subjected to a creep test (twenty four hours) to confirm their elastic behavior. This was followed by tensile testing of samples as done by Pelham and Wang (Pelham and Wang 1997) to determine elastic modulus using Hooke' s Law ($\sigma = E.\varepsilon$) where σ is stress in Pascals, ε is the strain and E the elastic modulus in Pascals. The number of replicates varied from a minimum of N=2 to a maximum of N=5 in the various treatment groups.

3.3 Results and Discussion

- Alkylsilane deposition kinetics on PDMS surface

Time of chlorodimethyloctyl silane (ODMS) vapor deposition on crosslinked 10% weight crosslinker PDMS networks was varied and its effect on surface chemistry was evaluated through water contact angle measurements. The water contact angle gives an indication of the relative strength of cohesive forces and adhesive forces between the water and the material surface (Figure 3.3). When the forces between molecules (cohesive force) within a droplet are stronger than the attractive forces between droplet and the surface (adhesive force), then the water does not wet the surface and it is described as hydrophobic, and *vice versa* (Ratner et al. 2013).

ODMS forms a covalent Si-OH bond with PDMS and HCl is released as a byproduct (Chruściel and Leśniak 2014). The objective of this experiment was to adopt an optimum alkylsilane deposition time to be followed for all future experiments related to PDMS surface modification, one that achieves a homogenous monolayer surface coverage on PDMS.

The results are illustrated in Figure 3.4, where the error bars represent deviation from mean of N=4 samples in each treatment group. It was found that the plasma cleaned PDMS surface which was very hydrophilic changed to a hydrophobic surface (97°±0.6) with just an hour long exposure. This rapid coverage by alkylsilane monolayers, on the order of a few minutes for chlorosilanes, has been reported previously (Kulkarni et al. 2005; Hussain, Krim, and Grant 2005). Longer exposure times conducted in this study were 3 hours, 24 hours, 48 hours, 6 days and 11 days, which yielded average measurements of 99°±3, 103°±3, 104°±1, 105±0.2 and 105±0.3 respectively. Full coverage of ODMS an monolayer on silicon is indicated by a contact angle of approximately 104°

(Gallant et al. 2007; Arkles 2006). A systematic pairwise comparison between the many groups revealed that there were statistically significant differences (p value<0.05) only for the shortest depositions times (1 and 3 hour) compared to the longer time depositions. The difference between the 24 hour and higher deposition times was insignificant; therefore, a 24 hour long exposure was chosen for all future experiments that followed. Spatially regulated ultraviolet ozone (UVO) oxidation treatment of the PDMS samples with the one hour and 3 hour alkylsilane deposition times resulted in sharp, step changes in hydrophobicity such that a position on the surface was either very hydrophilic or very hydrophobic (data not shown). Smooth and gradual gradients were obtained for PDMS samples that were exposed to alkylsilane vapor deposition for 24 hours or longer.

- Ultraviolet oxidation of alkylsilanes deposited on PDMS and characterization of surface chemistry

Monotonically increasing surface chemistry gradients were reproducibly generated on 10% weight crosslinker PDMS substrates. Detailed experiments and analysis of the surface gradients on these 10% weight crosslinker PDMS samples is the central focus of Chapter 4. In this chapter, surface chemistry gradients on the softer formulations of PDMS containing 2%, 1.67% and 1.43% weight crosslinker are illustrated. It was important to ascertain that surface gradients that were generated on the 10% weight PDMS could be easily translated to the softer formulation of PDMS that had lesser crosslinker weight%. This would be particularly important and useful for fabrication of combinatorial biomaterial with both a mechanical and surface chemistry gradient detailed in Chapter 6. Therefore, this preliminary experiment was conducted as a proof of concept

demonstrating monotonic gradients on PDMS formulations having 2%, 1.6% and 1.43% weight crosslinker concentration (Figure 3.5).

- Effect of Soxhlet extraction on PDMS surface modifications

The process of Soxhlet extraction of uniform silane deposited PDMS substrates does not significantly alter the hydrophobic (~102°) surface chemistry which was confirmed by water contact angle measurements. Figures 3.6 to 3.8 show the variations in surface chemistry for PDMS substrates that were Soxhlet extracted in 90% ethanol compared to non-extracted PDMS substrates. It was decided not to use more typical and organic solvents with higher solubility for PDMS such as toluene due to the possible problem from extensive swelling (55%) of PDMS, (Mata, Fleischman, and Roy 2005) which would be especially detrimental to the ~0.5mm thick PDMS cured on glass slide used in this study. Ideal solvents recommended for PDMS that is bonded to glass are low solubility solvents, alcohols such as ethanol being one of them. In fact, use of high solubility solvents can cause PDMS to undergo non uniform swelling and delaminate from glass, sometimes causing mechanical tears of PDMS (Lee, Park, and Whitesides 2003). Another independent study that investigated swelling caused to thin PDMS films cured on glass slide from solvent hexane showed that the degree of swelling in inversely proportional to the concentration of crosslinker in PDMS (Ogieglo et al. 2013). Use of ethanol for immersion of plasma treated PDMS has also been reported to prevent hydrophobic recovery (Wang et al. 2010).

UVO of unmodified (no alkylsilane) Soxhlet extracted (N=4) and non-extracted PDMS (N=4) substrates is reported in Figure 3.6. These experiments were performed as a control experiment to demonstrate that UVO treatment modifies the silane layer bound to PDMS surface and not the

bulk PDMS. This is evident from the negligible difference in surface chemistry for both extracted and non-extracted substrates prior to and post UVO treatment.

Plasma treatment of the PDMS surface makes it hydrophilic which is usually a short lived process with hydrophobic chains migrating back to surface (Evaraert, Mei, and Busscher 1996; Everaert et al. 1995; Zhao, Lee, and Sen 2012). It was found that non-extracted PDMS substrates (N=4) underwent recovery quicker than the Soxhlet extracted samples (N=2). Error bars depict standard deviation from mean. The recovery for extracted samples was 35% less than for the non-extracted samples (Figure 3.7). Extracted oxidized PDMS samples have shown to exhibit reduced recovery compared to oxidized non extracted PDMS (Lee, Park, and Whitesides 2003). Hydrophobic recovery after surface plasma treatment of PDMS has shown to be been delayed (Contact Angle 30° to 40° in 7 days) through immersion extraction of PDMS in multiple batches of trimethylamine and ethyl acetate prior to surface treatment (Vickers, Caulum, and Henry 2006).

Gradients generated on PDMS samples also were also short lived (detailed in Chapter 4) and underwent recovery. Since it was found that Soxhlet extracted samples had a delayed recovery rate after plasma treatment, the effect of extraction on gradient recovery of PDMS was investigated next. It was determined that extraction process did not prevent or delay the hydrophobic recovery of gradients on extracted PDMS (N=2, Figure 3.8). In fact, the recovery was identical to that of the control non-extracted PDMS gradient (N=1). Error bars represent standard deviation from the mean. The final decision to not extract PDMS for future experiments was made by also factoring in the extension of time it would incur to conduct an experiment each time since the extraction process is 48 hours long.

- Effect of time and temperature of curing on elastic modulus

The effect of variations in curing conditions, specifically lower or higher temperatures of curing and length of curing time itself on the elastic modulus of 10% and 2% weight crosslinker concentration containing PDMS networks were studied. The formulation with crosslinker of 1.67 weight% exhibited creep and therefore formulations softer than 2 weight% crosslinker concentration were excluded from this study since they exhibited some viscoelastic behavior. The elastic modulus was determined from tensile testing (Pelham and Wang 1997) and application of Hook's Law. This experiment was done to examine if differences in curing conditions were significant enough to yield an appreciable and wide range in elastic modulus. The aim was to obtain a difference in three orders or higher magnitude difference between the least and most stiff PDMS that would be great for making mechanical gradients spanning the widest possible range. The data in Figure 3.9 documents measurements for 65°C and 90°C for 1, 2, 4 and 8 days. The number of replicates varied from a minimum of N=2 to a maximum of N=5 in the various treatment groups with the error bars indicating standard deviation from mean. There exists an independent Y axis for the 10% and 2% crosslinker weight PDMS samples.

In general, a higher stiffness was measured for a higher temperature of curing for both 10% and 2% crosslinker weight PDMS samples. With respect to time of curing, the increase in stiffness mostly plateaued at day 4. It was concluded that prolonged storage at room temperature will not lead to an appreciable increase in modulus of elasticity. Most importantly, the difference in elastic modulus between the 10% and 2% formulations were of a two orders of magnitude for any time and/or temperature of curing. In fact, it was observed that the whole profile of the elastic modulus would trend slightly up or down for a given temperature. Therefore curing at an elevated

temperature did not provide a significantly wider range of elastic moduli between the stiff and soft PDMS formulations. Overall, the elastic moduli ranged from 1.68±0.4 to 0.02±0.004 MPa for the 10% and 2% respectively, including data from all different times and temperatures of curing. The range of modulus we obtained is comparable to the 1.8 MPa (10% PDMS) to 0.5 MPa (2% PDMS) previously reported in literature (Brown, Ookawa, and Wong 2005).

3.4 Conclusions

Alkylsilane deposition kinetics on PDMS surfaces was optimized for a time period of 24 hours. Soxhlet extraction of PDMS substrates in ethanol delayed and exhibited lower hydrophobic recovery after plasma treatment but did not prevent, delay or lessen the extent of recovery after gradient fabrication. The capability of surface modifications on softer formulations of PDMS including 2%, 1.67% and 1.43% crosslinker weight PDMS were demonstrated by generating monotonic increasing profiles of surface chemistry. Different curing conditions of 10% and 2% crosslinker weight PDMS formulations at varied time periods and temperatures produced a two order magnitude range in elastic moduli spanning from 1.68±0.4 MPa for 10weight% to 0.02±0.004 MPa for 2 weight%. Overall, these results provided a stepping stone for the experiments detailed in later chapters.

Figure 3.1 Photograph of PDMS substrates undergoing Soxhlet extraction in ethanol.

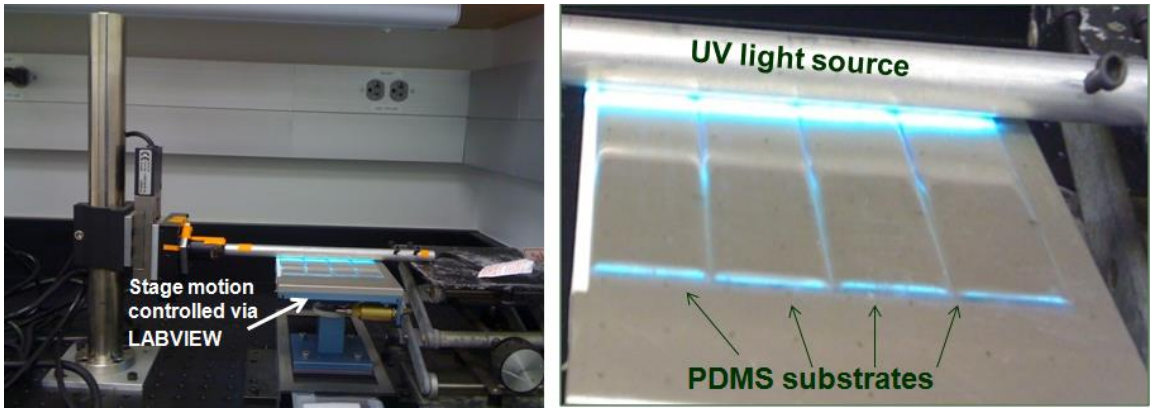

Figure 3.2 Image of PDMS substrates on moving stage beneath stationary UV lamp source.

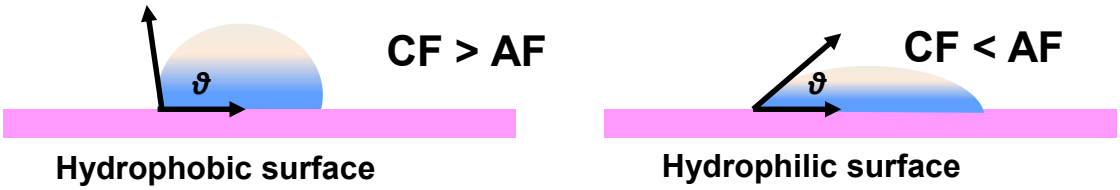

Figure 3.3 Illustration of the interplay of Cohesive Forces (CF) and Adhesive Forces (AF) of a water droplet on a hydrophobic vs hydrophilic surface.

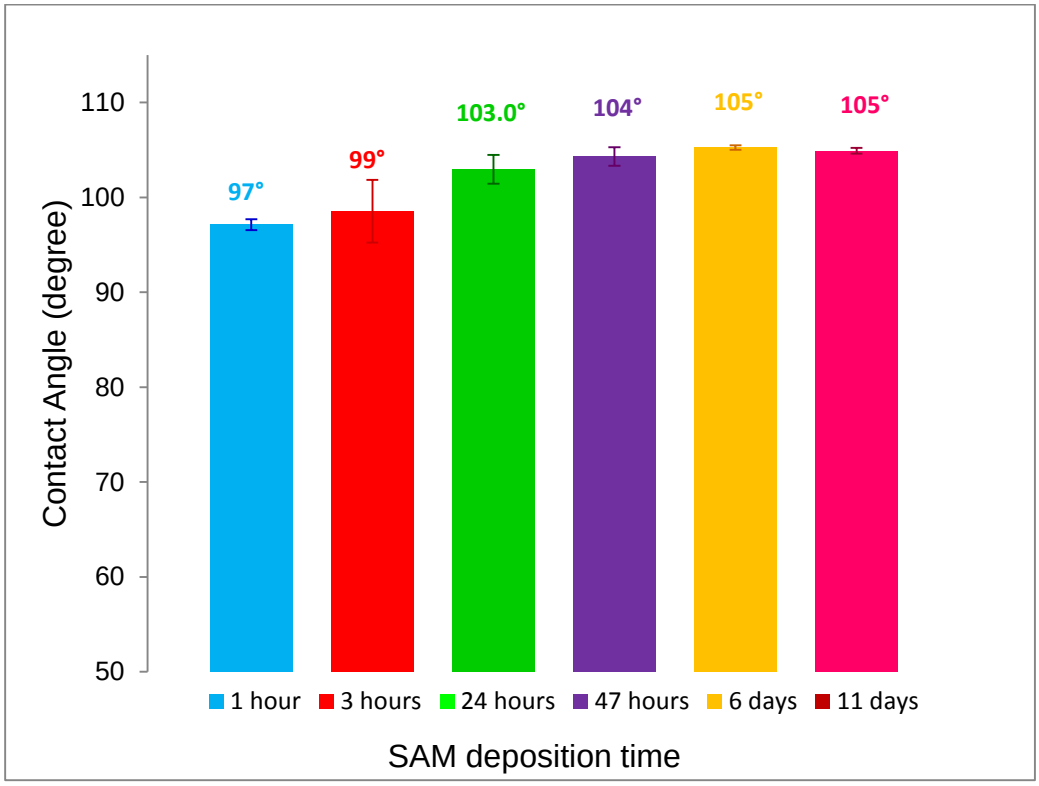

Figure 3.4 Effect of alkylsilane deposition time on hydrophobicity.

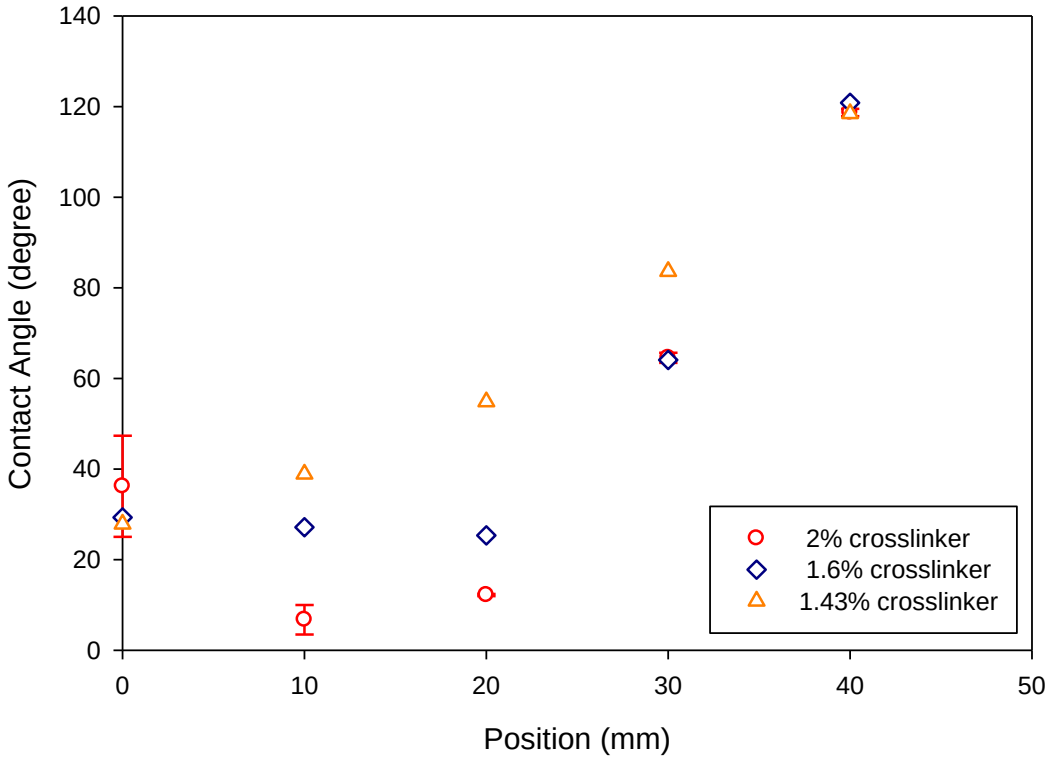

Figure 3.5 SAM gradients on softer PDMS formulations.

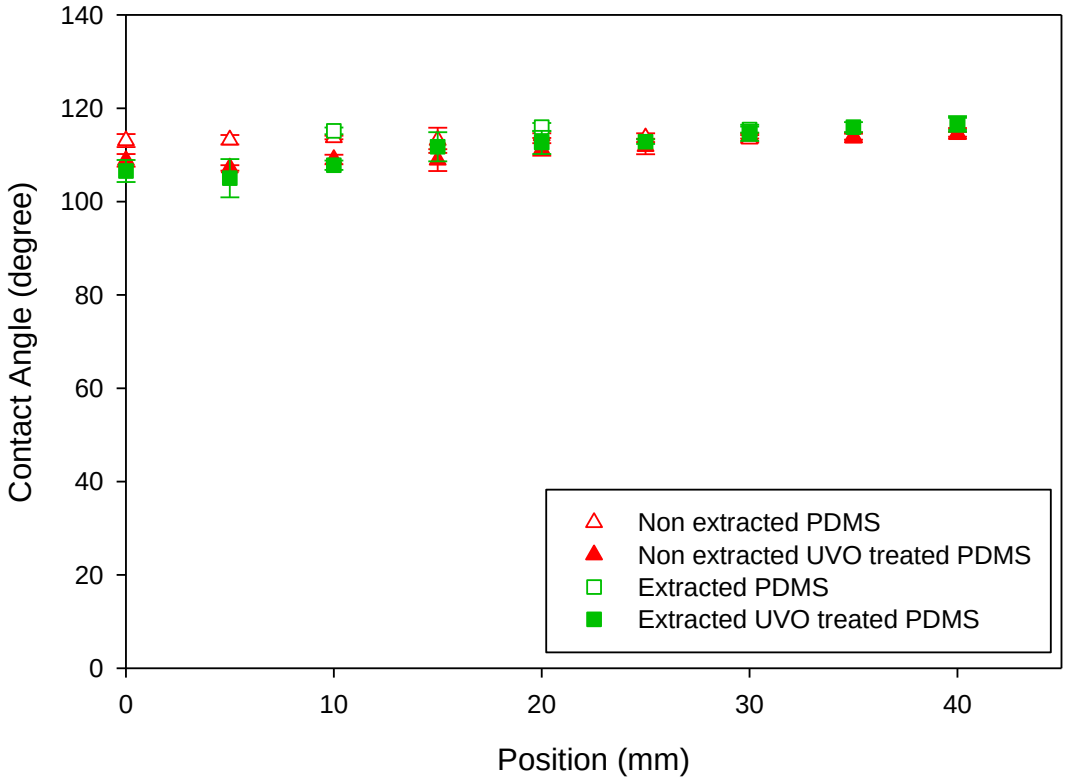

Figure 3.6 UVO treatment of unmodified, non silane deposited PDMS.

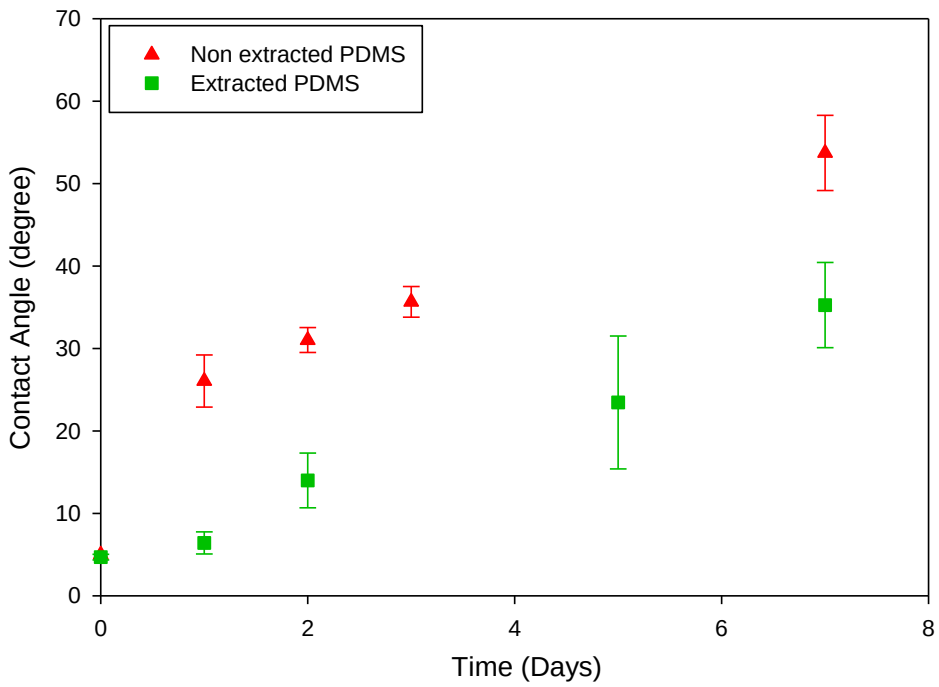

Figure 3.7 Rate of hydrophobic recovery of plasma treated PDMS in extracted and non extracted PDMS.

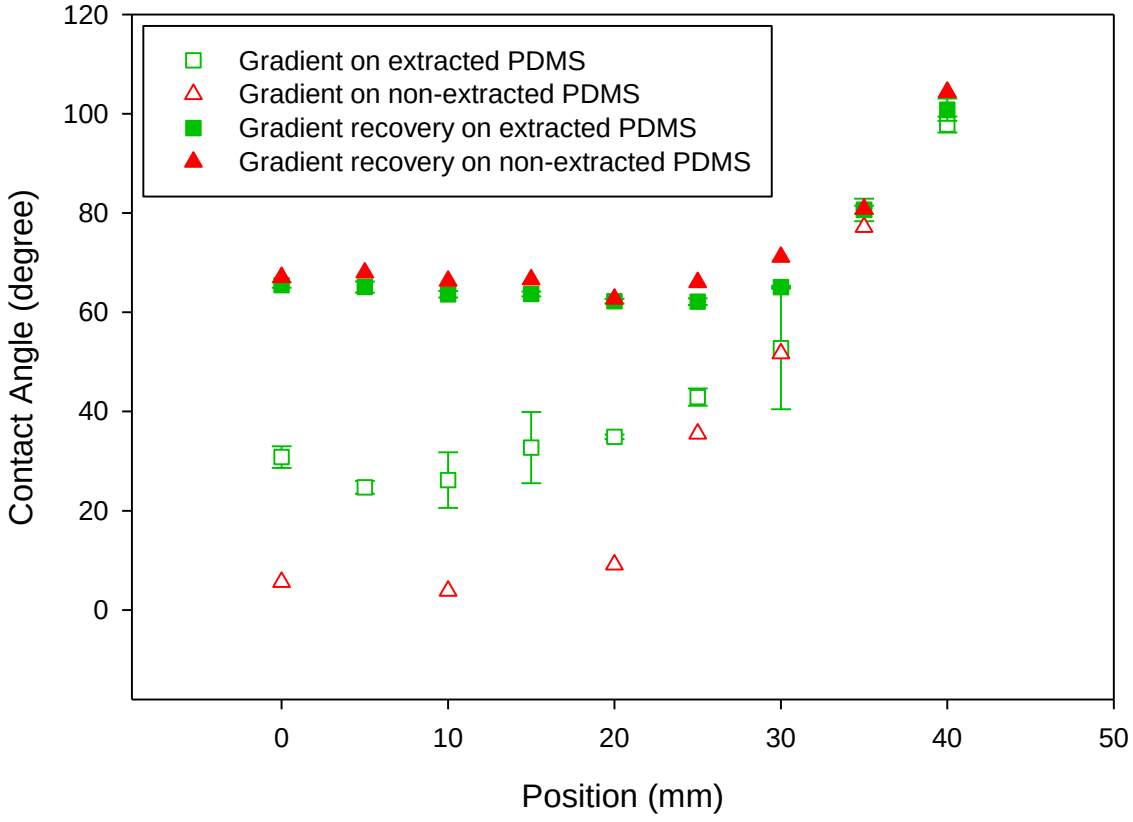

Figure 3.8 Gradient recovery on extracted vs non extracted PDMS.

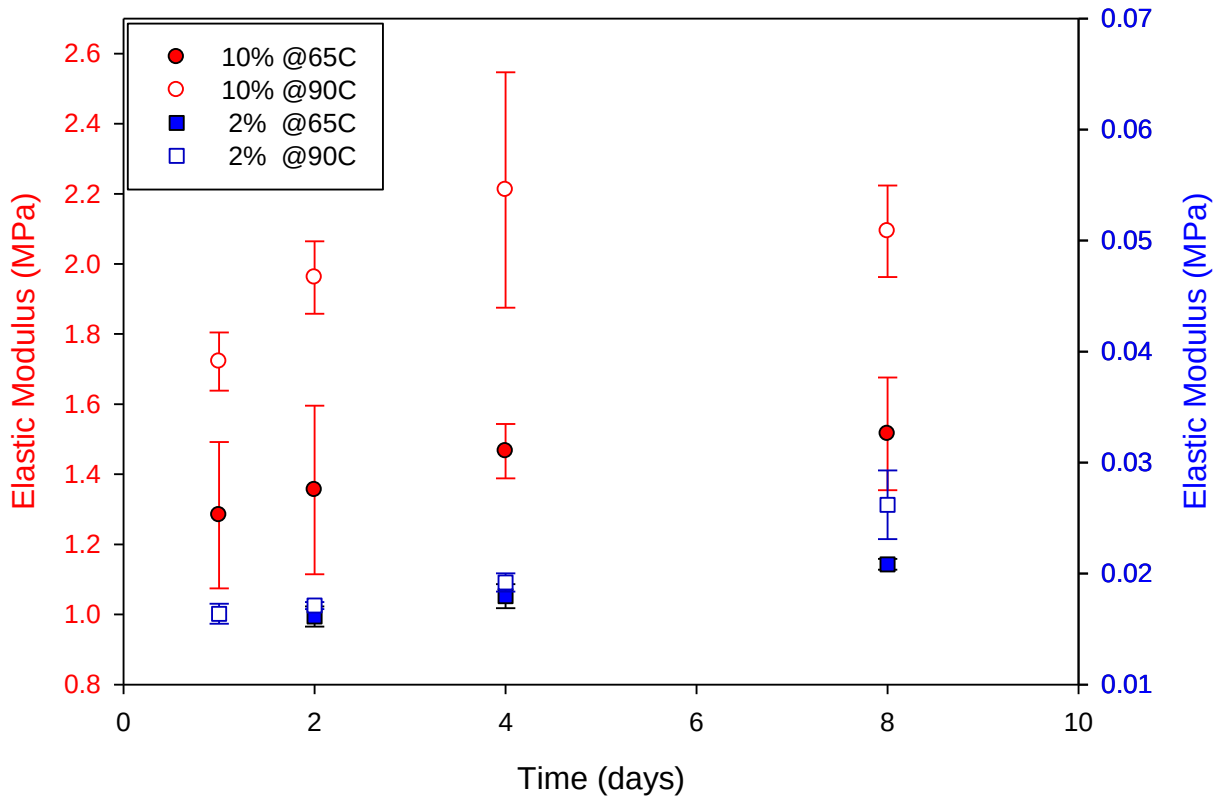

Figure 3.9 Effect of curing conditions on elastic modulus of PDMS.

3.5 References

Almutairi, Zeyad, Carolyn L. Ren, and Leonardo Simon. 2012. Evaluation of polydimethylsiloxane (PDMS) surface modification approaches for microfluidic applications. *Colloids and Surfaces A: Physicochemical and Engineering Aspects* 415 (0):406-412.

Arkles, Barry. 2006. Hydrophobicity, Hydrophilicity and Silane Surface Modification. Morrisville, PA: Gelest, Inc.

Beltran, Arnel B., Grace M. Nisola, Eulsaeng Cho, Erli Eros D. Lee, and Wook-Jin Chung. 2011. Organosilane modified silica/polydimethylsiloxane mixed matrix membranes for enhanced propylene/nitrogen separation. *Applied Surface Science* 258 (1):337-345.

Bhagat, Ali Asgar S., Preetha Jothimuthu, and Ian Papautsky. 2007. Photodefinable polydimethylsiloxane (PDMS) for rapid lab-on-a-chip prototyping. *Lab on a Chip* 7 (9):1192-1197.

Brown, Xin Q, Keiko Ookawa, and Joyce Y Wong. 2005. Evaluation of polydimethylsiloxane scaffolds with physiologically-relevant elastic moduli: interplay of substrate mechanics and surface chemistry effects on vascular smooth muscle cell response. *Biomaterials* 26 (16):3123-3129.

Candiello, Joseph, Manimalha Balasubramani, Emmanuel M. Schreiber, Gregory J. Cole, Ulrike Mayer, Willi Halfter, and Hai Lin. 2007. Biomechanical properties of native basement membranes. *FEBS Journal* 274 (11):2897-2908.

Chruściel, Jerzy J., and Elżbieta Leśniak. 2014. Modification of epoxy resins with functional silanes, polysiloxanes, silsesquioxanes, silica and silicates. *Progress in Polymer Science* (0).

Efimenko, Kirill, William E. Wallace, and Jan Genzer. 2002. Surface Modification of Sylgard-184 Poly(dimethyl siloxane) Networks by Ultraviolet and Ultraviolet/Ozone Treatment. *Journal of Colloid and Interface Science* 254 (2):306-315.

Evaraert, Emmannuel P., Henny C. Van Der Mei, and Henk J Busscher. 1996. Hydrophobic recovery of repeatedly plasma-treated silicone rubber. Part 2 A comparison of the hydophobic recovery in air,water,or liq.N2. *J. Adhesion Sci Technol. Vol. 10, No.4, pp 351-359* 10 (4):351-359.

Everaert, E P, H C Van der Mei, J De Vries, and H J Busscher. 1995. Hydrophobic recovery of repeatedly plasma-treated silicone rubber. Part 1. Storage in air. *Journal of Adhesion Science & Technology* 9 (9):1263-1278.

Fuard, D., T. Tzvetkova-Chevolleau, S. Decossas, P. Tracqui, and P. Schiavone. 2008. Optimization of poly-di-methyl-siloxane (PDMS) substrates for studying cellular adhesion and motility. *Microelectronic Engineering* 85 (5–6):1289-1293.

Gallant, N. D, K. A Lavery, E. J Amis, and M. L Becker. 2007. Universal Gradient Substrates for "Click" Biofunctionalization. *Advanced Materials* 19 (7):965-969.

Hemmilä, Samu, Juan V. Cauich-Rodríguez, Joose Kreutzer, and Pasi Kallio. 2012. Rapid, simple, and cost-effective treatments to achieve long-term hydrophilic PDMS surfaces. *Applied Surface Science* 258 (24):9864-9875.

Hong, Hun-Gi, and Wonchoul Park. 2005. A study of adsorption kinetics and thermodynamics of ω-mercaptoalkylhydroquinone self-assembled monolayer on a gold electrode. *Electrochimica Acta* 51 (4):579-587.

Hussain, Yazan, Jacqueline Krim, and Christine Grant. 2005. OTS adsorption: A dynamic QCM study. *Colloids and Surfaces A: Physicochemical and Engineering Aspects* 262 (1–3):81-86.

Jo, Kyungmin, Hua-Zhong Yu, and Haesik Yang. 2011. Formation kinetics and stability of phosphonate self-assembled monolayers on indium–tin oxide. *Electrochimica Acta* 56 (13):4828-4833.

Jo, Myeong Chan, and Rasim Guldiken. 2014. Effects of polydimethylsiloxane (PDMS) microchannels on surface acoustic wave-based microfluidic devices. *Microelectronic Engineering* 113 (0):98-104.

Karakoy, Mert, Evin Gultepe, Shivendra Pandey, Mouen A. Khashab, and David H. Gracias. 2014. Silane surface modification for improved bioadhesion of esophageal stents. *Applied Surface Science* 311 (0):684-689.

Kennedy, Scott B., Newell R. Washburn, Carl George Simon Jr, and Eric J. Amis. 2006. Combinatorial screen of the effect of surface energy on fibronectin-mediated osteoblast adhesion, spreading and proliferation. *Biomaterials* 27 (20):3817-3824.

Kulkarni, Sneha A., S. A. Mirji, A. B. Mandale, R. P. Gupta, and Kunjukrishna P. Vijayamohanan. 2005. Growth kinetics and thermodynamic stability of octadecyltrichlorosilane self-assembled monolayer on Si (100) substrate. *Materials Letters* 59 (29–30):3890-3895.

Lee, Jessamine Ng, Cheolmin Park, and George M. Whitesides. 2003. Solvent Compatibility of Poly(dimethylsiloxane)-Based Microfluidic Devices. *Analytical Chemistry* 75 (23):6544-6554.

Maji, Debashis, S. K. Lahiri, and Soumen Das. 2012. Study of hydrophilicity and stability of chemically modified PDMS surface using piranha and KOH solution. *Surface and Interface Analysis* 44 (1):62-69.

Mata, Alvaro, Aaron Fleischman, and Shuvo Roy. 2005. Characterization of Polydimethylsiloxane (PDMS) Properties for Biomedical Micro/Nanosystems. *Biomedical Microdevices* 7 (4):281-293.

Ogieglo, Wojciech, Hans van der Werf, Kristianne Tempelman, Herbert Wormeester, Matthias Wessling, Arian Nijmeijer, and Nieck E. Benes. 2013. n-Hexane induced swelling of thin PDMS films under non-equilibrium nanofiltration permeation conditions, resolved by spectroscopic ellipsometry. *Journal of Membrane Science* 431 (0):233-243.

Pelham, Robert J, and Yu-li Wang. 1997. Cell locomotion and focal adhesions are regulated by substrate flexibility. *Proceedings of the National Academy of Sciences* 94 (25):13661-13665.

Roberson, Sonya V., Albert J. Fahey, Amit Sehgal, and Alamgir Karim. 2002. Multifunctional ToF-SIMS: combinatorial mapping of gradient energy substrates. *Applied Surface Science* 200 (1“4):150-164.

Tzvetkova-Chevolleau, Tzvetelina, Angélique Stéphanou, David Fuard, Jacques Ohayon, Patrick Schiavone, and Philippe Tracqui. 2008. The motility of normal and cancer cells in response to the combined influence of the substrate rigidity and anisotropic microstructure. *Biomaterials* 29 (10):1541-1551.

Vickers, Jonathan A., Meghan M. Caulum, and Charles S. Henry. 2006. Generation of Hydrophilic Poly(dimethylsiloxane) for High-Performance Microchip Electrophoresis. *Analytical Chemistry* 78 (21):7446-7452.

Wang, Lin, Bing Sun, Katherine S. Ziemer, Gilda A. Barabino, and Rebecca L. Carrier. 2010. Chemical and physical modifications to poly(dimethylsiloxane) surfaces affect adhesion of Caco-2 cells. *Journal of Biomedical Materials Research Part A* 93A (4):1260-1271.

Wang, Peng-Yuan, Wei-Bor Tsai, and Nicolas H. Voelcker. 2012. Screening of rat mesenchymal stem cell behaviour on polydimethylsiloxane stiffness gradients. *Acta Biomaterialia* 8 (2):519-530.

Wheeler, Aaron R., Soonwoo Chah, Rebecca J. Whelan, and Richard N. Zare. 2004. Poly(dimethylsiloxane) microfluidic flow cells for surface plasmon resonance spectroscopy. *Sensors and Actuators B: Chemical* 98 (2–3):208-214.

Wong, Joyce Y., Jennie B. Leach, and Xin Q. Brown. 2004. Balance of chemistry, topography, and mechanics at the cell-biomaterial interface: Issues and challenges for assessing the role of substrate mechanics on cell response. *Surface Science* 570:119-133.

Xia, Younan, and George M. Whitesides. 1998. Soft Lithography. *Angewandte Chemie International Edition* 37 (5):550-575.

Zhao, Li Hong, Jennifer Lee, and Pabitra N. Sen. 2012. Long-term retention of hydrophilic behavior of plasma treated polydimethylsiloxane (PDMS) surfaces stored under water and Luria-Bertani broth. *Sensors and Actuators A: Physical* 181 (0):33-42.

Zhou, Jinwen, Amanda Vera Ellis, and Nicolas Hans Voelcker. 2010. Recent developments in PDMS surface modification for microfluidic devices. *Electrophoresis* 31 (1):2-16.

CHAPTER 4

SURFACE CHEMISTRY GRADIENT FORMULATION ON CROSS-LINKED PDMS NETWORKS

4.1 Note to Reader

Contents in this chapter have been published in the Journal of Biomedical Materials Research Part A, 2014. The Permission is included in Appendix A.

4.2 Introduction

A comprehensive understanding of cell-substrate interactions is imperative for the advancement of functional biomaterials. The effectiveness of materials at biological interfaces depends on, among many other aspects, the optimization of properties that can instruct cells to perform desired functions (Griffith and Naughton 2002). However, cell fate decisions are the consequence of extremely complex networks of events that depend on a multitude of factors present in a cell's microenvironment. Some of these, including biochemical signals (e.g. concentration of a growth factor, protein conformation), mechanical signals (e.g. rigidity of basement matrix) and biophysical cues (e.g. curvature, ridges on surface), can be incorporated into biomaterials that mimic native microenvironments (Nikkhah et al. 2012; Wong, Leach, and Brown 2004; Rape, Guo, and Wang 2011; Shekaran and Garcia 2011; Smeal et al. 2005).

Factors that influence cellular response are both numerous and complex. High throughput combinatorial platforms that allow rapid, broad spectrum analysis of the effect of physical, biological, chemical and mechanical properties provide several advantages for testing these responses. Such screening techniques, when available, are more efficient and effective than individual testing of parameters (Yliperttula et al. 2008; Moraes et al. 2010; Mei, Goldberg, and Anderson 2007). In this approach, detailed studies can be focused on positive hits identified from a large screening field of variables, or an optimal blend of multiple variables for a certain biomedical application may be identified (Hook et al. 2010; Neuss et al. 2008).

Surface wettabilities of biomaterials are an important parameter of biocompatibility. The interaction of plasma with surface of materials contributes to kind and quantity of protein adsorption and long term effect on cell functionality (Simon and Lin-Gibson 2011; Anderson, Rodriguez, and Chang 2008; Liu et al. 2007). Varying wettablities on soft substrates by Corona discharge from electrode has been shown to produce a gradient in surface wettabilities on Polyethylene (Lee et al. 2000; Lee et al. 1998). Plasma polymerization of dimethyl ether on coverslips and Si wafer coated with acrylic acid with use of a mask has been done to obtain surface chemistry gradients to study stem cell response (Harding et al. 2012). Surface chemistry gradients have been generated by controlled oxidation of a hydrophobic silane monolayer on conventional surfaces like glass and silicon wafers before (Roberson et al. 2002; Gallant et al. 2007; Kennedy et al. 2006). In this study, we fabricated surface chemistry gradients atop polydimethylsiloxane (PDMS), a silicone elastomer widely used in medical implants and other biomedical applications. PDMS was chosen as the model biomaterial for its ease of use and its amenability to surface modification. We successfully modified PDMS surfaces via silanization followed by spatially

controlled oxidation, which has been exploited in this study for constructing a surface chemistry gradient on this "soft" material.

4.3 Experimental Section

- Elastic biomaterial substrates

PDMS, a silicone elastomer, was used in this study as a biomaterial with "tissue-like" stiffness (Palchesko RN et al. 2012). Cross-linked networks of PDMS were prepared by mixing the precursor base and curing agent components (Sylgard 184; Dow Corning, Midland, MI) thoroughly in a 10:1 mass ratio and then degassing to remove air bubbles. 0.9 ml was dispensed onto a plasma cleaned 25x75 mm glass slide using a 1 ml syringe and cured overnight at 65 °C to obtain a 0.5 mm thick layer of PDMS on the supporting slide. Mechanical testing of PDMS strips was done according to the tensile test method described by Pelham and Wang to estimate its elastic modulus (Pelham and Wang 1997).

- Surface chemistry gradient fabrication

Gradients in surface chemistry were generated on glass slides according to the original procedure described and characterized by Roberson et al (Roberson et al. 2002). which has been used to investigate several cell-biomaterial interactions on rigid surfaces (Acharya et al. 2010; Gallant et al. 2007; Kennedy et al. 2006; Moore et al. 2010, 2011). Here this procedure was also adapted to fabricate similar gradients on PDMS. Although surface gradients have been generated on glass slides and silicon wafers previously, to our knowledge this is the first time they have been produced on PDMS, a material with elastic modulus of ~1.8 MPa or less (Brown, Ookawa, and Wong 2005).

Gradients on glass were also included in the experimental design to provide a direct comparison to previously published studies.

The fabrication process is illustrated in Figure 4.1. Briefly, plain glass slides or PDMS substrates were sonicated for 15 minutes in 75% ethanol and then vacuum dried in a desiccator. The dry samples were oxidized using a plasma cleaner (Plasma Etch PE-50, Carson City, NV) at 100 watts for 5 minutes to render the sample surfaces hydrophilic and conducive to silane functionalization. Chemical vapor deposition was used to modify the surfaces with a hydrophobic self-assembled monolayer (SAM) of chlorodimethyloctylsilane (ODMS) (Sigma-Aldrich). Glass and PDMS substrates were placed under vacuum for 24 hours in a glass desiccator that contained ODMS and toluene mixed in a 1:1 ratio, followed by rinsing with 70% ethanol and baking for one and half hours at 65 °C to drive out residual solvent and volatile species.

The alkylsilane monolayers were then spatially modified in a tightly regulated manner that created monotonically varying gradients of surface chemistry (Gallant et al. 2007). The samples were placed on an accelerating linear motion stage (Aerotech, Inc., Pittsburgh, PA) to undergo ultraviolet ozone (UVO) oxidation beneath a stationary low pressure Mercury (Hg) vapor lamp with a fused silica envelope (part #84-285-7, Jelight, Irvine, CA) enclosed in an aluminum casing. This UV wand lamp had a primary emission at 254 nm and a secondary emission at 185 nm. The UV light impinged on the substrate surfaces through a 2 mm wide aperture that ran along the length of the casing. The hydrophobic alkylsilane SAM was subjected to dose dependent ozonolysis from the UV lamp which generated oxygen containing species including, predominantly, carboxyl terminal groups (Kennedy et al. 2006; Roberson et al. 2002). The rate of stage motion, and

therefore the residence time of each position under the UV light, was controlled by a custom LabVIEW user interface. The stage advanced in 0.1 mm steps and was accelerated by decreasing the dwell time at each step. The result was a linear variation in exposure time over the length of the sample. The maximum UVO exposure occurred at the starting end and the exposure dose decreased over the length of the sample to zero exposure. The resulting hydrophobicity/COOH gradient correlated with the linear UVO exposure profile of the surface. Maximum exposure times of 300 s and 100 s were required on the PDMS and glass surfaces, respectively, to obtain similar hydrophobicity gradients. Accelerating exposure altered the surface over 4 cm, while a 1 cm zone with no UVO treatment served as the internal control for each sample.

- Characterization of surface chemistry gradients

Gradients fabricated by this procedure have been previously characterized with static and advancing water contact angle measurements to quantify surface energy and time-of-flight secondary ion mass spectrometry (ToF-SIMS) to analyze composition (Acharya et al. 2010; Gallant et al. 2007; Kennedy et al. 2006; Moore et al. 2010, 2011; Roberson et al. 2002). Hydrophobicity was characterized via static water contact angle goniometry with a CAM101 (KSV Instruments, Monroe, CT) and surface elemental composition was analyzed by x-ray photoelectron spectroscopy (XPS) with a PHI 5000 Versa Probe II (ULVAC-PHI, Inc.). Readings were taken every 5 mm along the entire length of gradient substrates for both characterization procedures.

For goniometry readings, the contact angle between the droplet and surface was estimated by the Young-Laplace fitting algorithm available in the CAM software. The presence of a homogenous

surface chemistry on substrates was confirmed by consistent water contact angle measurements along length of alkylsilane coated samples prior to the UVO exposure. Gradients in surface chemistry produced on substrates were similarly characterized through spatially resolved contact angle measurements. Surface modifications on PDMS are typically short lived due to the migration of lurking polymeric chains from the bulk material to surface (Brown, Ookawa, and Wong 2005; Evaraert, Mei, and Busscher 1996; Everaert et al. 1995). Hydrophobic recovery was quantified on N=4 gradient substrates characterized repeatedly at specific time points (Figure 4.2). This inherent hydrophobic recovery in PDMS necessitated immersion of gradient substrates in deionized H_2O before use (Figure 4.3) (Mata, Fleischman, and Roy 2005). Submerged gradients on glass and PDMS were used for subsequent experiments within 24 hours of fabrication. Hydrophobicity for cell adhesion samples was analyzed for four independent experiments (N=4) with two to six replicates in a single independent experiment for each of the treatment groups (Figure 4.5).

XPS measurements were performed using a PHI 5000 Versa Probe II spectrometer at the University of Florida Major Analytical Instrumentation Center. The x-ray source employed was monochromated aluminum, scanning over a binding energy range of 0 eV to 1100 eV with a dwell time of 20 ms. Each spectrum was collected over a 200 μm diameter sample area. The survey spectra were collected at each position with an analyzer pass energy of 93.9 eV, and the relative concentrations of O, C, and Si were obtained from the O 1s (532.5 eV), C 1s (285.0 eV), Si 2p (103.0 eV) peaks using a pass energy of 23.5 eV and 10 sweeps of 0.1 eV per step. Prior to XPS analysis, samples were Soxhlet extracted in ethanol (190 proof) for 48 hours before UVO exposure to remove volatile species that could interfere with achieving ultra-low vacuum operation.

The ratio of oxygen content on UVO-exposed surfaces to control no-UVO samples was quantified after the oxygen values were normalized to silicon for each specific position of the gradient. Controls consisted of uniform alkylsilane-coated PDMS in addition to the 40 mm positions of each gradient sample surface, which was subjected to zero UVO exposure. XPS data represent N=4 gradients for characterization to supplement data obtained from water contact angle measurements (Figure 4.6) and N=2 gradients for hydrophobic recovery of gradients when expose to ambient air overnight (Figure 4.7). The error bars in all the figures display standard deviation from the mean.

4.4 Results and Discussion

- Surface chemistry gradient fabrication on a "soft" biomaterial

Spatiotemporal UVO exposure of hydrophobic monolayers has previously been used to fabricate surface chemistry gradients on silicon wafers and glass slides (Gallant et al. 2007; Kennedy et al. 2006; Acharya et al. 2010; Moore et al. 2010, 2011; Roberson et al. 2002) and this procedure was modified to generate similar hydrophobicity gradients on flexible cross-linked networks of the silicone elastomer PDMS. The surface modification of PDMS involved oxygen plasma treatment, hydrophobic alkylsilane layer deposition and spatiotemporally regulated UVO exposure to obtain monotonic surface energy gradients (Figure 4.5). Error bars display the standard deviation from the mean among N=4 independent experiments with two to six replicates within each of the treatment group. Consistent with other treatments of PDMS, (Brown, Ookawa, and Wong 2005; Evaraert, Mei, and Busscher 1996; Everaert et al. 1995; Mata, Fleischman, and Roy 2005) this covalently bound and oxidized surface modification layer was short lived as rapid hydrophobic recovery was observed (Figure 4.2). XPS confirmed there was an average 13±4 % drop in surface oxygen from day 1 to day 2 (Figure 4.7, N=2 PDMS gradients). To overcome the challenge of

hydrophobic recovery, submerging the substrates in deionized H_2O (Mata, Fleischman, and Roy 2005) preserved the hydrophobicity gradients for at least 8 days (Figure 4.3). There were N=4 replicates in each treatment group in Figure 4.2 and 4.3 and the error bars show standard deviation from the mean.

After optimizing the gradient preservation and UVO exposure program for PDMS, water contact angle measurements were recorded using sessile drop goniometry before and after UVO treatment of glass and PDMS substrates (Figure 4.5). Gradients were generated on glass substrates to verify the surface gradients on PDMS were equivalent, and also for comparison of cell response on similar surface gradients on soft and stiff materials. Hydrophobic alkylsilane monolayers deposited on glass and PDMS substrates had a surface wettability of approximately 100°. Following UVO exposure, a range of surface wettabilities was obtained on glass and PDMS substrates with contact angles varying from ~10° to ~100° over 40 mm. Interestingly, longer exposure times were required to produce gradients on PDMS that are similar in profile to the gradients on glass. While it took only a 100 s maximum exposure time to render one end of the monolayer maximally hydrophilic on the glass substrates, PDMS substrates required 300 s of UVO exposure to obtain a hydrophilic end comparable to that on a glass slide. The 0 mm position corresponded to maximum UVO exposure which decreased linearly to the minimum (0 s) exposure at 40 mm. A one cm region beyond 40 mm that experienced no UVO exposure served as an internal control for each sample.

In addition to goniometry measurements, PDMS gradient surfaces were also characterized with XPS (Figure 4.6, N=4 PDMS gradients) to quantify oxygen content variation with respect to position on PDMS gradients. XPS analysis taken at 5 mm intervals on PDMS surface gradients

revealed that oxygen concentration was maximum at the hydrophilic end and decreased steadily toward the hydrophobic end. The normalized oxygenation at the hydrophilic end of gradient was 1.19 ± 0.12 compared to 0.97 ± 0.05 at the hydrophobic end of gradient. The relative increase in surface oxygen over no-UVO controls was quantified after the values were normalized to position-specific silicon quantities. This effectively corrected for measurement errors because silicon concentration should theoretically be invariant (Figure 4.6 Inset, N=4 PDMS gradients).

Additionally, native PDMS controls without any surface treatment maintained hydrophobicity (~115° water contact angle) following up to 5 min UVO exposure (results displayed in Chapter 3). This confirmed that the gradient was a result of the UVO oxidation of the alkylsilyl monolayer and not the oxidation of the PDMS surface. From data obtained from XPS characterization of gradients and the inability to obtain gradients on unmodified PDMS, it can be inferred that the surface chemistry profile trends of the PDMS gradients were similar to the gradients fabricated on glass, which have been previously characterized with ToF-SIMS to display linearly increasing concentrations of carboxylic acid spanning ~100 to ~400 pmol/cm^2 (Gallant et al. 2007; Moore et al. 2011).

Versatile combinatorial screening techniques can significantly contribute to a more rapid evolution of functional biomaterials for biomedical applications. We have successfully constructed surface chemistry gradients on PDMS, an elastomeric biomaterial with stiffness in the physiological range of numerous tissues, e.g. wall of aortic arch ~1.0 MPa (Wong, Leach, and Brown 2004; Brown, Ookawa, and Wong 2005). The elastic modulus of 1.55 MPa estimated from tensile testing PDMS is in agreement with the value of 1.78 MPa reported by Brown et al (Brown, Ookawa, and Wong

2005). Surface chemistry gradients were generated by adapting the technique reported by Roberson et al (Roberson et al. 2002) whereby alkylsilane monolayers on SiO_x were spatiotemporally modified by UVO exposure and were characterized through contact angle measurements and ToF-SIMS. The similarities in the structure of glass which is composed of abundant silica and PDMS that has repetitive siloxane units enabled this translation of surface chemistry from one material to the other. In this manner, we were able to generate equivalent gradient materials that varied monotonically in surface chemistry by UVO oxidation of alkysilyl monolayers on PDMS. Surface hydrophobicity spanned a range from ~10° to ~100° in water contact angle which arose from an approximately 23% difference in normalized oxygen content over the length of the gradients. Surface characterization was complicated by the similar compositions of the bulk PDMS and UVO-modified surface layer. However, UVO of bare PDMS (no alkylsilane monolayer) did not result in any significant change in hydrophobicity and confirmed that the variation of surface chemistry occurred in the hydrocarbon surface monolayer. Therefore it was concluded that these gradients had a profile in surface chemistry similar to those generated on alkylsilane-coated glass. The difference in the UVO exposure times required to modify PDMS and glass was perhaps due to the inherent hydrophobicity difference between the underlying bulk material properties: native PDMS is hydrophobic (~115°) while glass is hydrophilic (~25°). It is also possible that a difference in ODMS layer packing density exists between the PDMS and glass substrates. Determining the reason proportionally longer UVO exposure on PDMS was required to generate the same concentration of hydrophilic species (i.e. COOH) is beyond the scope of this study. These gradient materials were employed to gain a better insight into fundamental cell-material interactions, by the high throughput investigation of the morphological response to surface chemistry on a “soft” biomaterial using an automated

fluorescent microscopy system. The findings from cell based experiments are presented in Chapter 5.

4.5 Conclusions

Surface chemistry of alkylsilane monolayers on PDMS can be modified by UVO treatment which was demonstrated for the first time by the fabrication of continuous and monotonically increasing gradients in surface oxidation. The presence of gradients was successfully characterized using goniometric and XPS measurements.

4.6 Acknowledgements

We would like to thank Eric Lambers in the Major Analytical Instrumentation Center at University of Florida for performing XPS analysis and Joel R. Cooper for assistance with programming the Labview interface for gradient exposure automation.

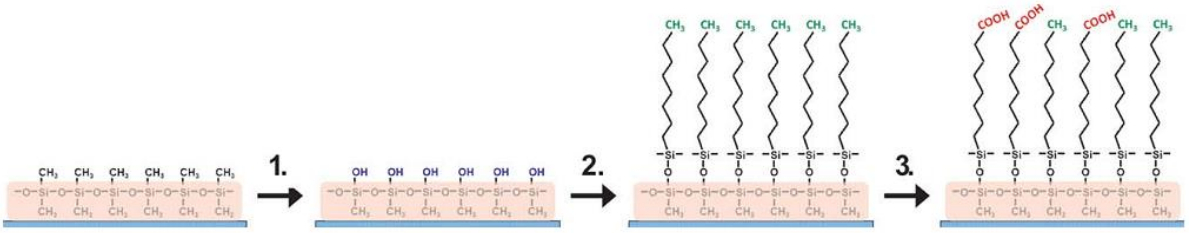

Figure 4.1 Schematic illustration of fabrication of surface chemistry gradients on cross-linked PDMS networks. PDMS samples were (1) oxidized by plasma treatment and then (2) modified with a hydrophobic alkylsilane SAM. (3) The SAM was spatiotemporally exposed to UVO to generate a surface chemistry gradient with oxygenated species increasing with UVO exposure.

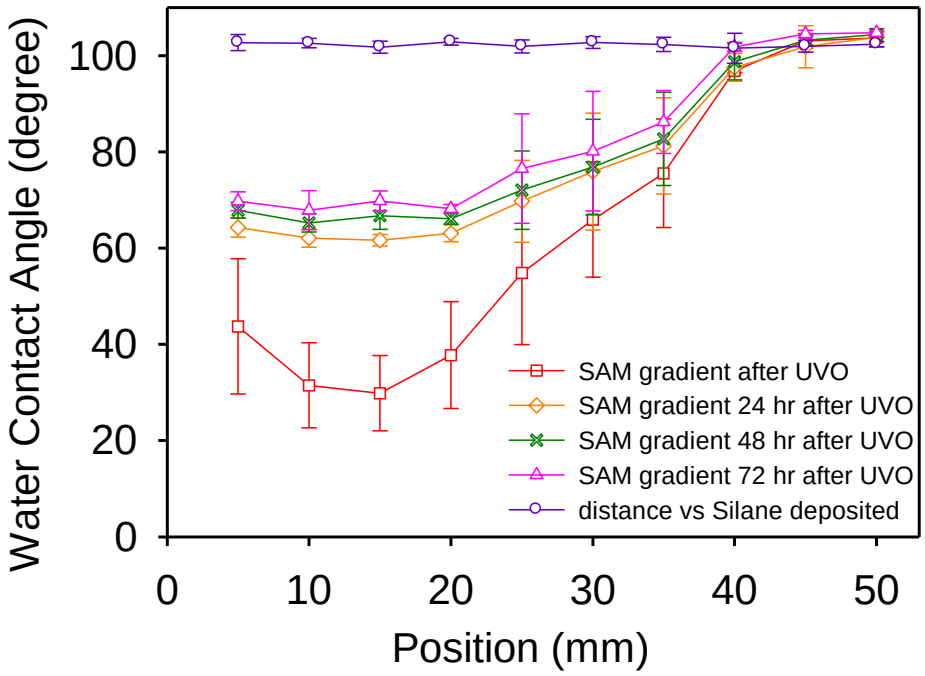

Figure 4.2 Hydrophobic recovery of modified PDMS surfaces. Surface chemistry gradients on PDMS rapidly degraded when stored in ambient atmosphere (N = 4). Time-course data represent repeated measurements on the same samples for each experiment.

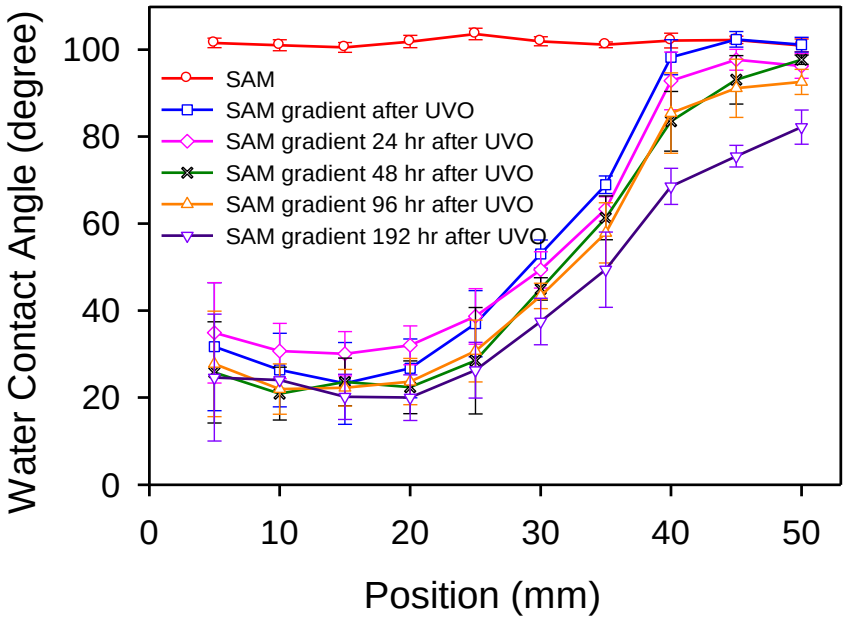

Figure 4.3 Hydrophobic recovery was avoided by water immersion of gradient substrates which preserves the surface chemistry gradients. Hydrophobic recovery was avoided by water immersion of gradient substrates which preserves the surface chemistry gradients (N = 4). Time-course data represent repeated measurements on the same samples for each experiment.

Figure 4.4 Photograph of spreading water droplet profiles along PDMS surface gradient. The spreading of water drops on PDMS and glass surface gradients indicate the variation of the SAM chemistry induced by spatiotemporal UVO exposure.

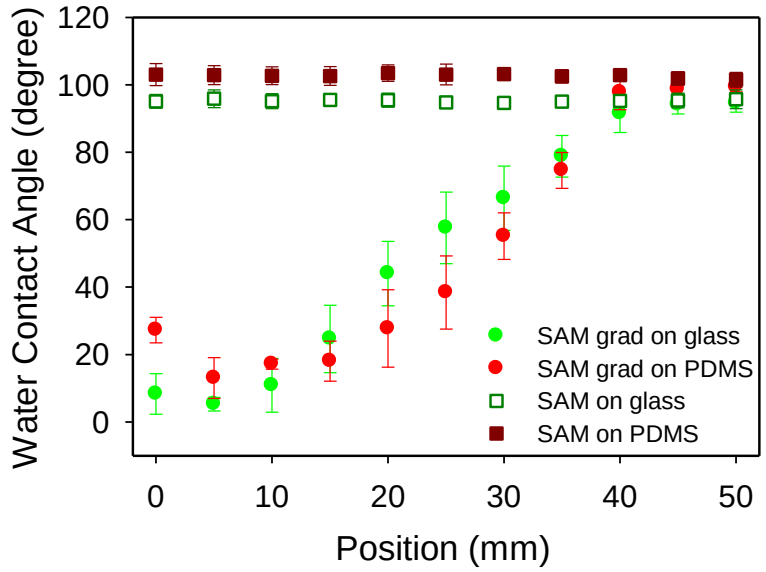

Figure 4.5 Contact angle measurements along glass and PDMS substrates before and after UVO. The measurements show the transformation from a uniform hydrophobic surface chemistry to a gradient on both PDMS and glass substrates. Data were obtained from N = 4 independent experiments with two to six replicates in each experiment.

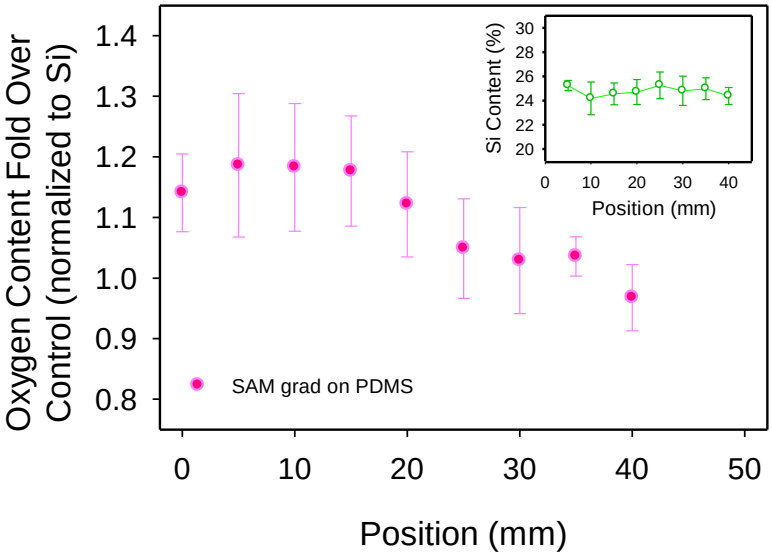

Figure 4.6 Surface oxygen concentration (relative to uniform controls and normalized to silicon) decreased with UVO exposure (N=4). Inset: Atomic fraction of silicon on gradient surface.

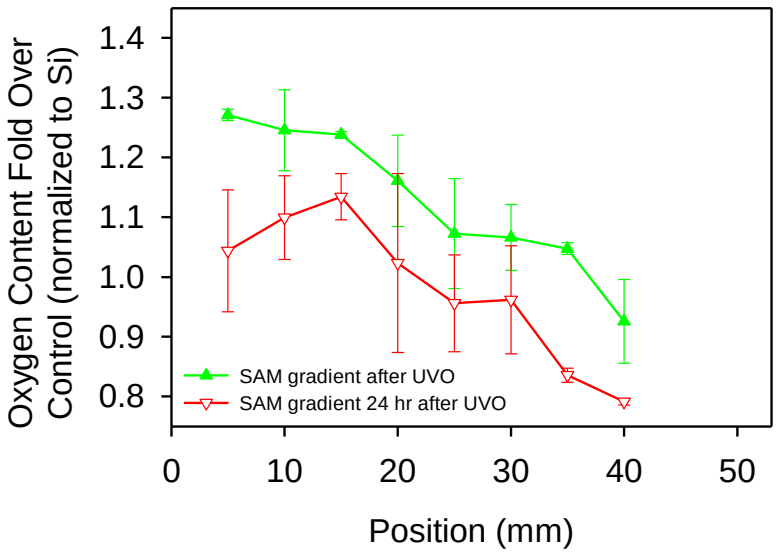

Figure 4.7 Surface oxygen concentration (relative to uniform controls and normalized to silicon) decreased over 24 h ambient atmosphere. Inset: Atomic fraction of silicon on gradient surface. Time-course data represent repeated measurements on the same samples for each experiment.

4.7 References

Acharya, Abhinav P., Natalia V. Dolgova, Nicole M. Moore, Chang-Qing Xia, Michael J. Clare-Salzler, Matthew L. Becker, Nathan D. Gallant, and Benjamin G. Keselowsky. 2010. The modulation of dendritic cell integrin binding and activation by RGD-peptide density gradient substrates. *Biomaterials* 31 (29):7444-7454.

Anderson, J M., A Rodriguez, and D T. Chang. 2008. Foreign Body Reaction to Biomaterials. *Seminars in immunology* 20 (2):86-100.

Brown, Xin Q, Keiko Ookawa, and Joyce Y Wong. 2005. Evaluation of polydimethylsiloxane scaffolds with physiologically-relevant elastic moduli: interplay of substrate mechanics and surface chemistry effects on vascular smooth muscle cell response. *Biomaterials* 26 (16):3123-3129.

Evaraert, Emmannuel P., Henny C. Van Der Mei, and Henk J Busscher. 1996. Hydrophobic recovery of repeatedly plasma-treated silicone rubber. Part 2 A comparison of the hydophobic recovery in air,water,or liq.N2. *J. Adhesion Sci Technol. Vol. 10, No.4, pp 351-359* 10 (4):351-359.

Everaert, E P, H C Van der Mei, J De Vries, and H J Busscher. 1995. Hydrophobic recovery of repeatedly plasma-treated silicone rubber. Part 1. Storage in air. *Journal of Adhesion Science & Technology* 9 (9):1263-1278.

Gallant, N. D, K. A Lavery, E. J Amis, and M. L Becker. 2007. Universal Gradient Substrates for "Click" Biofunctionalization. *Advanced Materials* 19 (7):965-969.

Griffith, Linda G., and Gail Naughton. 2002. Tissue Engineering--Current Challenges and Expanding Opportunities. *Science* 295 (5557):1009-1014.

Harding, Frances J., Lauren R. Clements, Robert D. Short, Helmut Thissen, and Nicolas H. Voelcker. 2012. Assessing embryonic stem cell response to surface chemistry using plasma polymer gradients. *Acta Biomaterialia* 8 (5):1739-1748.

Hook, Andrew L., Daniel G. Anderson, Robert Langer, Paul Williams, Martyn C. Davies, and Morgan R. Alexander. 2010. High throughput methods applied in biomaterial development and discovery. *Biomaterials* 31 (2):187-198.

Kennedy, Scott B., Newell R. Washburn, Carl George Simon Jr, and Eric J. Amis. 2006. Combinatorial screen of the effect of surface energy on fibronectin-mediated osteoblast adhesion, spreading and proliferation. *Biomaterials* 27 (20):3817-3824.

Lee, Jin Ho, Gilson Khang, Jin Whan Lee, and Hai Bang Lee. 1998. Interaction of Different Types of Cells on Polymer Surfaces with Wettability Gradient. *Journal of Colloid and Interface Science* 205 (2):323-330.

Lee, Jin Ho, Sang Jin Lee, Gilson Khang, and Hai Bang Lee. 2000. The Effect of Fluid Shear Stress on Endothelial Cell Adhesiveness to Polymer Surfaces with Wettability Gradient. *Journal of Colloid and Interface Science* 230 (1):84-90.

Liu, Xiaomei, Jung Yul Lim, Henry J. Donahue, Ravi Dhurjati, Andrea M. Mastro, and Erwin A. Vogler. 2007. Influence of substratum surface chemistry/energy and topography on the human fetal osteoblastic cell line hFOB 1.19: Phenotypic and genotypic responses observed in vitro. *Biomaterials* 28 (31):4535-4550.

Mata, Alvaro, Aaron Fleischman, and Shuvo Roy. 2005. Characterization of Polydimethylsiloxane (PDMS) Properties for Biomedical Micro/Nanosystems. *Biomedical Microdevices* 7 (4):281-293.

Mei, Ying, Michael Goldberg, and Daniel Anderson. 2007. The development of high-throughput screening approaches for stem cell engineering. *Current Opinion in Chemical Biology* 11 (4):388-393.

Moore, Nicole M., Nancy J. Lin, Nathan D. Gallant, and Matthew L. Becker. 2010. The use of immobilized osteogenic growth peptide on gradient substrates synthesized via click chemistry to enhance MC3T3-E1 osteoblast proliferation. *Biomaterials* 31 (7):1604-1611.

Moore, Nicole M., Nancy J. Lin, Nathan D. Gallant, and Matthew L. Becker. 2011. Synergistic enhancement of human bone marrow stromal cell proliferation and osteogenic differentiation on BMP-2-derived and RGD peptide concentration gradients. *Acta Biomaterialia* 7 (5):2091-2100.

Moraes, Christopher, GongHao Wang, Yu Sun, and Craig A. Simmons. 2010. A microfabricated platform for high-throughput unconfined compression of micropatterned biomaterial arrays. *Biomaterials* 31 (3):577-584.

Neuss, Sabine, Christian Apel, Patricia Buttler, Bernd Denecke, Anandhan Dhanasingh, Xiaolei Ding, Dirk Grafahrend, Andreas Groger, Karsten Hemmrich, Alexander Herr, Willi Jahnen-Dechent, Svetlana Mastitskaya, Alberto Perez-Bouza, Stephanie Rosewick, Jochen Salber, Michael Waltje, and Martin Zenke. 2008. Assessment of stem cell/biomaterial combinations for stem cell-based tissue engineering. *Biomaterials* 29 (3):302-313.

Nikkhah, Mehdi, Faramarz Edalat, Sam Manoucheri, and Ali Khademhosseini. 2012. Engineering microscale topographies to control the cell-substrate interface. *Biomaterials* 33 (21):5230-5246.

Palchesko RN, Zhang L, Sun Y, and Feinberg AW. 2012. Development of Polydimethylsiloxane Substrates with Tunable Elastic Modulus to Study Cell Mechanobiology in Muscle and Nerve. *PLoS ONE* 7 ((12): e51499. doi:10.1371/journal.pone.0051499).

Pelham, Robert J, and Yu-li Wang. 1997. Cell locomotion and focal adhesions are regulated by substrate flexibility. *Proceedings of the National Academy of Sciences* 94 (25):13661-13665.

Rape, Andrew D., Wei-hui Guo, and Yu-li Wang. 2011. The regulation of traction force in relation to cell shape and focal adhesions. *Biomaterials* 32 (8):2043-2051.

Roberson, Sonya V., Albert J. Fahey, Amit Sehgal, and Alamgir Karim. 2002. Multifunctional ToF-SIMS: combinatorial mapping of gradient energy substrates. *Applied Surface Science* 200 (1):150-164.

Shekaran, Asha, and Andres J. Garcia. 2011. Nanoscale engineering of extracellular matrix-mimetic bioadhesive surfaces and implants for tissue engineering. *Biochimica et Biophysica Acta (BBA) - General Subjects* 1810 (3):350-360.

Simon, Carl G., and Sheng Lin-Gibson. 2011. Combinatorial and High-Throughput Screening of Biomaterials. *Advanced Materials* 23 (3):369-387.

Smeal, RoyM, Richard Rabbitt, Roy Biran, and PatrickA Tresco. 2005. Substrate Curvature Influences the Direction of Nerve Outgrowth. *Annals of Biomedical Engineering* 33 (3):376-382.

Wong, Joyce Y., Jennie B. Leach, and Xin Q. Brown. 2004. Balance of chemistry, topography, and mechanics at the cell-biomaterial interface: Issues and challenges for assessing the role of substrate mechanics on cell response. *Surface Science* 570:119-133.

Yliperttula, Marjo, Bong Geun Chung, Akshay Navaladi, Amir Manbachi, and Arto Urtti. 2008. High-throughput screening of cell responses to biomaterials. *European Journal of Pharmaceutical Sciences* 35 (3):151-160.

CHAPTER 5

CELL RESPONSES TO SURFACE CHEMISTRY GRADIENTS AND THE SIGNIFICANCE OF THE PROTEIN ADHESIVE INTERFACE

5.1 Note to Reader

Parts of this chapter have been published in the Journal of Biomedical Materials Research Part A, 2014. The Permission is included in Appendix A.

5.2 Introduction

High-throughput and combinatorial approaches developed previously for pharmaceutics and material science are now finding applications in synthesis of biomaterials and screening cell-material interactions. Both combinatorial material microarrays and gradient materials have demonstrated potential for optimization of cell microenvironments for cell adhesion, proliferation and differentiation (Yliperttula et al. 2008). For instance, Anderson et al. (Anderson, Levenberg, and Langer 2004) screened embryonic stem cell attachment and spreading and other cell-material interactions with an array of more than 1700 polymeric materials. In another example, a gradient approach for immunomodulation was demonstrated by Acharya et al (Acharya et al. 2010) who performed a systematic characterization of dendritic cell adhesion and activation on arginine-glycine-aspartic acid (RGD) peptide density gradients.

Surface properties of biomaterials, including the extracellular matrix mimicking parameters described earlier, have shown to be key modulators of cell functionality. Adsorbed proteins or tethered biomolecules form the interfacial adhesive layer that cells interact with primarily using specialized receptors called integrins (García 2005; Hynes 2002). Therefore, the biomaterial surface properties and how they modulate the structural and functional characteristics of adsorbed proteins have been shown to have a predominant role in regulating cell behavior (Garcia, Vega, and Boettiger 1999; Lan et al. 2005; Michael et al. 2003). Fibronectin is one such important protein which is found in soluble form in blood and insoluble form in stromal connective tissues and basement membranes (Mosher and Furcht 1981; Ruoslahti 1988). Integrin receptors recognize and bind specifically to adhesion motifs with specific sequences of amino acids such as the RGD tripeptide found in numerous extracellular matrix proteins including fibronectin, laminin, and vitronectin (Hernandez et al. 2007; Elineni and Gallant 2011). Differential binding of integrins is caused by structural and functional changes to the ligand upon adsorption (e.g. $\alpha_5\beta_1$ specific binding to adsorbed fibronectin) and results in tight regulation of cell functions such as adhesion, differentiation and proliferation (Michael et al. 2003; Iuliano, Saavedra, and Truskey 1993; Lan et al. 2005; Garcia, Vega, and Boettiger 1999). For instance, Keselowsky et al (Keselowsky, Collard, and Garcia 2005; Keselowsky, Collard, and García 2003) showed that surfaces with different chemistries induce differences in fibronectin adsorption and conformation which influence initial osteoblast cell adhesion and have different capacities to mature osteoblasts and up-regulate matrix mineralization. The unique surface properties of a biomaterial, therefore, are central design parameters that must be investigated to obtain optimum functionality and direct cell response. However, few studies have combined the application of high throughput methods to screen cell response with variations in surface properties of materials, especially low modulus biomaterials

(Lee et al. 2000; Lee et al. 1998; Kennedy et al. 2006; Acharya et al. 2010; Gallant et al. 2007; Moore et al. 2010, 2011; Zapata et al. 2007; Chatterjee et al. 2010).

Surface chemistry gradients were generated on alkylsilane coated cross-linked networks of PDMS and the influence of hydrophobicity on NIH3T3 and HUVEC cell functionality was investigated through screening cell-material interactions in terms of fibroblast cell morphology on adsorbed fibronectin coatings. In addition, structural and functional changes in the adhesive protein interface were examined to gain insight into the intermediary events that translate the chemical and physical properties of the underlying substrate into this specific cell response. This technology will enable the development of multifunctional materials that can be surface functionalized with instructive cues (Gallant et al. 2007; Moore et al. 2010, 2011) on substrates with mechanical properties that are tunable over a physiologically relevant range (Palchesko RN et al. 2012).

5.3 Experimental Section

- Cell culture

NIH/3T3, a mouse embryonic fibroblast cell line, was purchased from American Type Culture Collection (ATCC) and cultured on tissue culture polystyrene in Dulbecco's Modified Eagle's Medium (DMEM, Invitrogen) that contained 100 units/ml penicillin and 100 ug/ml streptomycin (Invitrogen) and 10% new born calf serum (Invitrogen). HUVEC, human umbilical cord vein endothelial cells, a primary cell line was purchased from Lonza and was cultured in EBM-2 basal medium (CC-3156) and EGM-2 SingleQuot Kit Suppl. & Growth Factors (CC-4176) as per manufacturer's instructions.

Control and gradient substrates were sterilized for 10 min in 70% ethanol and then rinsed with Dulbecco's phosphate buffered saline (DPBS, Invitrogen) three times. The substrates were first precoated with 10 μg/ml human plasma fibronectin (Gibco, Invitrogen) for 30 minutes and subsequently blocked with 1% bovine serum albumin (BSA, Fisher Scientific) for 30 minutes. Cells released from tissue culture dishes using Trypsin/EDTA (Invitrogen) were seeded cells at 40 cells/mm^2. Freshly seeded cells were left undisturbed in the biosafety cabinet for 30 minutes to facilitate cell attachment before transfer to the incubator. Plain glass slides acted as a control to confirm that changes in cell morphology were due to underlying gradients and not an artifact of the seeding procedure

- High throughput cell morphology analysis: automated image capture and data extraction

After incubation for 16 hours, cells were fixed with 3.7% by mass formaldehyde (Invitrogen) in DPBS and permeabilized for 10 minutes using 0.5% by mass Triton X-100 in buffered saline. For high throughput imaging, cell nuclei (Hoechst 33342, Invitrogen) and bodies (AlexaFluor 488 maleimide, Invitrogen) were fluorescently labeled for one hour. Cells were imaged and analyzed using NIS Elements software and a Nikon Eclipse Ti-U microscope (Nikon Instruments, Melville NY) equipped with fluorescence filter sets. A computer controlled stage was automated to capture 3 non overlapping images every 2 mm along the gradient axis over 50 mm starting from the point of maximum UVO exposure extending to 10 mm beyond the point of minimum UVO treatment. Approximately 96 mm^2 was analyzed on each sample. A binary mask was created by automatically applying contrast thresholding to each image so that cell spreading area and nuclei count could be automatically extracted. The spreading data for NIH3T3 cells presented in this paper represents four independent experiments (N=4) with two to six replicates in a single independent experiment

for each of the treatment groups, unless mentioned otherwise. The spreading and adhesion data for HUVEC cells are from N=3 replicates for each of the treatment groups.

- Characterization of fibronectin adsorption on PDMS for a range of hydrophobicity

PDMS networks on glass coverslips with discrete surface chemistries were created by uniform UVO exposure of the entire alkylsilane coated sample surface (Efimenko, Wallace, and Genzer 2002; Efimenko et al. 2005; Toworfe et al. 2004) and characterized with water contact angle measurements. These measurements were made on small uniform samples (~500 mm^2, 0.5 mm thick) to minimize the required quantity of labeled fibronectin and to facilitate the use of a soluble enzymatic substrate to study protein conformation. Three independent experiments (N=3) were conducted for both fibronectin adsorption and conformation studies.

Adsorption on PDMS samples was quantified using AlexaFluor 488 labeled fibronectin. The instructions provided in the protein labeling kit (A10235, Invitrogen) were followed to conjugate and purify the fluorescent fibronectin (Figure 5.1). Protein concentration and degree of labeling were determined and the final product was stored at 4°C (Williams et al. 2011). Discrete PDMS substrates were washed in 70% ethanol, rinsed three times with DPBS, and then incubated in 10 μg/ml AlexaFluor 488 conjugated fibronectin for 30 minutes. All samples were thoroughly rinsed twice with DPBS and deionized H_2O for five minutes each prior to mounting in a preservative medium (Fluoro-gel, Fisher Scientific) under a coverslip. A Nikon Ti-U microscope equipped with a FITC filter cube was used to capture 5 images on each sample. The average intensity of fluorescent protein adsorbed on sample substrate was recorded for each image. The background

intensity measured on a plain glass control slide at the time of each analysis was subtracted from experimental sample measurements.

The conformation of the adsorbed fibronectin was examined by adopting the approach described in Keselowsky et al (Keselowsky, Collard, and García 2003) using mouse anti-human monoclonal antibody HFN7.1 (Developmental Studies Hybridoma Bank, Iowa City, IA) which is specific to the cell binding domain of fibronectin. Differences in HFN7.1 binding indicates a change in the spatial relationship between the RGD and PHSRN sequences on the 9^{th} and 10^{th} type III repeats of the fibronectin and correlates to integrin $\alpha_5\beta_1$ binding (Garcia, Vega, and Boettiger 1999; Keselowsky, Collard, and García 2003; Lan et al. 2005) which requires optimal positioning of these motifs. Briefly, PDMS samples (~500 mm^2) modified with a range of wettabilities were precoated with 10 μg/ml fibronectin for 30 minutes followed by blocking with 1% BSA. Samples were incubated with HFN7.1 for an hour at 37°C, washed three times with 1% BSA, and then incubated in goat anti-mouse secondary antibody conjugated with alkaline phosphatase (Jackson Immunoresearch Laboratories, West Grove, PA) for an hour at 37°C. After washing, an equal volume of the substrate p-nitrophenylphosphate (pNPP) (Sigma Aldrich) was added to each sample. After incubation for 45 minutes at 37°C, 125 μl from each supernatant was transferred to a 96 well plate and the absorbance at 405 nm was detected using a microplate spectrophotometer (Biotek, Winooski, VT).

- Statistical and correlation analyses

SigmaPlot 11.0 (Systat Software, San Jose, CA) was used to perform regression analyses and curve fits on obtained data. A *p*-value of <0.01 obtained for the regression line slope was considered a

significant correlation between the concerned variables. All plotted data for NIH3T3 indicate the mean of N independent experiments ± one standard deviation. The error bars in HUVEC data shows standard deviation from mean among replicates. It is noted that the method of unbiased binning of data for distance or contact angle intervals from multiple quantification techniques caused some mismatch between some variables and therefore resulted in the unequal distribution of data points within correlation plots. However, no data points were neglected and data spanning the complete range of surface chemistries was included in order to identify trends and correlations.

5.4 Results and Discussion

- Cell spreading area on gradient substrates

Cell spreading and morphology is considered to be an important regulator of cell functionality (Chen et al. 1997). It is also an indication of initial differential adhesion to the proteins adsorbed or matrix assembled on a biomaterial surface which can modulate long term function. (Gallant, Michael, and Garcia 2005; Garcia, Vega, and Boettiger 1999; Keselowsky, Collard, and Garcia 2005; Keselowsky, Collard, and García 2003; Lan et al. 2005). Initial cell response in terms of morphology was analyzed against position along the length of the gradient substrate (Figure 5.2). As expected, cell spreading area on control plain glass slides (~20° water contact angle) did not show any specific trend thereby indicating that the observed trends in cell morphology were in response to the underlying gradients and not an artifact of the cell seeding procedure. On gradients, in general, NIH3T3 cell spreading was lowest at the hydrophilic end and highest at the hydrophobic end. The last one cm on each gradient, which was the hydrophobic zone between 40 mm and 50 mm, represented an internal control that equally supported maximal spreading. The spreading area on the stiffer glass gradients demonstrated a 76% (1.8 fold) rise in spreading by increasing from

1398 ± 175 μm^2 to 2467 ± 295 μm^2. On the softer PDMS gradient substrates, this phenomenon of increasing cell spreading was more pronounced as it increased 127% (2.3 fold) from 1010 ± 326 μm^2 to 2294 ± 218 μm^2. Comparing the different supporting materials, NIH3T3 cell spreading on the hydrophilic zone was 38% greater on glass gradients than PDMS gradients, although the spreading areas at the hydrophobic end on both glass and PDMS gradients were comparable.

HUVEC spreading with respect to position on gradient is displayed in Figure 5.3 Spreading on the control plain glass did not follow any specific trend. Cell spreading of HUVECs showed a similar trend to that of NIH3T3 in that cell spreading was minimum at the hydrophilic end and maximum at the hydrophobic end. However, this phenomenon was much sharper on PDMS gradients with a 193% (2.9 fold) increase in spreading from 1644±529 μm^2 to 4824±299 μm^2. The spreading increase on glass gradients was much more subdued with a modest increase of 42% (1.4 fold) from 2963±687 μm^2 to 4206±763 μm^2. Representative low (10x) and high magnification (60x) images of fluorescently stained cells are shown at selected positions on both glass gradients and PDMS for NIH3T3 in Figure 5.4 and 5.5 respectively and on PDMS for HUVECs in Figure 5.6. The position and the surface wettability for each image are reported. (Scale bar of all images is 100μm).

- Correlation between cell spreading area and surface chemistry

Gradients in surface chemistry were obtained as illustrated in Figure 4.5 of Chapter 4, and the trend of NIH3T3 and HUVEC cell spreading area at regular intervals along the entire length of substrates are shown in Figure 5.2 and Figure 5.3. However, spreading data of NIH3T3 and HUVEC were binned methodically for 5 mm increments to match contact angle measurements reported every 5 mm to obtain correlation plots which showed increasing cell spreading with rising

hydrophobicity on both glass and PDMS gradients. In fact, for NIH3T3 cells (Figure 5.7), the correlation was almost identical for both glass and PDMS gradients with R values of 0.97 and 0.98, respectively, and *p*-values <0.0001. The correlation was equally strong for HUVEC (Figure 5.8) on PDMS and glass gradients with R value of 0.96 for both and *p* values of <0.0001 and 0.002 respectively. Furthermore, the slope of the linear fit was considerably higher for HUVEC on PDMS gradients than a slope of ~12 for HUVEC on glass gradients and NIH3T3 on PDMS and glass gradients. The bidirectional error bars show standard deviations of the binned data corresponding to the respective axes. These results showing the exceptionally strong correlation between cell spreading and increasing hydrophobicity on gradient substrates led to further investigation of the effect of surface chemistry on the adsorbed fibronectin which mediated adhesion at the interface.

- Cell shape on surface gradients

Cell circularity is a coefficient that is generated based on the area and perimeter of selected objects and its value ranges from 0 to1. It is an indication of relative comparison to a circular object with a value of 1 indicating that object has shape of a circle. Cell circularity for NIH3T3 (N=4) and HUVEC (N=3) cells with respect to position on PDMS gradients are plotted in Figure 5.9 and Figure 5.10, respectively. The circularity followed a sigmoid curve with more a pronounced trend for HUVEC than for NIH3T3. The R^2 value of sigmoid curve fit was only 0.49 for NIH3T3 with a *p* value of 0.0005 while it was 0.88 with a *p* value of <0.0001 for HUVEC.

- Cell adhesion on surface gradients

NIH3T3 adhesion in terms of cell density (cells/μm^2) on control, glass and PDMS gradients did not follow any particular trend or pattern (data not shown). However, with HUVECs, while there was no significant pattern for cells on glass gradients; the adhesion on PDMS gradients followed a trend that was lesser on the hydrophilic part of the gradient and higher on the hydrophobic part of the gradient (Figure 5.11). The lowest cell density was 32±9 cells/μm^2 and the highest was 88±15 cells/μm^2. Similar to the correlation plot for cell spreading, correlation for HUVEC adhesion (Figure 5.12) with surface chemistry was also determined. A high correlation with R of 0.94 for PDMS gradients and lower R value of 0.69 for glass gradients with p values of <0.0001 and 0.06 respectively were obtained.

- Adsorption of fibronectin on surface modified PDMS

Since human plasma fibronectin pre-adsorbed onto the gradients primarily mediated the specific interactions between the biomaterial and cells, the density and conformation of the fibronectin were investigated. Fluorescence imaging of AlexaFluor-488 dye conjugated fibronectin coated on PDMS substrates with a range of uniform surface chemistries were analyzed to quantify adsorption (Figure 5.13). Values of relative fluorescence intensity reflect the proportional density of fibronectin adsorbed on PDMS substrates with a range of surface wetting properties. Fibronectin adsorption increased monotonically with hydrophobicity. A line fit reveals a proportional relationship (R^2=0.69) between fibronectin adsorption and hydrophobicity with a *p*-value <0.0001. Fitting higher order polynomials did not yield better correlations. Figure 5.14 shows the difference in fibronectin absorbance in relative fluorescence intensity at the two extreme ends of the surface

chemistry gradients. An analysis of variance yielded that the difference was statistically significant with a *p* value of 0.002 ($p<0.05$).

To understand the relationship between NIH3T3 cell spreading area and fibronectin adsorption, data were systematically binned for 15 degree intervals of water contact angle. The regression indicated cell spreading has a strong correlation with fibronectin adsorption (R=0.80) with a *p*-value of 0.06 (Figure 5.15). The bidirectional error bars show standard deviations of the binned data corresponding to the respective axes.

- Conformation of fibronectin on surface modified PDMS

The functional activity of the protein fibronectin on surfaces with different chemistries was also evaluated by assessing the accessibility of the cell binding domain with HFN7.1, a monoclonal antibody that mimics the binding affinity of integrin $\alpha_5\beta_1$ (Keselowsky, Collard, and García 2003; Llopis-Hernandez et al. 2011). HFN7.1 binds to the cell binding domain of fibronectin between the RGD and PHSRN sequences and is sensitive to relative spatial changes between these two motifs. HFN7.1 antibody binding was quantified with a modified ELISA procedure on PDMS substrates with uniform surface chemistry (Figure 5.16). Open symbols represent raw absorbance values of the substrate product normalized to control. The symbol shapes correspond to the samples from N = 3 independent experiments which demonstrated similar biphasic trends. The closed symbols represent the same data binned into 15 degree increments and then normalized to the corresponding fibronectin adsorbed quantity to decouple the roles of quantity and conformation. HFN7.1 binding increased from negligible amounts for extremely hydrophilic surfaces (<15°) to maximum at approximately 75°. However, a marked decrease was observed for

highly hydrophobic surfaces (>90°). Since this measurement does not account for the variation in the density of the adsorbed protein, the analysis was extended to normalize the ELISA data to account for differences in fibronectin density and represent only relative differences in conformation. Thus, all conformation and adsorption data were methodically binned for 15 degree contact angle intervals and the conformation mean values were scaled by the adsorption values to estimate the relative influence of conformation alone (Figure 5.17). A similar biphasic trend was observed, and accordingly the Pearson's correlation coefficient (R) was 0.24. When only the data up to 75° contact angle were considered, cell spreading and fibronectin conformation were highly correlated (R = 0.99, *p*-value = 0.001).

- NIH3T3 spreading and adhesion on soft and stiff PDMS

PDMS with less crosslinker (1.43% weight crosslinker), the *soft* PDMS, and more (10% weight crosslinker), the *stiff* PDMS, in discrete forms were used to study NIH3T3 cell response. An analysis of variance based on the numerous images (no. of images = 66) taken on the *soft* and *stiff* PDMS show statistical difference for cell spreading (Figure 5.18) and cell adhesion (Figure 5.19) with the same *p* value of <0.001 for both.

Cell spreading has been established as a critical regulator of cell functions including survival and transcription (Chen et al. 1997; Li et al. 2008). The spreading area of NIH/3T3 fibroblasts increased with hydrophobicity over a range of ~10° to ~100° water contact angle. It was interesting to note that although spreading area was minimum at the extremely hydrophilic region with <15°, it did not deter cell adhesion in that region. Kennedy et al (Kennedy et al. 2006) found that maximum osteoblast spreading was reached at an intermediate wettability on fibronectin coated

surface gradients on glass while the osteoblast proliferation was highest on the most hydrophobic end of the gradient. This differs from our observations that NIH/3T3 fibroblast spreading continued to rise with increasing hydrophobicity on both glass and PDMS substrates, though the difference is likely attributed to numerous dissimilarities in the experimental systems including the cell type, fibronectin coating concentration, and substrate material.

One of the most striking and definitive results from this study is the strong dependence of cell spreading on surface chemistry (Figure 5.7 and Figure 5.8). Although this correlation was similar on the glass gradients and PDMS gradients, the cell spreading was lower on the PDMS gradients compared to the glass gradients for the entire range of hydrophobicity. Despite the fact that the surface chemical interfaces on both were comparable, there existed a vast difference in their underlying stiffnesses. The elastic modulus of glass is ~ 50 GPa, while cross-linked PDMS is ~1.8 MPa. The role of substrate stiffness in cell functionality has been well documented in previous studies,(Pelham and Wang 1997; Brown, Ookawa, and Wong 2005; Engler et al. 2006; Discher, Janmey, and Wang 2005; Discher DE 2009; Ghosh et al. 2007) and enhanced fibroblast spreading on and durotaxis toward stiffer substrates in comparison with softer substrates has also been reported (Lo et al. 2000; Pelham and Wang 1997; Georges and Janmey 2005; Discher DE 2009). The differences in matrix mechanical properties are sensed by transmembrane integrin receptors that transmit information back and forth between the inside of cell and the extracellular matrix. This process is called mechanotransduction and involves integrin binding and clustering, focal adhesion complex formation, and signaling processes linked to the actin-myosin contractile machinery (Dumbauld et al. 2010; Gallant, Michael, and Garcia 2005; Geiger B. 2001; Hynes 2002).

Cells interact with biomaterial surfaces as they do in their native microenvironments – through binding the proteins at the interface. Cell adhesion to extracellular matrices is mediated primarily through integrin receptor binding to proteins such as fibronectin (Hynes 2002). In this work, prior to cell attachment, both experimental and control samples were coated with fibronectin. This was done to introduce a common adhesive environment where fibronectin would be the predominant protein cells interacted with over the time course of these experiments. Both fibronectin adsorption density and fibronectin conformation on different material surfaces are established key players that have profound impacts on cell functionality (Leahy DJ 1996; Keselowsky, Collard, and García 2003; Michael et al. 2003; Phillips et al. 2010; Allen et al. 2006). Therefore, fibronectin adsorption behavior on PDMS with varied wettablities was probed in this study to understand the adhesive environment mediating the correlation between surface chemistry and cell spreading. Using fluorescently labeled fibronectin, it was found that maximum adsorption occurred on the most hydrophobic surfaces whereas minimum adsorption was measured on the most hydrophilic surfaces, which is in good agreement with many previously reported studies (Lee et al. 2006; Keselowsky, Collard, and García 2003; Llopis-Hernandez et al. 2011). For instance, fibronectin adsorption on surfaces with different self-assembled monolayer (SAM) chemistries was established to follow the trend OH<COOH<NH_2<CH_3 (Lee et al. 2006). Similarly, the surfaces investigated here contain a spatially controlled continuous variation from completely CH_3 to predominantly COOH (and to a lesser degree, other oxygen containing entities) proportional to the UVO exposure time, (Moore et al. 2011; Roberson et al. 2002) which regulated adsorption. Subsequently, regression analysis revealed that a positive correlation exists between cell spreading and fibronectin adsorption. However, the *p*-value of 0.06 in the linear regression indicates some

uncertainty in the fit parameters (i.e., slope) and suggests a linear model may not accurately predict the dependence of spreading on fibronectin adsorption for these surfaces.

Fibronectin conformation on PDMS with UVO modulated surface chemistries was assessed with an antibody based assay for the cell binding domain between the 9th and 10th type III repeats that corresponds to $\alpha_5\beta_1$ integrin binding, the primary fibronectin receptor for NIH/3T3 fibroblasts. The affinity of the antibody was highly sensitive to an optimum distance between the RGD and PHSRN motifs of fibronectin (Keselowsky, Collard, and García 2003; Leahy DJ 1996). Unlike the adsorption studies, the results from these conformation experiments yielded a biphasic trend where the amount of antibody bound increased with hydrophobicity up to about 75° before sharply decreasing on the most hydrophobic (91°-105°) surfaces. After normalizing to the fibronectin density, the HFN 7.1 binding on the most hydrophobic surface was ~3 fold less than the maximum binding. The absence of a correlation ($R = 0.24$) between cell spreading and fibronectin conformation over the entire gradient range was primarily due to the hydrophobic end of the gradient where spreading was maximum but the HFN7.1 binding was low. An analysis of only the range of contact angle up to 75° revealed a strong correlation ($R = 0.99$) between cell spreading and fibronectin conformation for hydrophilic to intermediate hydrophobicity on PDMS substrates. Together these results on fibronectin functional activity suggest that $\alpha_5\beta_1$ does not dominate cell interactions at the hydrophobic end of the gradient. One possible explanation is that total integrin binding may regulate spreading, rather than an individual receptor class, on the denatured fibronectin that is present in high density on the hydrophobic region of these materials, suggesting further investigation into the specific binding of all fibronectin receptors and their role in regulating cell functions such as spreading is warranted. Recently, Llopis-Hernandez et al.

examined both fibronectin adsorption and conformation on SAM surfaces with different wettabilities obtained using mixtures of distinct terminal OH and CH_3 alkanethiols (Llopis-Hernandez et al. 2011). Their results on fibronectin adsorption and conformation follow similar profiles and corroborate our results; however, their findings on fibronectin conformation, following normalization, did not display the distinct biphasic trend that our results have shown.

Collectively, these results reflect the level of complexity in protein adsorption and adhesive interactions at the cell-biomaterial interface that leads to a specific cell response. The strong linear correlation observed in this study, between steady-state cell spreading and surface chemistry is a surprising outcome given the complexity of the interactions at the interface. As discussed earlier, the factors that influence cell fate are numerous and are a combination of surface chemistry and other additional matrix properties. For instance, although not the focus of the present work, it can also be inferred that elastic modulus may have led to the difference in cell spreading on PDMS gradients versus the glass gradients in this study. These factors are not independent in that the specificity of integrin binding (e.g., $\alpha_5\beta_1$ instead of $\alpha_v\beta_3$) can regulate the cellular mechanosensory machinery which influences cell shape and therefore higher order functions such as proliferation or matrix production.

5.5 Conclusions

Using these gradient materials as adhesive substrates demonstrated that cell morphology strongly depended on surface hydrophobicity, and that this correlation arose from complex interactions with the surface. Analysis of the fibronectin at the adhesive interface showed a strong correlation between cell spreading and fibronectin density, and a distinctly biphasic relationship between

spreading and fibronectin conformation over the range of approximately 10-100° contact angle on PDMS. These findings provide insight into what regulates the strong positive correlation between surface chemistry and fibronectin-mediated cell shape control on elastic surfaces. This study also demonstrated the potential of soft combinatorial biomaterials to identify significant trends or patterns in biological responses over large ranges of matrix properties.

5.6 Acknowledgement

HFN7.1 antibody was obtained from the Developmental Studies Hybridoma Bank, which was developed under the auspices of the National Institute of Child Health and Human Development and is maintained by the University of Iowa, Department of Biological Sciences.

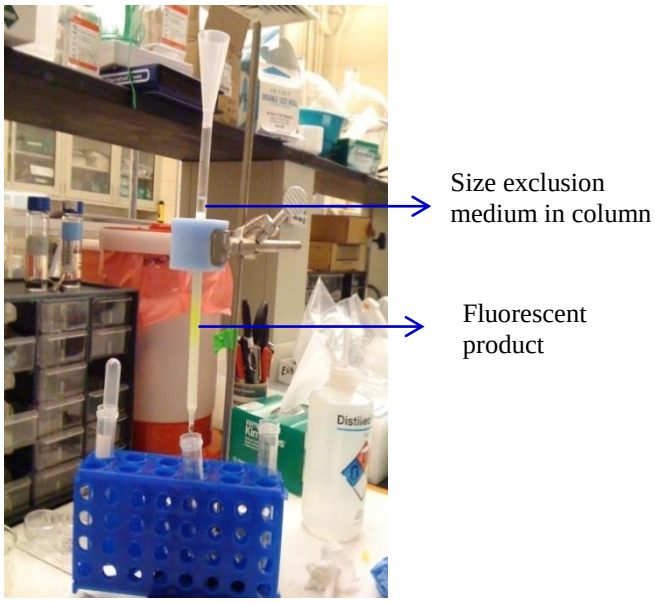

Figure 5.1 Column chromatography purification of fluorescently labeled fibronectin.

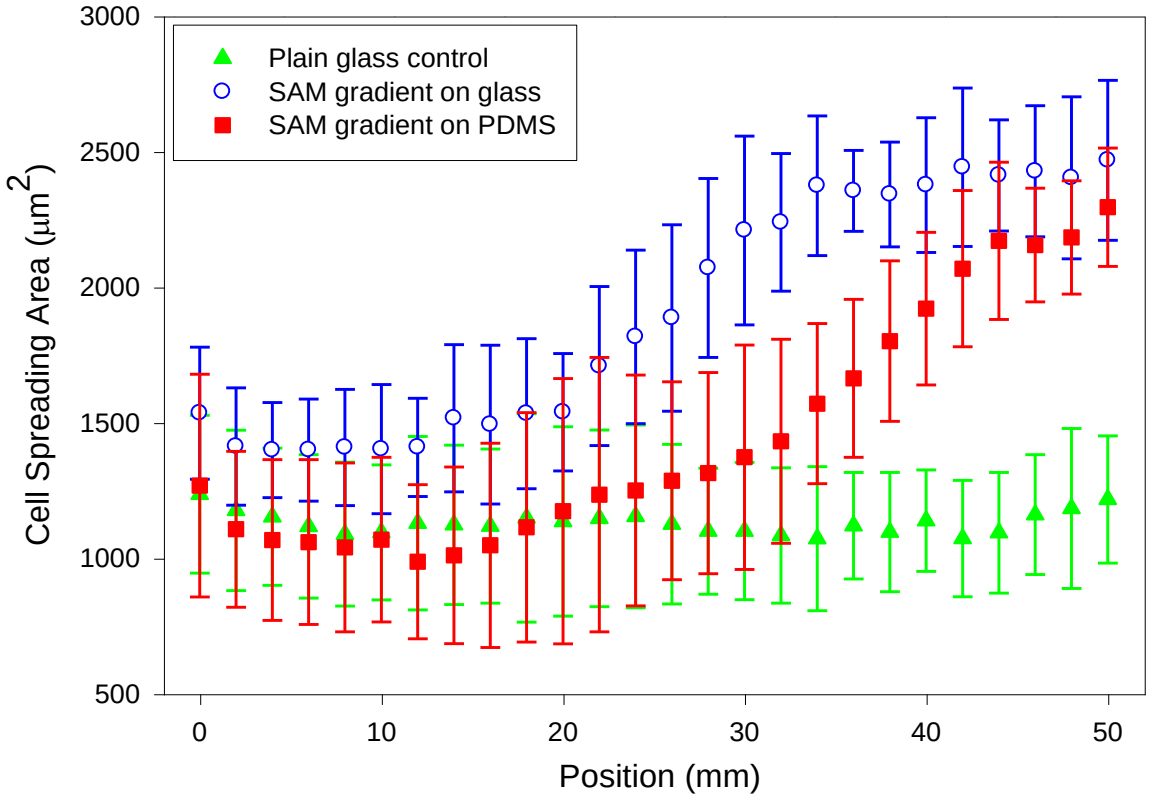

Figure 5.2 Steady-state (16 h) NIH3T3 spreading on surface chemistry gradients. Automated image analysis of cell morphology indicates cell spreading on fibronectin coated surfaces varies with position on surface chemistry gradients. Data were obtained from N = 4 independent experiments with two to six replicates in each experiment.

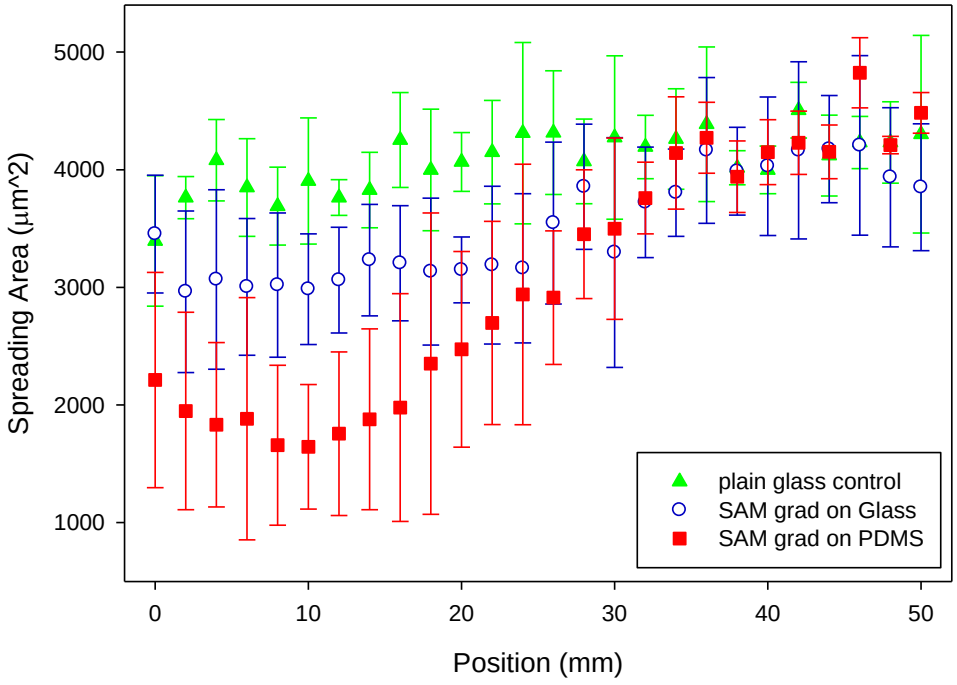

Figure 5.3 Steady-state (16 h) HUVEC spreading on surface chemistry gradients. Automated image analysis of cell morphology indicates cell spreading on fibronectin coated surfaces varies with position on surface chemistry gradients. Data were obtained from N = 3 replicates in each treatment group.

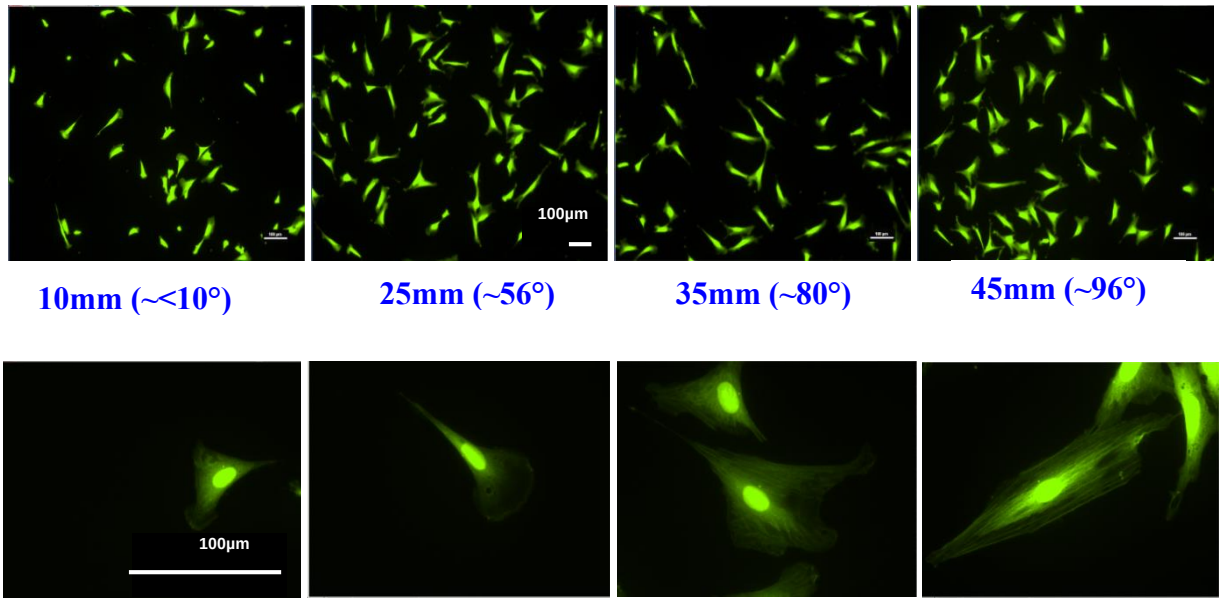

Figure 5.4 Representative NIH3T3 images on glass gradients are shown. The top row images were taken at lower magnification (10x) and higher magnification (60x). Scale bar 100 µm.

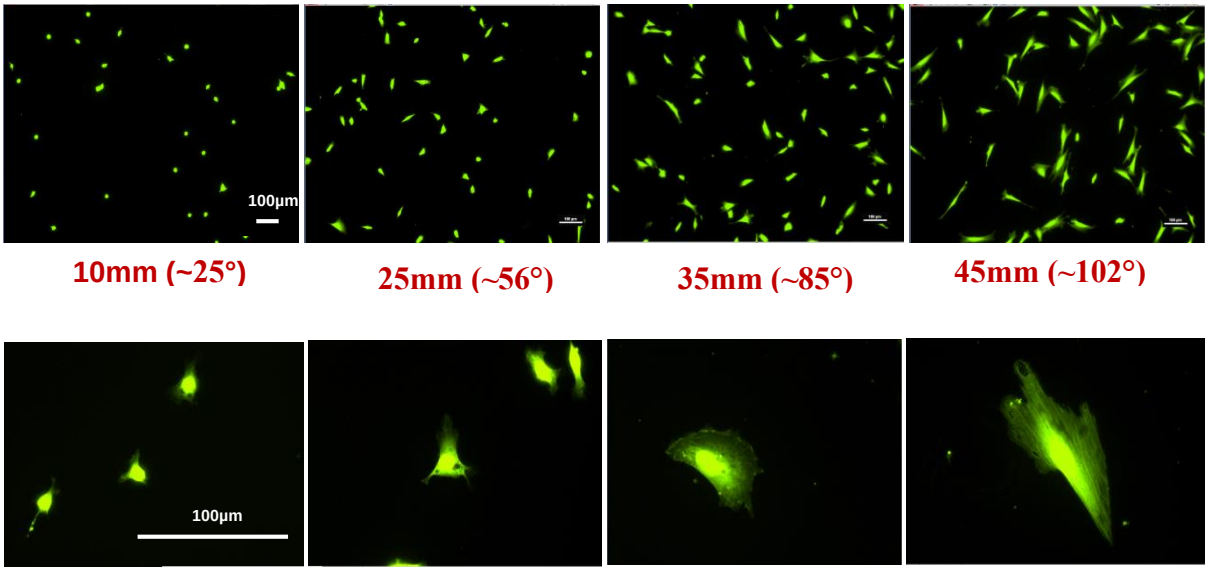

Figure 5.5 Representative NIH3T3 images on PDMS gradients are shown. The top row images were taken at lower magnification (10x) and higher magnification (60x). Scale bar 100 µm.

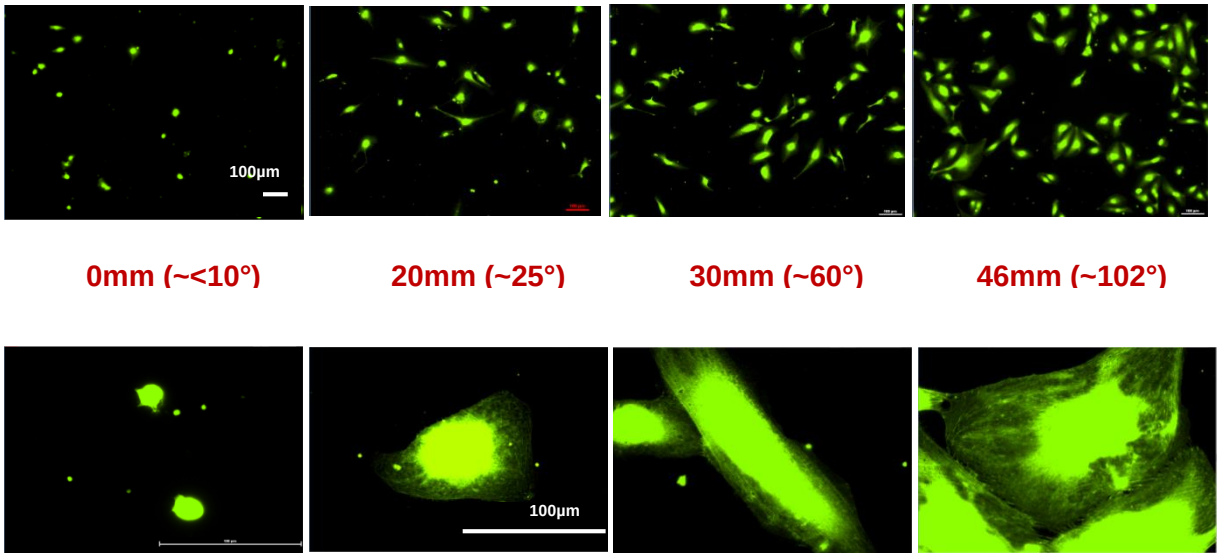

Figure 5.6 Representative HUVEC images on PDMS gradients are shown. The top row images were taken at lower magnification (10x) and higher magnification (60x). Scale bar 100 μm.

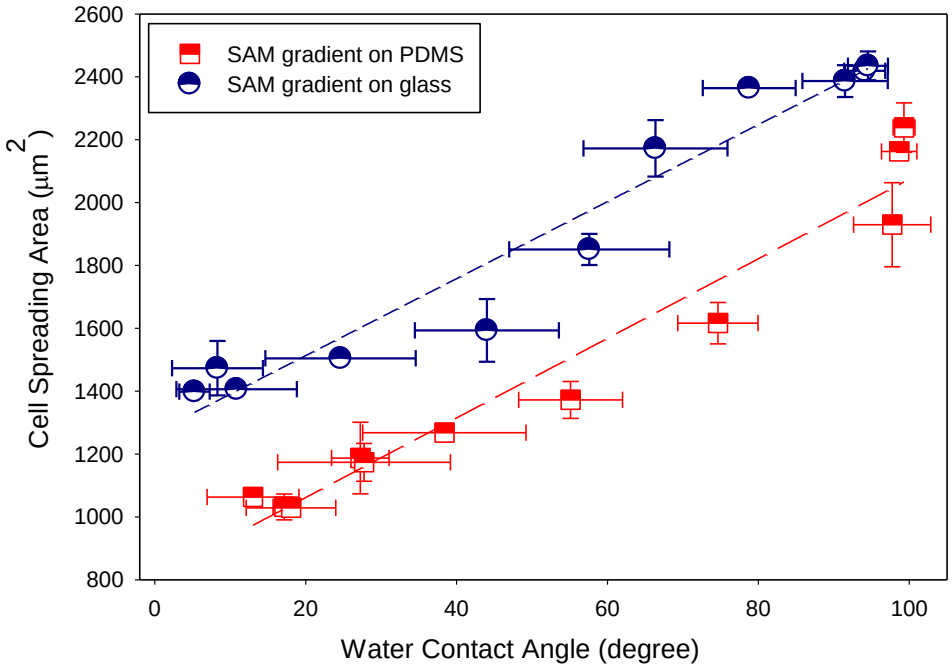

Figure 5.7 Correlation of NIH3T3 spreading with surface chemistry gradients. Spreading area and contact angle measurements on surface chemistry gradients were binned into 5 mm increments to examine their correlation. The linear regression analyses on PDMS (long dash) and glass (short dash) substrates had coefficients of correlation of 0.98 ($p < 0.0001$) and 0.97 ($p<0.0001$), respectively. The bidirectional error bars show standard deviations of the binned data corresponding to the respective axes.

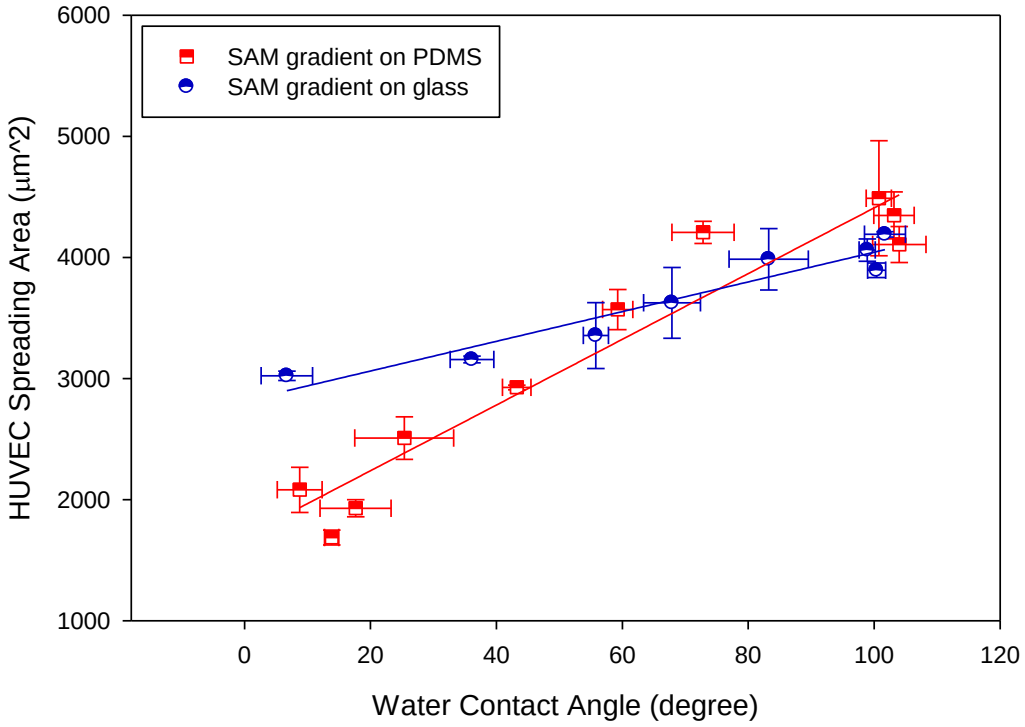

Figure 5.8 Correlation of HUVEC spreading area with surface chemistry gradients. Spreading area and contact angle measurements on surface chemistry gradients were binned into 5 mm increments to examine their correlation. The linear regression analyses on PDMS (red line) and glass (blue line) substrates had coefficients of correlation of 0.96 ($p<0.0001$) and 0.96 ($p=0.002$), respectively. The bidirectional error bars show standard deviations of the binned data corresponding to the respective axes.

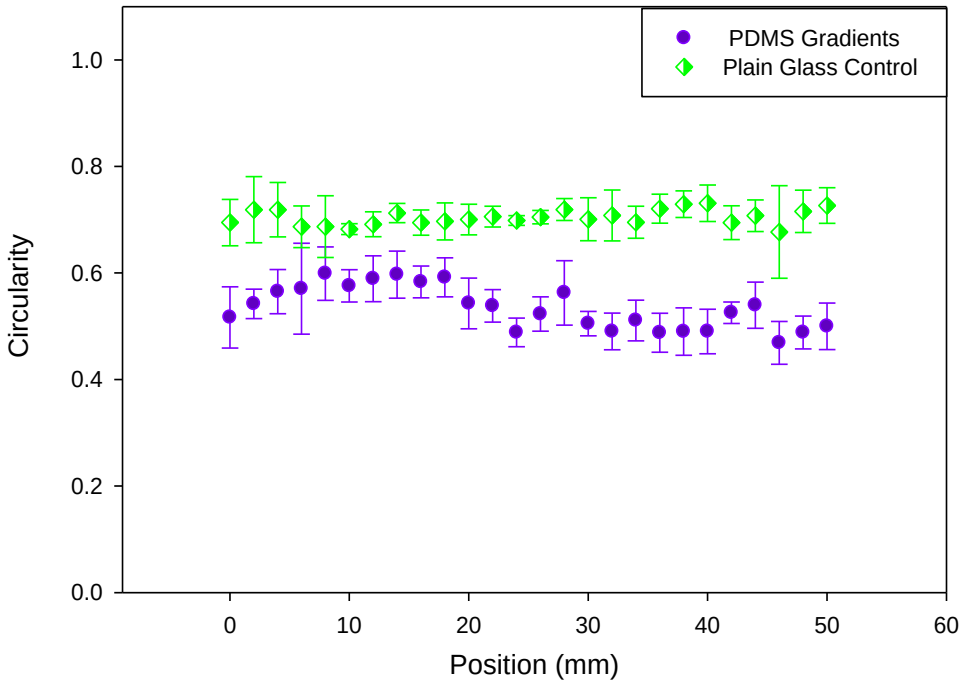

Figure 5.9 NIH3T3 circularity on PDMS surface chemistry gradients. A sigmoid trend (R^2=0.49) was observed with respect to circularity for an increase in PDMS surface hydrophobicity for N=4 replicates.

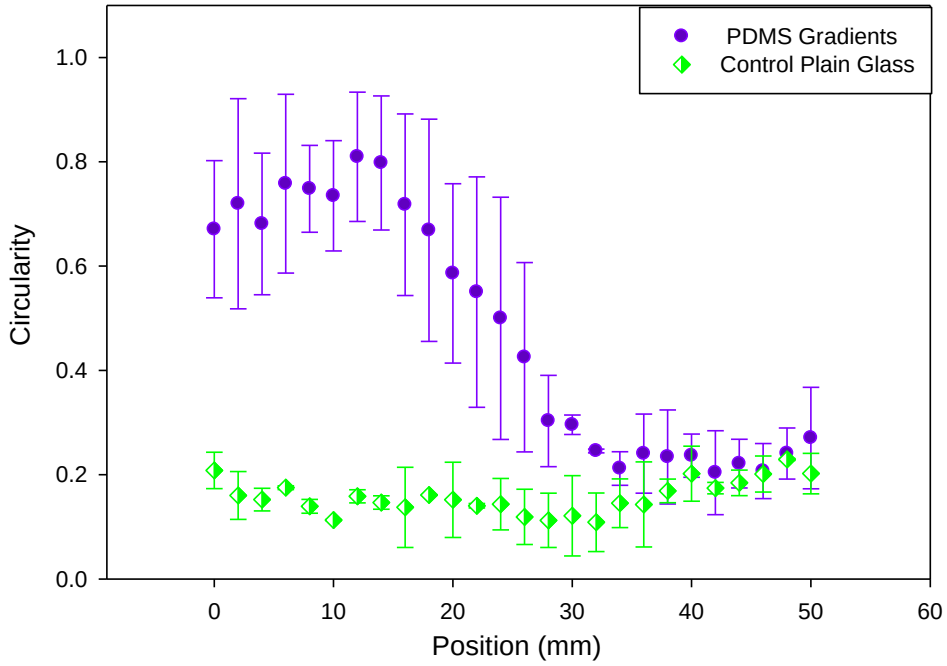

Figure 5.10 HUVEC circularity on PDMS surface chemistry gradients. A prominent sigmoid trend (R^2=0.88) was observed with respect to circularity for an increase in PDMS surface hydrophobicity for N=3 replicates.

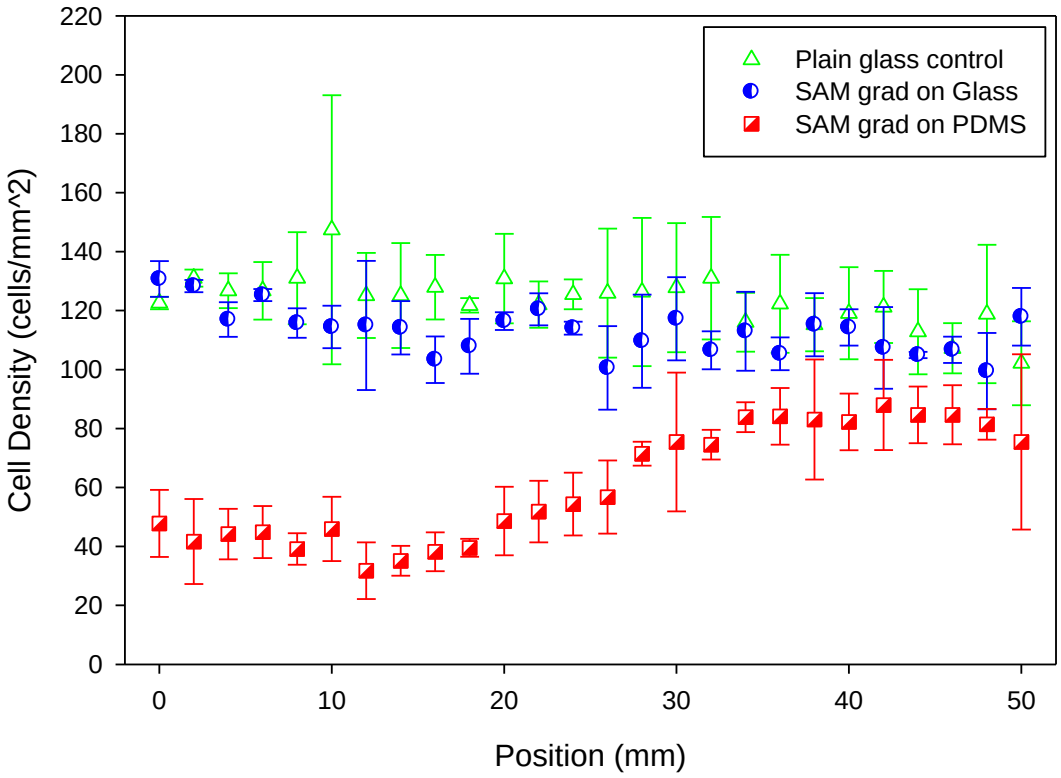

Figure 5.11 HUVEC adhesion on surface chemistry gradients. An increase in cell density with hydrophobity was observed for cells on PDMS gradients. N=3 replicates in each treatment group.

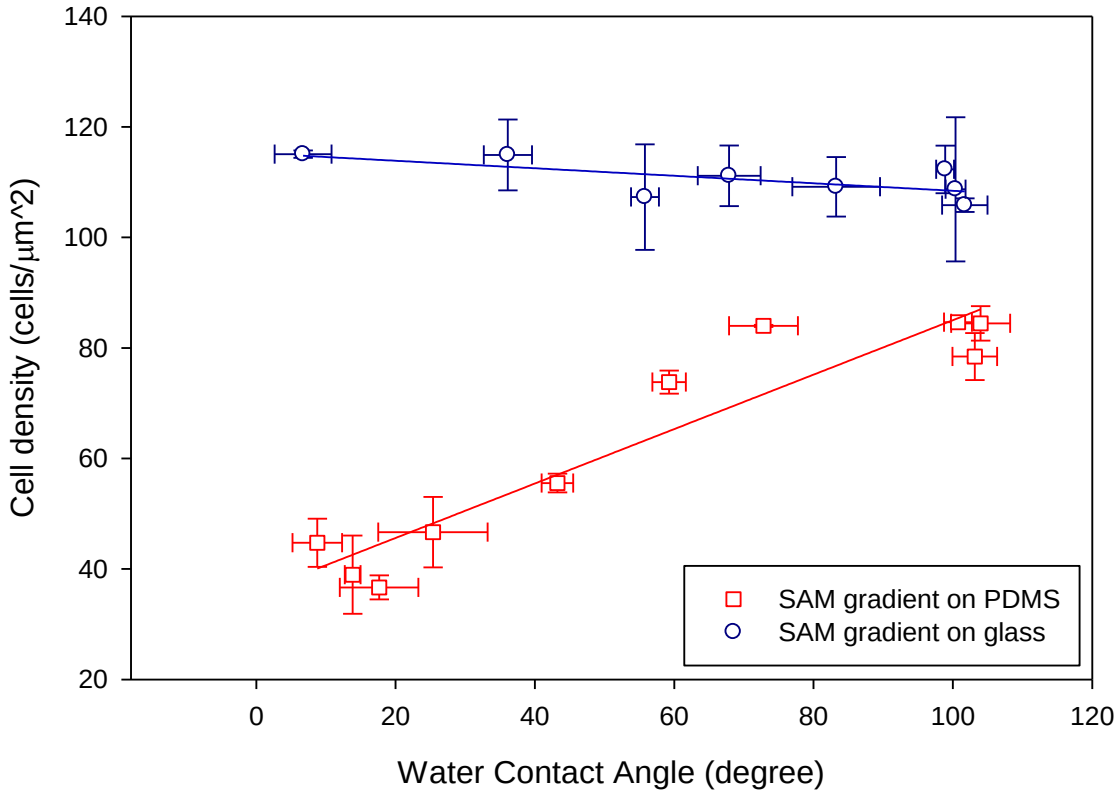

Figure 5.12 Correlation of HUVEC adhesion with surface chemistry gradient. Cell density and contact angle measurements on surface chemistry gradients were binned into 5 mm increments to examine their correlation. The linear regression analyses on PDMS (red line) and glass (blue line) substrates had coefficients of correlation of 0.94 ($p<0.0001$) and 0.69 ($p=0.06$), respectively. The bidirectional error bars show standard deviations of the binned data corresponding to the respective axes.

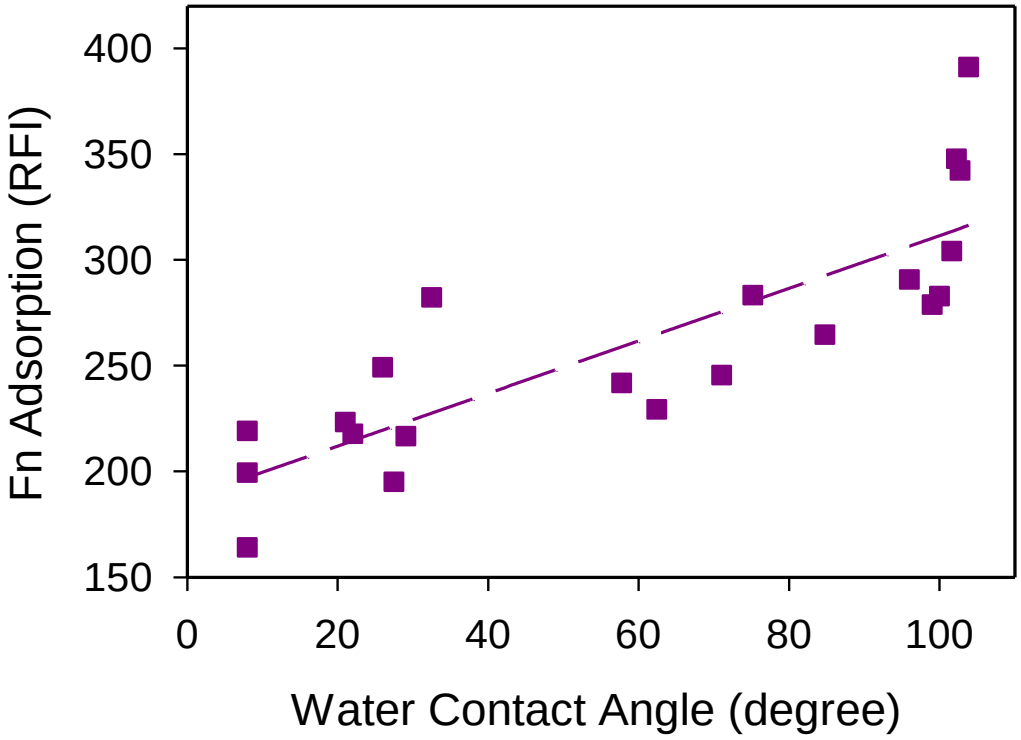

Figure 5.13 Fibronectin adsorption on PDMS with varying hydrophobicities. The adsorption of fluorescently labeled fibronectin was quantified by image analysis of the relative fluorescence intensity (N=3 independent experiments). A linear regression (dashed line, y= 187+1.2 x) had an R^2=0.69.

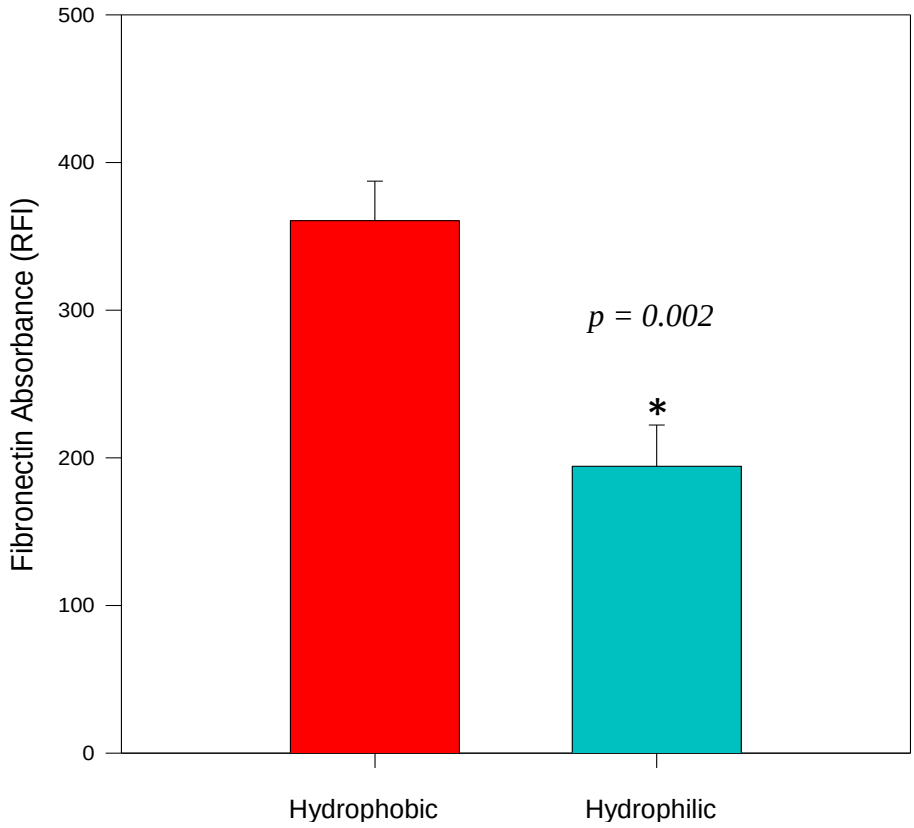

Figure 5.14 Fibronectin adsorption on hydrophilic and hydrophobic PDMS. The difference in fibronectin absorbance in relative fluorescence intensity at the two extreme ends of the surface chemistry gradients is shown. An analysis of variance yielded that the difference was statistically significant with a *p* value of 0.002 ($p<0.05$)

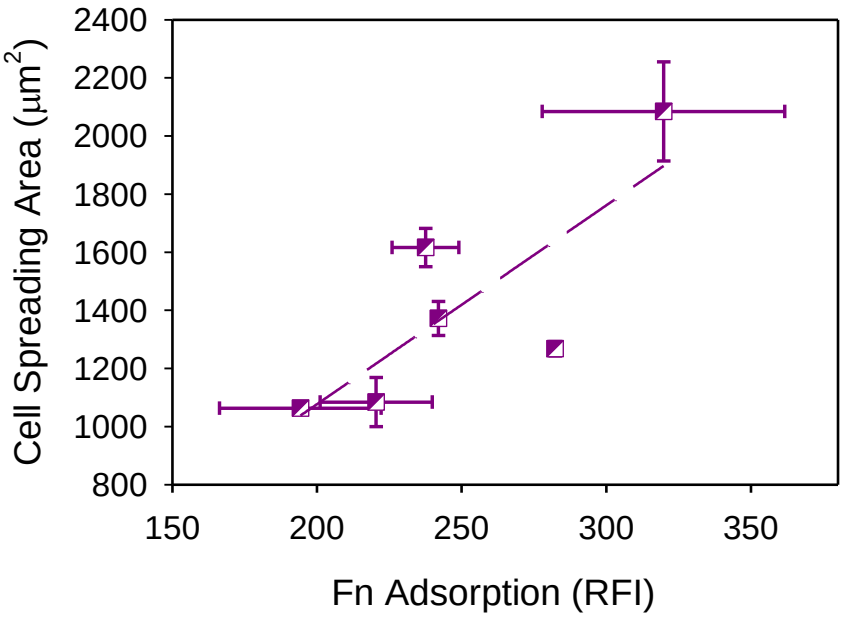

Figure 5.15 Correlation of NIH3t3 spreading with fibronectin adsorption on PDMS gradients. NIH/3T3 fibroblast spreading area and fibronectin adsorption measurements were binned into 15° contact angle increments to examine their correlation (R=0.80, p=0.06). The bidirectional error bars show standard deviations of the binned data corresponding to the respective axes.

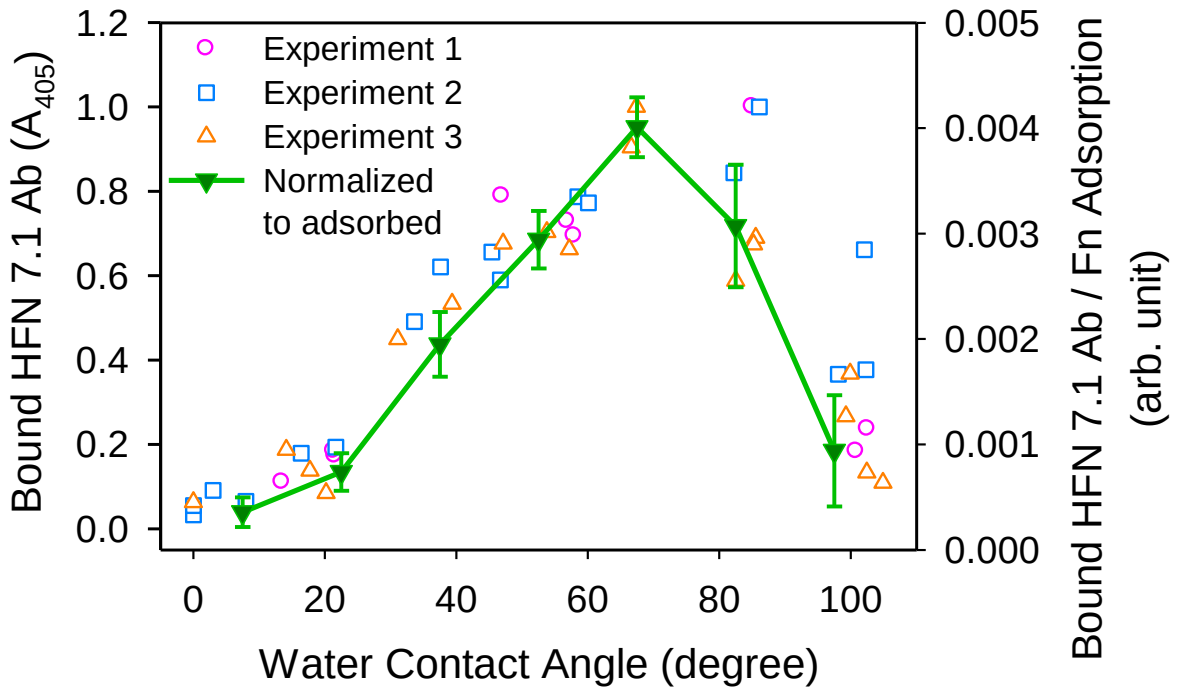

Figure 5.16 Conformation of fibronectin adsorbed on PDMS with varied surface chemistries. HFN7.1 antibody binding was quantified by ELISA. Open symbols represent raw absorbance values of the substrate product normalized to control. The symbol shapes correspond to the samples from N=3 independent experiments which demonstrated similar biphasic trends. The closed symbols represent the same data binned into 15° increments and then normalized to the corresponding fibronectin adsorbed quantity to decouple the roles of quantity and conformation.

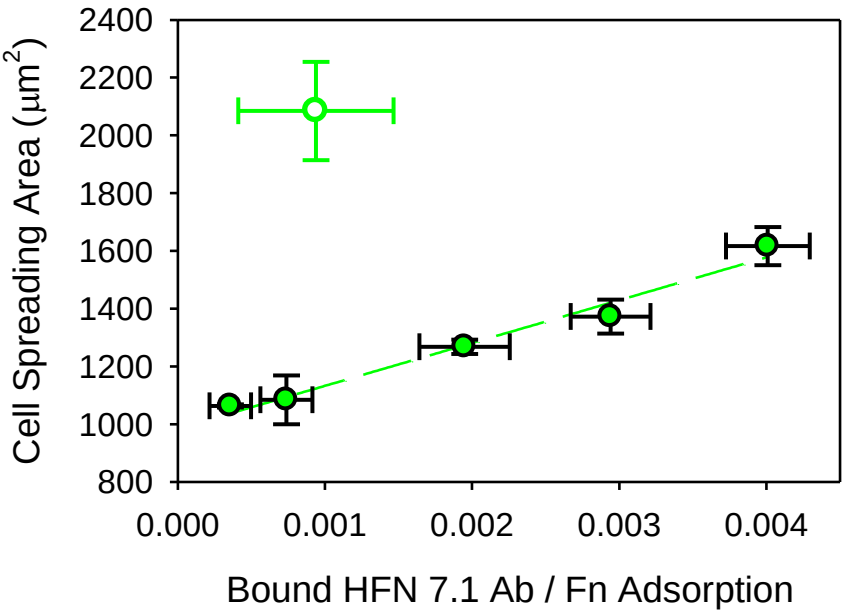

Figure 5.17 Correlation of NIH/3T3 spreading and fibronectin conformation (normalized to adsorption). Measurements were binned into 15° contact angle increments to examine their correlation (open and closed circles; R=0.24, p=0.65 over the entire range). The dashed line represents the regression for contact angles spanning 0–75 only (closed circles; R5 0.99, p=0.001). The bidirectional error bars show standard deviations of the binned data corresponding to the respective axes.

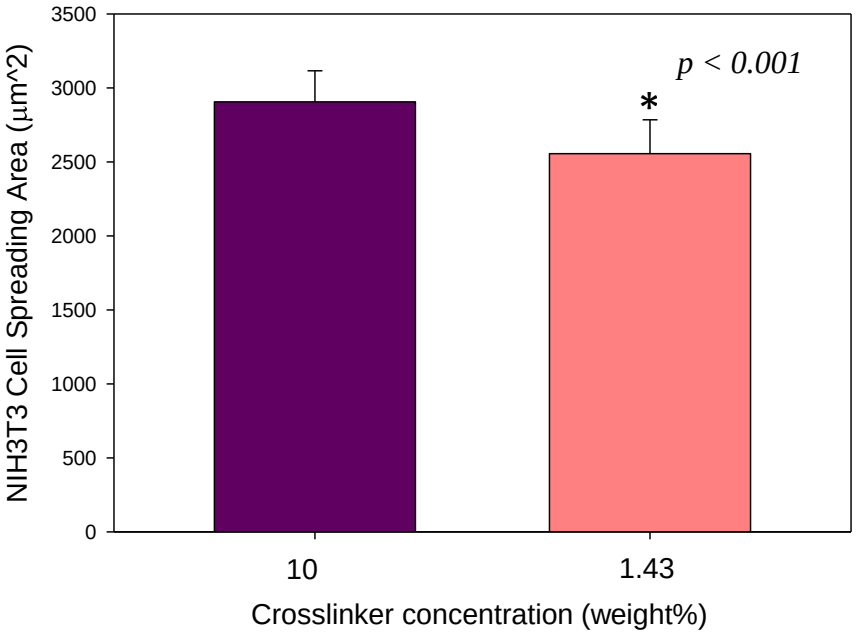

Figure 5.18 NIH3T3 cell spreading on discrete stiff and soft PDMS.

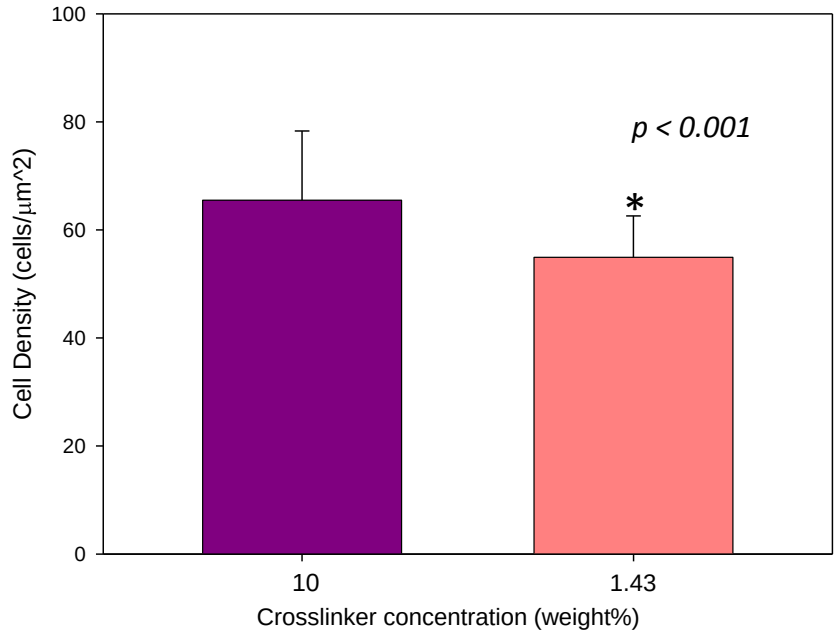

Figure 5.19 NIH3T3 cell adhesion on discrete stiff and soft PDMS.

5.7 References

Acharya, Abhinav P., Natalia V. Dolgova, Nicole M. Moore, Chang-Qing Xia, Michael J. Clare-Salzler, Matthew L. Becker, Nathan D. Gallant, and Benjamin G. Keselowsky. 2010. The modulation of dendritic cell integrin binding and activation by RGD-peptide density gradient substrates. *Biomaterials* 31 (29):7444-7454.

Allen, Lorcan T., Miriam Tosetto, Ian S. Miller, Darran P. O' Connor, Stephen C. Penney, Iseult Lynch, Alan K. Keenan, Stephen R. Pennington, Kenneth A. Dawson, and William M. Gallagher. 2006. Surface-induced changes in protein adsorption and implications for cellular phenotypic responses to surface interaction. *Biomaterials* 27 (16):3096-3108.

Anderson, Daniel G., Shulamit Levenberg, and Robert Langer. 2004. Nanoliter-scale synthesis of arrayed biomaterials and application to human embryonic stem cells. *Nature Biotechnology* 22 (7):863-866.

Brown, Xin Q, Keiko Ookawa, and Joyce Y Wong. 2005. Evaluation of polydimethylsiloxane scaffolds with physiologically-relevant elastic moduli: interplay of substrate mechanics and surface chemistry effects on vascular smooth muscle cell response. *Biomaterials* 26 (16):3123-3129.

Chatterjee, Kaushik, Sheng Lin-Gibson, William E. Wallace, Sapun H. Parekh, Young Jong Lee, Marcus T. Cicerone, Marian F. Young, and Carl G. Simon Jr. 2010. The effect of 3D hydrogel scaffold modulus on osteoblast differentiation and mineralization revealed by combinatorial screening. *Biomaterials* 31 (19):5051-5062.

Chen, Christopher S., Milan Mrksich, Sui Huang, George M. Whitesides, and Donald E. Ingber. 1997. Geometric Control of Cell Life and Death. *Science* 276 (5317):1425-1428.

Discher DE, Mooney DJ, Zandstra PW. 2009. Growth factors, matrices, and forces combine and control stem cells. *Science* (324):1673-1677.

Discher, Dennis E., Paul Janmey, and Yu-li Wang. 2005. Tissue Cells Feel and Respond to the Stiffness of Their Substrate. *Science* 310 (5751):1139-1143.

Dumbauld, David W., Kristin E. Michael, Steven K. Hanks, and Andrés J. García. 2010. Focal adhesion kinase-dependent regulation of adhesive forces involves vinculin recruitment to focal adhesions. *Biology of the Cell* 102 (4):203-213.

Efimenko, Kirill, Julie A. Crowe, Evangelos Manias, Dwight W. Schwark, Daniel A. Fischer, and Jan Genzer. 2005. Rapid formation of soft hydrophilic silicone elastomer surfaces. *Polymer* 46 (22):9329-9341.

Efimenko, Kirill, William E. Wallace, and Jan Genzer. 2002. Surface Modification of Sylgard-184 Poly(dimethyl siloxane) Networks by Ultraviolet and Ultraviolet/Ozone Treatment. *Journal of Colloid and Interface Science* 254 (2):306-315.

Elineni, K K , and N D Gallant. 2011. Regulation of Cell Adhesion Strength by Peripheral Focal Adhesion Distribution. *Biophysical journal* 101 (12):2903-2911.

Engler, Adam J., Shamik Sen, H. Lee Sweeney, and Dennis E. Discher. 2006. Matrix Elasticity Directs Stem Cell Lineage Specification. *Cell* 126 (4):677-689.

Gallant, N. D, K. A Lavery, E. J Amis, and M. L Becker. 2007. Universal Gradient Substrates for "Click" Biofunctionalization. *Advanced Materials* 19 (7):965-969.

Gallant, Nathan D., Kristin E. Michael, and Andres J. Garcia. 2005. Cell Adhesion Strengthening: Contributions of Adhesive Area, Integrin Binding, and Focal Adhesion Assembly. *Molecular Biology of the Cell* 16 (9):4329-4340.

Garcia, A J, M D Vega, and D Boettiger. 1999. Modulation of Cell Proliferation and Differentiation through Substrate-dependent Changes in Fibronectin Conformation. *Molecular Biology of the Cell* 10 (3):785-798.

García, Andrés J. 2005. Get a grip: integrins in cell–biomaterial interactions. *Biomaterials* 26 (36):7525-7529.

Geiger B., Bershadsky A., Pankov R. and Yamada K.M. 2001. Transmembrane crosstalk between the extracellular matrix and the cytoskeleton. *Nature Reviews Molecular Cell Biology* 2:793-805.

Georges, Penelope C., and Paul A. Janmey. 2005. Cell type-specific response to growth on soft materials. *Journal of Applied Physiology* 98 (4):1547-1553.

Ghosh, Kaustabh, Zhi Pan, E. Guan, Shouren Ge, Yajie Liu, Toshio Nakamura, Xiang-Dong Ren, Miriam Rafailovich, and Richard A. F. Clark. 2007. Cell adaptation to a physiologically relevant ECM mimic with different viscoelastic properties. *Biomaterials* 28 (4):671-679.

Hernandez, J C R, M S Sanchez, J M Soria, J L Ribelles, and M M Pradas. 2007. Substrate Chemistry-Dependent Conformations of Single Laminin Molecules on Polymer Surfaces are Revealed by the Phase Signal of Atomic Force Microscopy. *Biophysical journal* 93 (1):202-207.

Hynes, Richard O. 2002. Integrins: Bidirectional, Allosteric Signaling Machines. *Cell* 110 (6):673-687.

Iuliano, Denise J., Steven S. Saavedra, and George A. Truskey. 1993. Effect of the conformation and orientation of adsorbed fibronectin on endothelial cell spreading and the strength of adhesion. *Journal of Biomedical Materials Research* 27 (8):1103-1113.

Kennedy, Scott B., Newell R. Washburn, Carl George Simon Jr, and Eric J. Amis. 2006. Combinatorial screen of the effect of surface energy on fibronectin-mediated osteoblast adhesion, spreading and proliferation. *Biomaterials* 27 (20):3817-3824.

Keselowsky, B G., D M. Collard, and A J. Garcia. 2005. Integrin binding specificity regulates biomaterial surface chemistry effects on cell differentiation. *Proceedings of the National Academy of Sciences* 102 (17):5953-5957.

Keselowsky, Benjamin G., David M. Collard, and Andrés J. García. 2003. Surface chemistry modulates fibronectin conformation and directs integrin binding and specificity to control cell adhesion. *Journal of Biomedical Materials Research Part A* 66A (2):247-259.

Lan, Michael A., Charles A. Gersbach, Kristin E. Michael, Benjamin G. Keselowsky, and Andres J. Garcia. 2005. Myoblast proliferation and differentiation on fibronectin-coated self assembled monolayers presenting different surface chemistries. *Biomaterials* 26 (22):4523-4531.

Leahy DJ, Aukhil I , Erickson HP. 1996. 2.0 A crystal structure of a four-domain segment of human fibronectin encompassing the RGD loop and synergy. *Cell* 84:155-164.

Lee, Jin Ho, Gilson Khang, Jin Whan Lee, and Hai Bang Lee. 1998. Interaction of Different Types of Cells on Polymer Surfaces with Wettability Gradient. *Journal of Colloid and Interface Science* 205 (2):323-330.

Lee, Jin Ho, Sang Jin Lee, Gilson Khang, and Hai Bang Lee. 2000. The Effect of Fluid Shear Stress on Endothelial Cell Adhesiveness to Polymer Surfaces with Wettability Gradient. *Journal of Colloid and Interface Science* 230 (1):84-90.

Lee, Mark H., Paul Ducheyne, Laura Lynch, David Boettiger, and Russell J. Composto. 2006. Effect of biomaterial surface properties on fibronectin-alpha5beta1 integrin interaction and cellular attachment. *Biomaterials* 27 (9):1907-1916.

Li, Fang, Bin Li, Qing-Ming Wang, and James H. C. Wang. 2008. Cell shape regulates collagen type I expression in human tendon fibroblasts. *Cell Motility and the Cytoskeleton* 65 (4):332-341.

Llopis-Hernandez, V, Patricia Rico, J Ballester-Beltran, David Moratal, and M Salmeron-Sanchez. 2011. Role of Surface Chemistry in Protein Remodeling at the Cell-Material Interface. *PLoS ONE* 6 (5):1-11.

Lo, Chun-Min, Hong-Bei Wang, Micah Dembo, and Yu-li Wang. 2000. Cell Movement Is Guided by the Rigidity of the Substrate. *Biophysical journal* 79 (1):144-152.

Michael, KE, VN Vernekar, BG Keselowsky, JC Meredith, RA Latour, and AJ Garcia. 2003. Adsorption-induced conformational changes in fibronectin due to interactions with well-defined surface chemistries. *Langmuir* 19:8033-8040.

Moore, Nicole M., Nancy J. Lin, Nathan D. Gallant, and Matthew L. Becker. 2010. The use of immobilized osteogenic growth peptide on gradient substrates synthesized via click chemistry to enhance MC3T3-E1 osteoblast proliferation. *Biomaterials* 31 (7):1604-1611.

Moore, Nicole M., Nancy J. Lin, Nathan D. Gallant, and Matthew L. Becker. 2011. Synergistic enhancement of human bone marrow stromal cell proliferation and osteogenic differentiation on BMP-2-derived and RGD peptide concentration gradients. *Acta Biomaterialia* 7 (5):2091-2100.

Mosher, Deane F, and Leo T Furcht. 1981. Fibronectin: Review of its Structure and Possible Functions. *J Investig Dermatol* 77 (2):175-180.

Palchesko RN, Zhang L, Sun Y, and Feinberg AW. 2012. Development of Polydimethylsiloxane Substrates with Tunable Elastic Modulus to Study Cell Mechanobiology in Muscle and Nerve. *PLoS ONE* 7 ((12): e51499. doi:10.1371/journal.pone.0051499).

Pelham, Robert J, and Yu-li Wang. 1997. Cell locomotion and focal adhesions are regulated by substrate flexibility. *Proceedings of the National Academy of Sciences* 94 (25):13661-13665.

Phillips, J. E., T. A. Petrie, F. P. Creighton, and A. J. Garcia. 2010. Human mesenchymal stem cell differentiation on self-assembled monolayers presenting different surface chemistries. *Acta Biomaterialia* 6 (1):12-20.

Roberson, Sonya V., Albert J. Fahey, Amit Sehgal, and Alamgir Karim. 2002. Multifunctional ToF-SIMS: combinatorial mapping of gradient energy substrates. *Applied Surface Science* 200 (1“4):150-164.

Ruoslahti, E. 1988. Fibronectin and its receptors. *Annu Rev. Biochem* 57:375-413.

Toworfe, George K., Russell J. Composto, Christopher S. Adams, Irving M. Shapiro, and Paul Ducheyne. 2004. Fibronectin adsorption on surface-activated poly(dimethylsiloxane) and its effect on cellular function. *Journal of Biomedical Materials Research Part A* 71A (3):449-461.

Williams, Corin, Angela W. Xie, Masayuki Yamato, Teruo Okano, and Joyce Y. Wong. 2011. Stacking of aligned cell sheets for layer-by-layer control of complex tissue structure. *Biomaterials* 32 (24):5625-5632.

Yliperttula, Marjo, Bong Geun Chung, Akshay Navaladi, Amir Manbachi, and Arto Urtti. 2008. High-throughput screening of cell responses to biomaterials. *European Journal of Pharmaceutical Sciences* 35 (3):151-160.

Zapata, Pedro, Jing Su, Andrés J. García, and J. Carson Meredith. 2007. Quantitative High-Throughput Screening of Osteoblast Attachment, Spreading, and Proliferation on Demixed Polymer Blend Micropatterns. *Biomacromolecules* 8 (6):1907-1917.

CHAPTER 6

FABRICATION OF COMBINATORIAL BIOMATERIALS TO SCREEN CELL MECHANOTRANSDUCTION

6.1 Introduction

Biomaterials for tissue engineering have evolved over the years and increasingly need to be functional materials that elicit specific responses at the cellular and molecular levels. Cells constantly perceive and respond to multiple stimuli in the context of the microenvironment which influences cell behavior. Some important factors include soluble chemical signals, interacting protein sequences and the mechanical properties of the extracellular matrix: both the topography of the surface and the inherent bulk material properties (Wong, Leach, and Brown 2004). These signals can trigger migration in the form of chemotaxis, mechanotaxis and haptotaxis (Redd et al. 2006; Haga et al. 2005). Also, cell-matrix adhesion is a dynamic process that includes both outside-in and inside-out signaling events at the interface (Gallant ; Garcia and Gallant 2003). This makes it imperative to comprehend the multifaceted aspects of cell-biomaterial interfacial communication.

Matrix property gradients are also seen naturally *in vivo* in the form of graded differences in mineral density and porosity of core bone structure to outer trabecular bone (Karageorgiou and Kaplan 2005), structural variations in teeth, interfacial tissues like cartilage to bone and ligament to bone, and in physiological processes such as embryogenesis and wound healing (Wu et al. 2012; Singh, Berkland, and Detamore 2008; Seidi et al. 2011).

Fabrication of single gradient materials, especially surface chemistry, and their effect on cell functionality was discussed in Chapter 5. For instance, gradients in growth factors have shown to have an impact on cell migration as exhibited by directionality and migration of vascular smooth muscle cells toward high density regions of basic fibroblast growth factor (Wu et al. 2014). Since numerous factors contribute to cell response, sorting through each of them individually can cause considerable delay to move a new product from conception to reaching market (Simon and Lin-Gibson 2011). Therefore, multifactor materials that have variations in two or more different properties allow for obtaining more information from an experiment with a gradient of a single independent variable. Moreover, there is the additional advantage of assessing cell response in a more comprehensive manner that more closely mimics the complexity of the native extracellular matrix.

While there have been some studies with multiple gradients, many of them involve the gradients varying in chemical properties and blends of different polymers. 2D gradient materials that have biaxial or dual gradients in bulk physical properties in combination with another parameter gradient, especially using the same principal material are limited to the following. Orthogonal gradients with thiol based surface chemistry gradients on gold with different terminal functional groups have been reported (Beurer et al. 2010; Venkataraman et al. 2014). A two dimensional gradient was made with plasma polymerization of allylamine on polypropylene material and was used to screen cell adhesion which correlated with amine content on gradients.(Mangindaan, Kuo, and Wang 2013). Another instance of 2D surface gradients through plasma polymerization was used to study mesenchymal stem cells adhesion that correlated with acrylic acid coating. (Wang et al. 2015) Meredith et al developed an orthogonal combinatorial gradient with two polymeric

blends that was orthogonally annealed with a gradient in temperature which was instrumental in finding increased osteoblast differentiation at equal blend of both polymers at 105°C.(Meredith et al. 2003). Osteoblast proliferation was found to be enhanced on the smoother polymer of a two polymer orthogonal strip film gradient that was also annealed to obtain a gradient in roughness (Simon Jr et al. 2005).

Our aim was to fabricate 2D gradient biomaterials with gradients of surface chemistry cues and matrix stiffness to screen cell response. Discrete compositions of PDMS with varying stiffness have been investigated before by combining different formulations of commercially available PDMS (Palchesko RN et al. 2012) or by varying the concentration of crosslinking agents (Brown, Ookawa, and Wong 2005). A gradient in mechanical stiffness using PDMS has been reported by controlling the directionality of the curing process of PDMS by placing the PDMS base and crosslinker mixture vertically on hot plate, although the resulting range of stiffness was narrow (Wang, Tsai, and Voelcker 2012). In chapters 4 and 5, the fabrication of a single gradient biomaterial with a gradient in surface chemistries on PDMS and cell interactions with it were discussed in detail. Since cells respond to multiple cues *in vivo*, a biomaterial for *in vitro* investigations that has both a physical parameter gradient in the form of mechanical stiffness and a surface chemistry gradient takes us a step closer to recapitulating the complexity of cell microenvironment and understanding how cells process multiple signals. To our knowledge, this is the first time that a 2D gradient platform with mechanical stiffness and surface chemistry gradients has been engineered using PDMS.

6.2 Experimental Section

- Tensile testing of discrete PDMS formulations with varying crosslinker concentrations

Mechanical characterization of discrete PDMS having varying crosslinking concentrations were done to estimate their Elastic Moduli. This was done to estimate elastic modulus and approximately ensure a wide range of stiffness in the future PDMS material that would have a continuous Young's modulus gradient. Crosslinked networks of PDMS samples with varying stiffness were created with modulation of base to cross linker ratio. Mechanical testing to estimate elastic modulus of these samples was performed using conventional tensile testing method and elastic moduli of discrete samples were determined (Brown, Ookawa, and Wong 2005; Pelham and Wang 1997).

Varying combinations of base to cross-linker ratios of PDMS were mixed, degassed and cured for 4 days at 65°C.Cured polymeric samples were first subjected to a creep test (twenty four hours) to confirm their elastic behavior. This was followed by tensile testing of samples as done by Pelham and Wang(Pelham and Wang 1997) to determine elastic modulus using Hooke's Law ($\sigma = E.\varepsilon$) where σ is stress in Pascals, ε is the strain and E the elastic modulus in Pascals. Samples with varying cross linker concentrations of 10% (n=5), 5% (n=4), 3.3% (n=4), 2.5% (n=2) and 2% (n=3) mass fraction were found to be elastic. The formulation with crosslinker of 1.67 weight % exhibited creep and therefore was excluded from tensile testing since it exhibited some viscoelastic behavior.

- Combinatorial biomaterial fabrication

The assembly of combinatorial biomaterial using PDMS was done in two phases. Briefly, the first phase involved the fabrication of mechanical gradient material using PDM having a bulk stiffness gradient where one end had the highest modulus of elasticity that gradually tapered to the least modulus of elasticity at the other end. In the second phase, the surface of a crosslinked mechanical stiffness gradient material was modified with silane chemistry and ultraviolet oxidation treatment to obtain a surface chemistry gradient atop the stiffness gradient. In this manner, a truly spatiotemporal combinatorial biomaterial was procured, encompassing wide ranges of both mechanical and chemistry gradients. The details of fabrication are furnished below.

- Mechanical stiffness gradient fabrication

Two formulations of the PDMS (Sylgard 184, Dow corning) was used to create the mechanical gradient. One formulation contained 10% by weight crosslinker (*stiff* PDMS) while the other mixture had 1.43% by weight crosslinker (*soft* PDMS). The base and crosslinker was mixed thoroughly and then degassed under vacuum to remove air bubbles. A red dye, Sudan IV (Sigma Aldrich, St Louis, MO) was added to the *soft* PDMS mixture to aid in visualization of the gradient after deposition. The dye itself was dissolved in toluene (~35mg in 2000 ul) and filtered using a 0.45 µm syringe filter after which 500 ul was added to 50 ml of *soft* PDMS.

The *soft* and *stiff* PDMS fractions/combinations were then separately loaded in two 10 ml syringes (BD, New Jersey) and mounted on NE 1000 single syringe pumps (New Era Pump Systems, Inc, Farmingdale, NY). The experimental set up used to fabricate mechanical gradients is shown in Figure 6.1. The two pumps were run using the software SyringePumpPro, where one had a linearly

increasing profile from 0 to 125 ml/hr while the other ramped down linearly from 125 to 0 ml/hr over 50 s (plus 14 s constant pressure to expel the mixed solution). These inverse ramping profiles of the syringe pumps were adapted from method described in Smith Callahen et al (Smith Callahan, Ganios, et al. 2013; Smith Callahan, Policastro, et al. 2013). The contents from both syringes flowed into a Y connecter and were mixed well downstream using a static mixer (Omega Engineering Inc., Stamford, CT). The combined gradient was deposited onto a glass slide (75x50, Fisher Scientific) that was placed/perched on a moving stage (PHD 2000 Syringe Pump, Instech Laboratories Inc., PA).The gradient was deposited on 50 x 50 mm of the original 75 x 50 mm of glass slide. The PDMS mechanical gradients were cured overnight in the oven at 65°C.

- Surface chemistry gradient fabrication on mechanical gradient

The mechanical gradient was first sonicated in 75% ethanol to remove physical impurities. After drying the gradient substrate under vacuum, it was oxygen plasma cleaned (Plasma Etch PE-50, Carson City, NV) for 5 minutes at 100 watts. A monolayer of silane, octyldimethylcholorosilane (ODMS) was deposited through 24 hours of chemical vapor deposition. This was done under vacuum with the sample exposed to vapor of 1:1 mixture of ODMS and toluene solution. The silane layer on the mechanical gradient was then subjected to a stringently controlled Ultraviolet Oxidation (UVO) treatment. Ultraviolet light with 254 and 185 nm wavelength from a /fixed immobile lamp shone on sample placed on a moving stage that was controlled via LabVIEW interface The orientation of the newly generated surface chemistry gradient was perpendicular to the original mechanical stiffness gradient. Extended exposure time with a maximum of 380s seconds at one end of sample, that systematically reduced to a minimum of 0s exposure at the other

end In this manner a combinatorial biomaterial was fabricated with a mechanical gradient running across the ‘x’ axis and a surface chemistry gradient along the ‘y’ axis.

- Combinatorial biomaterial characterization

Mechanical gradients were characterized using a combination of compression tests and spectrophotometric analysis based on the Sudan IV dye added to the *soft* PDMS mixture during manufacture of mechanical gradient to facilitate visualization of the gradient. This meant that one end of gradient was a darker red with the color fading out across the length with the other end being clear typical of PDMS.

A standard curve was created using discrete blends of the 10% weight *stiff* PDMS and the 1.43% weight *soft* PDMS which contained the Sudan IV dye (Sigma Aldrich) in a 0.01% weight composition. The six discrete compositions had the following crosslinker concentrations: 10%, 7.9%, 5.7%, 3.6%, 2.5% and 1.43 crosslinker weight. Both compression testing and spectrophotometric analysis were conducted on each of these six discrete samples to obtain a standard curve that deduced the correlation between the measured elastic modulus and spectroscopic reading. This was followed by statistical curve fit on the standard curve data obtained from compression test and spectrophotometric analyses using Sigma Plot 11.2. The statistical data fit allowed for estimation of elastic modulus from spectrophotometric analysis of mechanical gradients. Spectroscopic analysis of mechanical gradient generated readings from 5 x 5 points on the gradient. This was preferred over the more labor intensive and time consuming process of compression tests. However, a comparison of data from direct compression testing and the indirect spectroscopic analysis on a mechanical gradient was also performed.

Spectroscopic scans involved a full visible spectrum scan (300 nm-700 nm) with an interval of 10 nm was performed on the discrete samples containing *stiff* and *soft* PDMS blends and three mechanical gradient samples. The entire 50x50 mm area was scanned during spectroscopic analysis of the three mechanical gradients. Spectroscopy analysis of the mechanical gradients enabled to indirectly gauge the stiffness gradient The maximum absorbance peak at 520 nm is distinctive of the Sudan 1V dye (Di Anibal et al. 2009).

During the compression testing procedure, strain was limited up to 10% by using different weight loads. This was to ensure that displacement occurred within the elastic range of PDMS. The elastic modulus is obtained using the following equation that has been previously used to determined modulus of soft tissue (Krouskop et al. 1998).

$$E = \frac{2\left(1-\nu^2\right)qa}{w}$$

The elastic modulus is represented by E, radius of loaded area is a, q is the stress and υ is the poisson ratio with a value of 0.5. While the above mentioned spectroscopic analyses and compression tests characterization techniques gives a trend in mechanical properties of the gradient, a more detailed, automated and thorough characterization of the mechanical gradient using other procedures such as nanoindentation is still warranted.

The surface chemistry gradient was characterized through water goniometry/ contact angle measurements. Readings were taken along multiple columns and rows in a grid like pattern to ensure a comprehensive characterization. Water droplets were released from a syringe on the combinatorial sample every 5 mm along y axis and every 10 mm apart on the x axis. The Young Laplace fitting algorithm was then used to measure the contact angles.

- Cell culture

NIH/3T3 , a mouse embryonic fibroblast cell line, was purchased from American Type Culture Collection (ATCC) and cultured on tissue culture polystyrene in Dulbecco's Modified Eagle's Medium (DMEM, Invitrogen) that contained 100 units/ml penicillin and 100 ug/ml streptomycin (Invitrogen) and 10% new born calf serum (Invitrogen).

Control and 2D combinatorial gradient substrates were sterilized for 10 min in 70% ethanol and then rinsed with Dulbecco's phosphate buffered saline (DPBS, Invitrogen) three times. The substrates were first precoated with 10 μg/ml human plasma fibronectin (Gibco, Invitrogen) for 30 minutes and subsequently blocked with 1% bovine serum albumin (BSA, Fisher Scientific) for 30 minutes. Cells released from tissue culture dishes using Trypsin/EDTA (Invitrogen) were seeded cells at 40 cells/mm^2. Freshly seeded cells were left undisturbed in the biosafety cabinet for 30 minutes to facilitate cell attachment before transfer to the incubator. Plain glass slide (50x75mm) acted as a control to confirm that changes in cell morphology were due to underlying gradients on 2D combinatorial platform and not an artifact of the seeding procedure.

- High throughput cell functionality analysis: automated image capture and data extraction

After incubation for 16 hours, cells were fixed with 3.7% by mass formaldehyde (Invitrogen) in DPBS and permeabilized for 10 minutes using 0.5% by mass Triton X-100 in buffered saline. For high throughput imaging of NIH3t3 cells, nuclei (Hoechst 33342, Invitrogen) and bodies (AlexaFluor 488 maleimide, Invitrogen) were fluorescently labeled for one hour.

Cells were imaged and analyzed using NIS Elements software and a Nikon Eclipse Ti-U microscope (Nikon Instruments, Melville NY) equipped with fluorescence filter sets. A computer controlled stage was automated to capture 90 images on the 2D gradient. This included 3 non overlapping images at 30 points along 5 rows and 6 columns spread over the 50 x 50 mm substrate. A binary mask was created by automatically applying contrast thresholding to each image so that cell spreading area and nuclei count could be automatically extracted.

- Statistical and correlation analyses

SigmaPlot 11.0 (Systat Software, San Jose, CA) was used to perform regression analyses and curve fits on obtained data. A *p*-value of <0.05 obtained for the regression line slope was considered a significant correlation between the concerned variables. Error bars in all graphs indicate standard deviation from the mean.

6.3 Results and Discussion

- Tensile testing of discrete PDMS formulations with varying crosslinker concentrations

Initial creep testing of differently crosslinked polymeric specimens indicated elastic behavior for formulations containing 10, 5, 3.3, 2.5 and 2.0 weight% crosslinker concentration. Formulations with less crosslinking agent such as the 1.67% exhibited viscoelastic behavior and were excluded from the tensile testing study. Figure 6.2 depicts elastic moduli of different PDMS compositions ranging from 1.55 ± 0.12 MPa to 0.02±0.001 MPa. A hundred fold magnitude of mechanical stiffness range was obtained by varying crosslink density. These values concur with reports of Brown et al for mechanical characterization of PDMS networks that ranged from 1.78MPa for 10 weight% to 0.05 for 2.0 weight% (Brown, Ookawa, and Wong 2005).

- Combinatorial biomaterial characterization

Compression testing of the discrete blends of *soft* and *stiff* PDMS in different ratios yielded their elastic moduli respective to the total crosslinker concentration in the blend and this data is shown in Figure 6.3. Error bars show standard deviation from n=5 measurements on each sample. Spectroscopic analysis was also conducted on these discrete blends of *stiff* and *soft* PDMS based on the absorbance of the Sudan IV dye at 520 nm that was mixed into the *soft* PDMS, and this is illustrated in Figure 6.4. The error bars represent standard deviation among n=16 readings on each of the 6 samples. The data from Figure 6.3 and 6.4 was utilized to generate a standard curve as shown in Figure 6.5. Multiple types of data fitting were attempted with the inverse third order fitting emerging with the highest coefficient of determination R^2 of 0.97. The coefficient of correlation obtained was 0.98 showing dependence of elastic modulus on the absorbance at 520 nm for each crosslinker concentration.

Spectrophotometric analysis was used to scan mechanical gradients (N=3) over the entire visible spectrum, with the peak at 520 nm. As expected, the highest peak was observed at the least stiff end of the gradient which had the maximum amount of the Sudan IV dye since it was added to the *soft* PDMS. Absorbance readings were obtained from 25 points along 5 rows and 5 columns on each mechanical gradient. The dye concentration which progressively diminished across the sample as the blend composition changed to stiff (10% crosslinker weight) PDMS was well reflected in the trend of decreased absorbance at 520 nm. Figure 6.6 shows the reduction in the absorption peak from a mechanical gradient. The absorbance data obtained from three mechanical gradients is shown in Figure 6.7 with the variation within each gradient displayed by error bars. The equation of the fitted inverse third order curve obtained from Figure 6.5,

f=y0+ (a/x) + (b/x^2) +(c/x^3), was used to estimate the elastic moduli indirectly for mechanical gradients from their spectrophotometric measurements depicted in in Figure 6.7. The estimated stiffness of three mechanical gradients ranged from 1.97±0.24 MPa to 0.06±0.004 MPa (Figure 6.8).

Compression tests were performed on a mechanical gradient for comparison with the indirect estimated stiffness of the same gradient from spectroscopic measurements (Figure 6.9). It was observed that while there was a major variation at one position on the mechanical gradient, the other values were in close agreement. Also, the overall range of stiffness in a mechanical gradient from the direct compression tests (1.9 to 0.004 MPa) and indirect estimation from spectroscopic characterizations (2.2 to 0.06 MPa) indicated a similar trend.

The direct compression test measurements and indirect spectroscopic measurements provided the trend and an approximate range of elastic modulus from one end of gradient to the other. However, a more accurate and high throughput mode of characterization, such as nanoindentation, is required for accurate characterization of fabricated mechanical gradients.

Contact angle measurements were taken along three columns with five readings separated by 10mm on alkylsilane deposited mechanical gradients. The average contact angle was 107±1°. After UVO treatment, water contact angle measurements were taken along four columns that spans the 50mm width on each sample. Nine measurements were taken every 5 mm apart in each column. The variation in surface chemistry gradients between different columns within one 2D gradient can be viewed in Figure 6.10. The hydrophilic end was 16±6° and the hydrophobic end was 91±9°.

Figure 6.11 displays alkylsilane deposited chemistries and surface gradient chemistries of N=3 2D gradients. The average uniform chemistry was at 107±1°. Post UVO, the surface chemistries ranged from 16±1° to 92±4°. Figure 6.12 shows the experimental set up for fabricating surface gradients on mechanical gradients. Also, it shows the flexibility of making different types of 2D combinatorial materials by tweaking the directionality of the surface gradient with respect to the mechanical gradient. For instance, Figure 6.13 demonstrates a 2D gradient with the surface gradient that runs along the direction parallel to the mechanical gradient. The hydrophilic end of the surface gradient is at the stiffest end while the hydrophobic is at the softest end. The surface gradient directionality may also be reversed as well with maximum UVO at the softest end of the mechanical gradient.

- NIH3T3 spreading on 2D combinatorial gradients

Fibroblast cells were seeded on both a control plain glass slide (50x75 mm, N=1) and 2D combinatorial biomaterials (50x50 mm, N=2). This was done as a preliminary experiment to gauge the scope of the newly fabricated 2D combinatorial gradient. Cell spreading on the control plain glass (Figure 6.14) was largely invariant and ranged from approximately 900-1200 μm^2. On the 2D combinatorial gradients, the maximum cell spreading was observed in the most hydrophobic region in an area of intermediate stiffness (2255±449 μm^2 at 20mm along mechanical gradient and 0mm on surface chemistry gradient) while the minimum cell spreading was on the hydrophilic region of the softer stiffness zone (716±391 μm^2 at 10 mm on mechanical gradient and 20mm on surface chemistry gradient). Another secondary region of enhanced spreading was also seen at a more hydrophilic zone of intermediate stiffness. These findings also highlight the fact that the maximum spreading was surprisingly not at the stiffest and most hydrophobic corner of the 2D

sample. This contrasts to the maximum fibroblast spreading on the hydrophobic regions on the stiff PDMS which represented the 1D surface chemistry gradients reported in Chapter 5 and the generally higher fibroblast spreading reported in literature on stiffest substrates used in each study (Gray, Tien, and Chen 2003; Lo et al. 2000; Pelham and Wang 1997). It was positive to note that regions of synergy and antagonism or 'hot spots' could be easily identified on the experimental samples and that cells responded differently to the presented combination of the dual gradients in surface chemistry and mechanical stiffness. Another important take away was that cell response on a 2D gradient substrate may vary from predictions based on observations of response to 1D material property gradients.

6.4 Conclusions

Tensile testing of differently cross linked PDMS networks through regulation of cross linker concentration yielded substrates that spanned a wide and physiologically relevant range of stiffness (1.55 ± 0.12 MPa to 0.02±0.001 MPa). A combinatorial biomaterial was successfully fabricated by computer controlled mixing of high and low crosslinker concentration solutions of the model biomaterial PDMS. This combinatorial biomaterial, 50mm by 50mm, encompasses within it two orthogonal gradients. One is a mechanical stiffness gradient that has been estimated indirectly to range from approximately 1.97±0.24 MPa to 0.06±0.004 MPa, and the second along the axis perpendicular to this stiffness gradient is a surface chemistry gradient ranging from 16±1° to 92±4° in water contact angle. The efficient methods in which the physical and chemical properties of the model material PDMS were modulated enabled the engineering of the final combinatorial platform presented in this study. Preliminary results from fibroblast spreading on the combinatorial biomaterial demonstrated that cell response was varied across the 2D gradient platform and also

displayed the potential to identify regions of synergy and antagonism that influence cell behavior. The findings also underscored the fact that cell response to two independently varied matrix properties will likely differ from superposition of cell responses to two single material properties.

6.5 Acknowledgements

I would like to thank Anthony Novak for help with tensile testing. I would also like to thank my lab mate Asma Sharfeddin for conducting compression tests, Erin Childers from the University of Akron who provided information for initial set up of the syringe pump system and Tim Burgess, CEO of SyringePumpPro based in Australia who provided customer service for using software that controls the pump system.

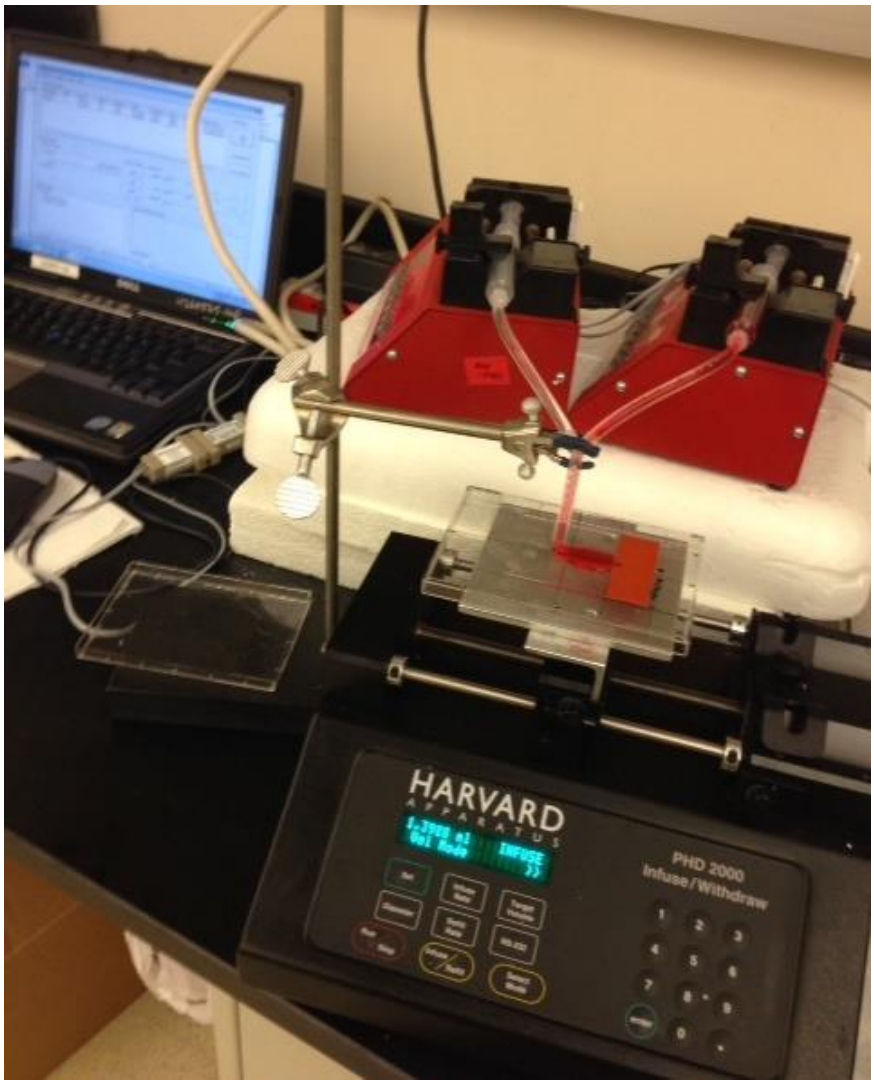

Figure 6.1 Experimental apparatus setup for mechanical gradient fabrication.

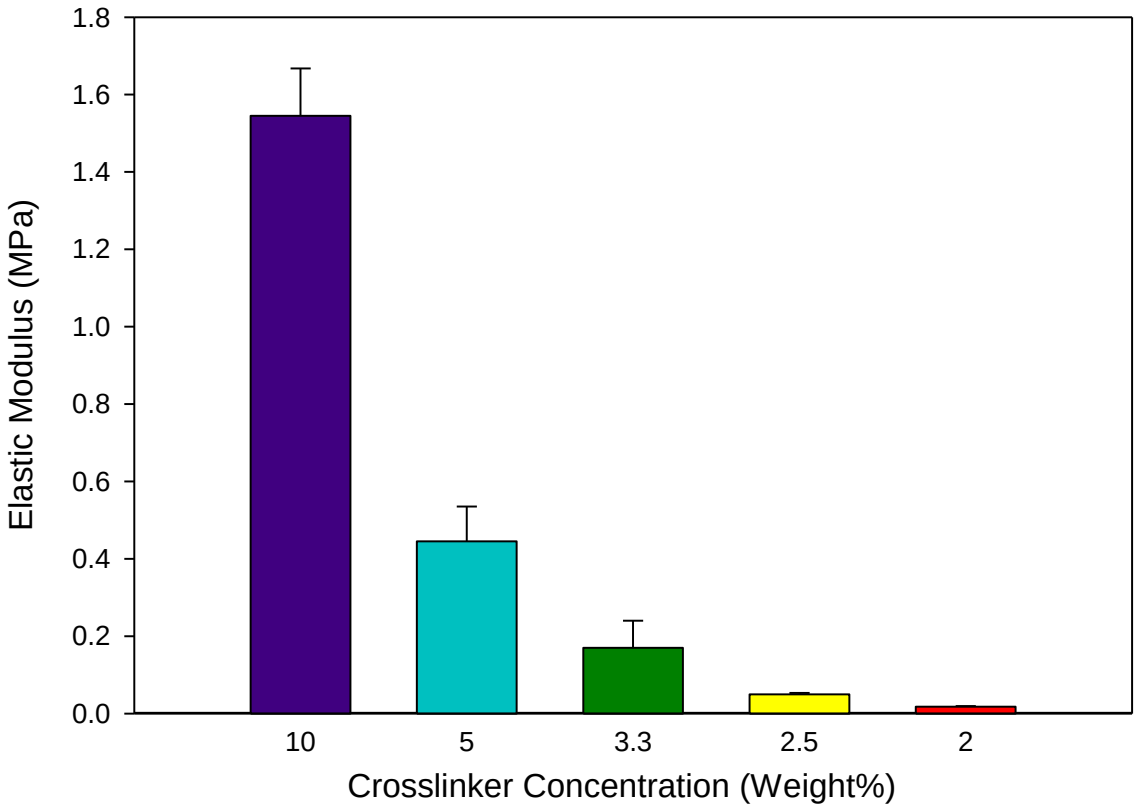

Figure 6.2 Elastic moduli of discrete PDMS networks with different formulations of crosslinker concentrations.

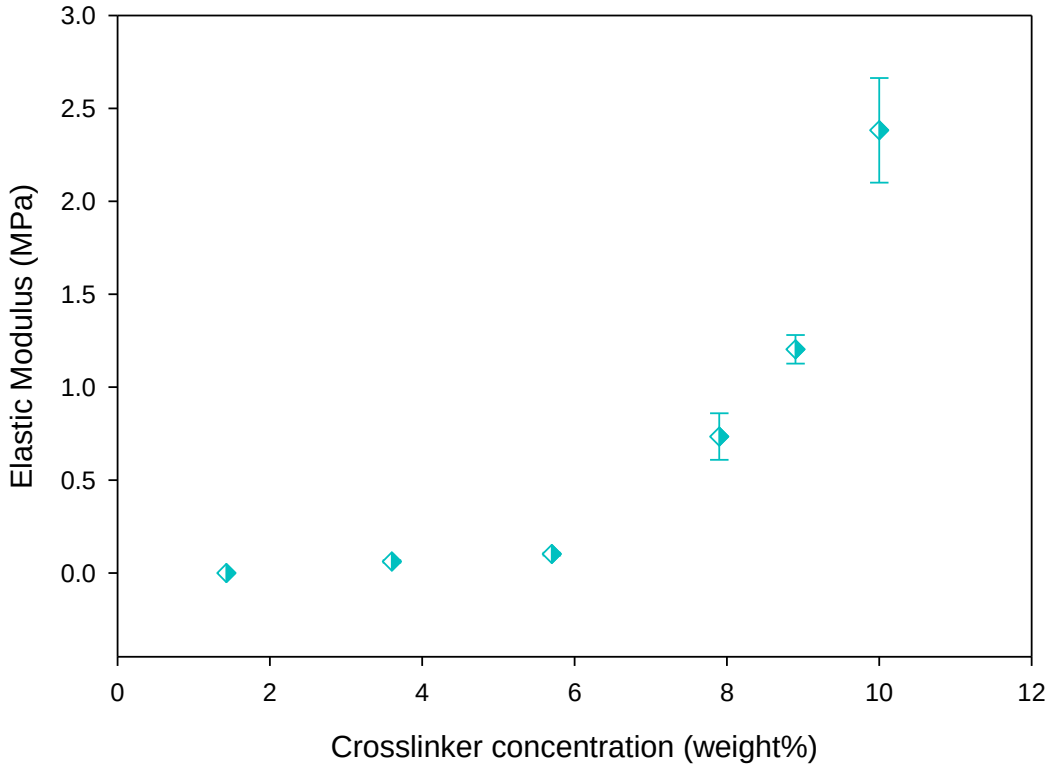

Figure 6.3 Elastic moduli from compression testing of discrete polymeric blends of *stiff* and *soft* PDMS.

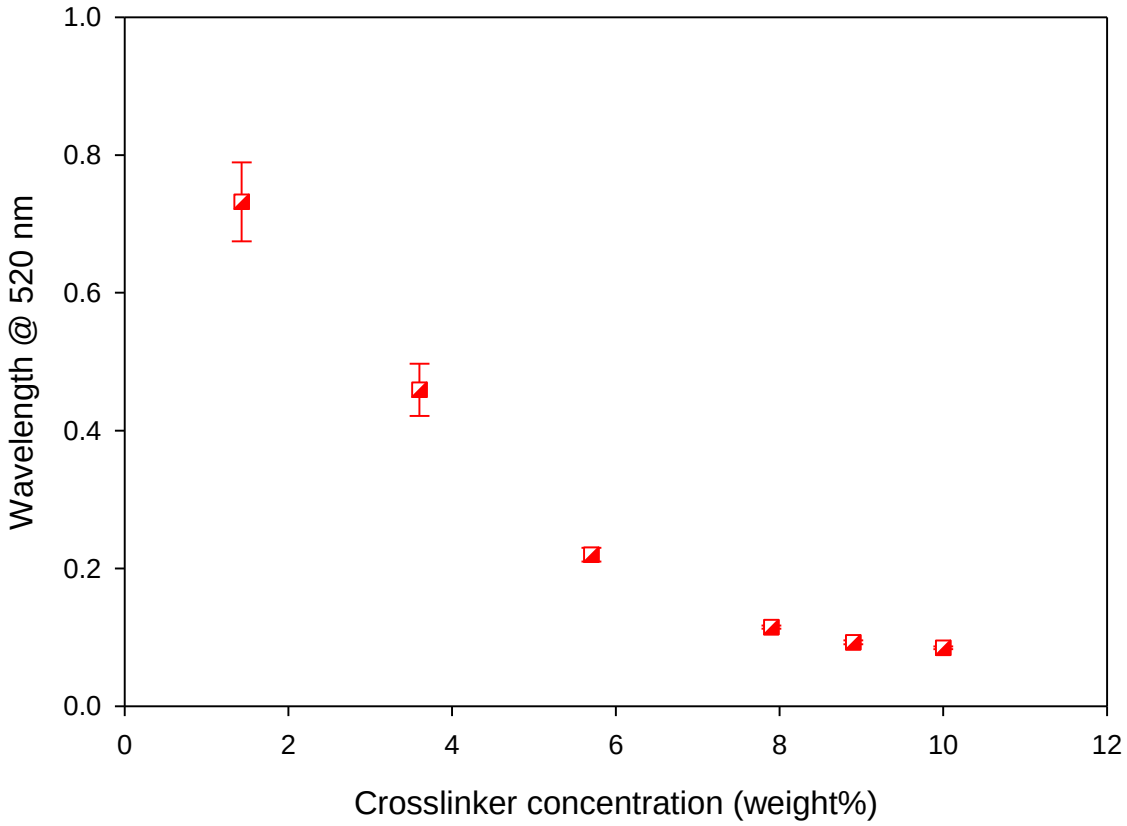

Figure 6.4 Absorbance at 520nm of discrete polymeric blends of *stiff* and *soft* PDMS. The differences in Sudan IV concentration in the discrete samples were measured using spectrophotometric analyses.

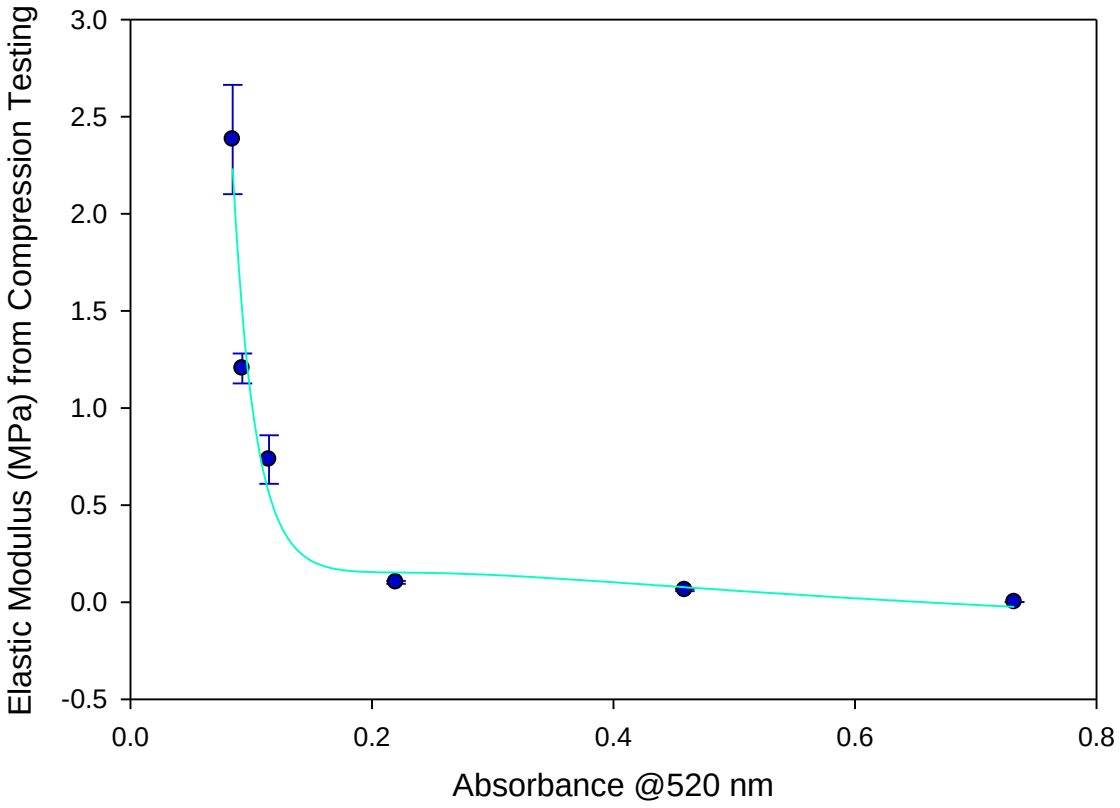

Figure 6.5 An inverse third order fit on a standard curve to obtain estimated elastic modulus on mechanical gradients. The standard curve was generated from a combination of direct compression testing and indirect spectroscopic absorbance measurements on discrete polymeric blends of *stiff* and *soft* PDMS.

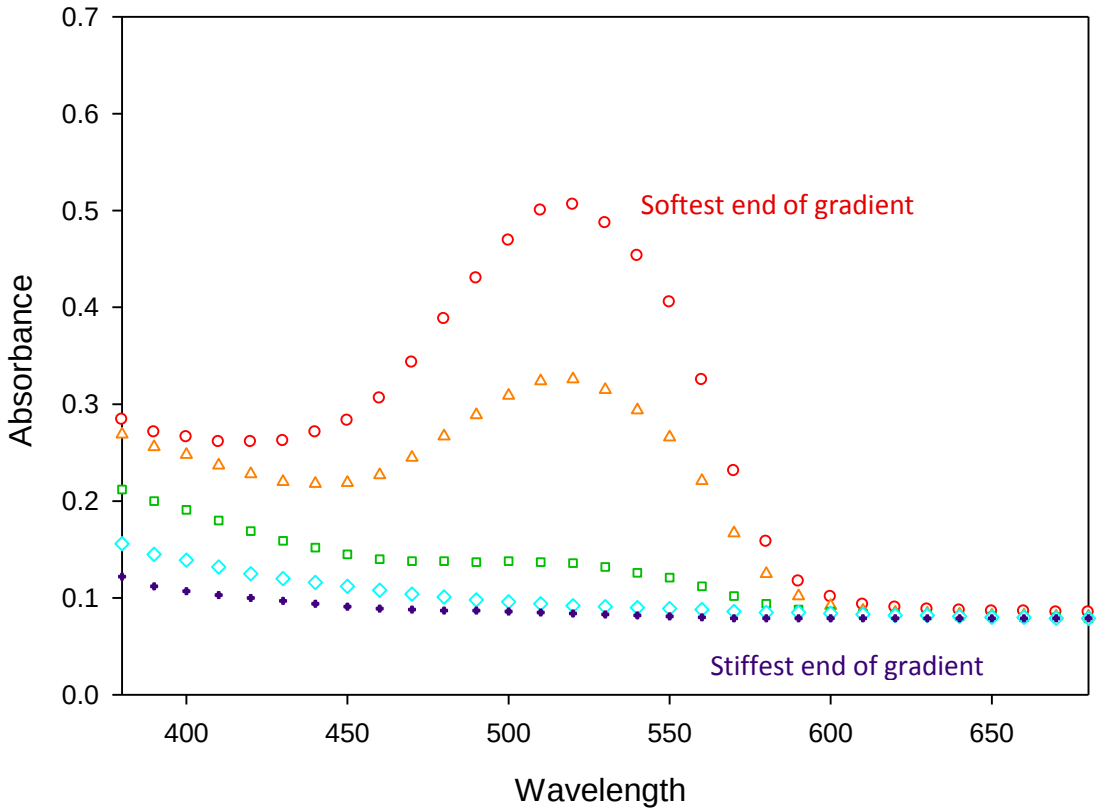

Figure 6.6 UV-vis absorbance spectra across a mechanical gradient sample. Higher absorbance peak correlates to higher dye concentration and lower modulus.

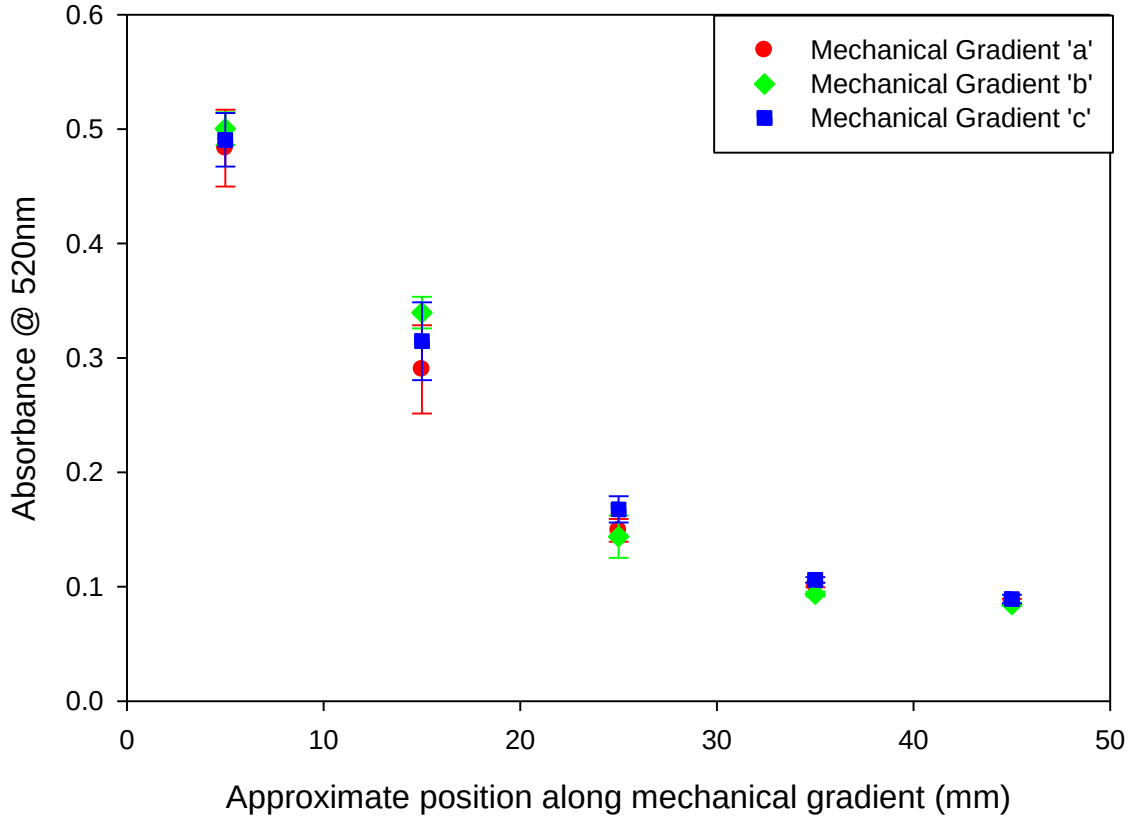

Figure 6.7 Variation in absorbance at 520 nm within and between three mechanical gradients. Highest absorbance is at the softest end of mechanical gradient that gradually decreases to a minimum at the stiffest end.

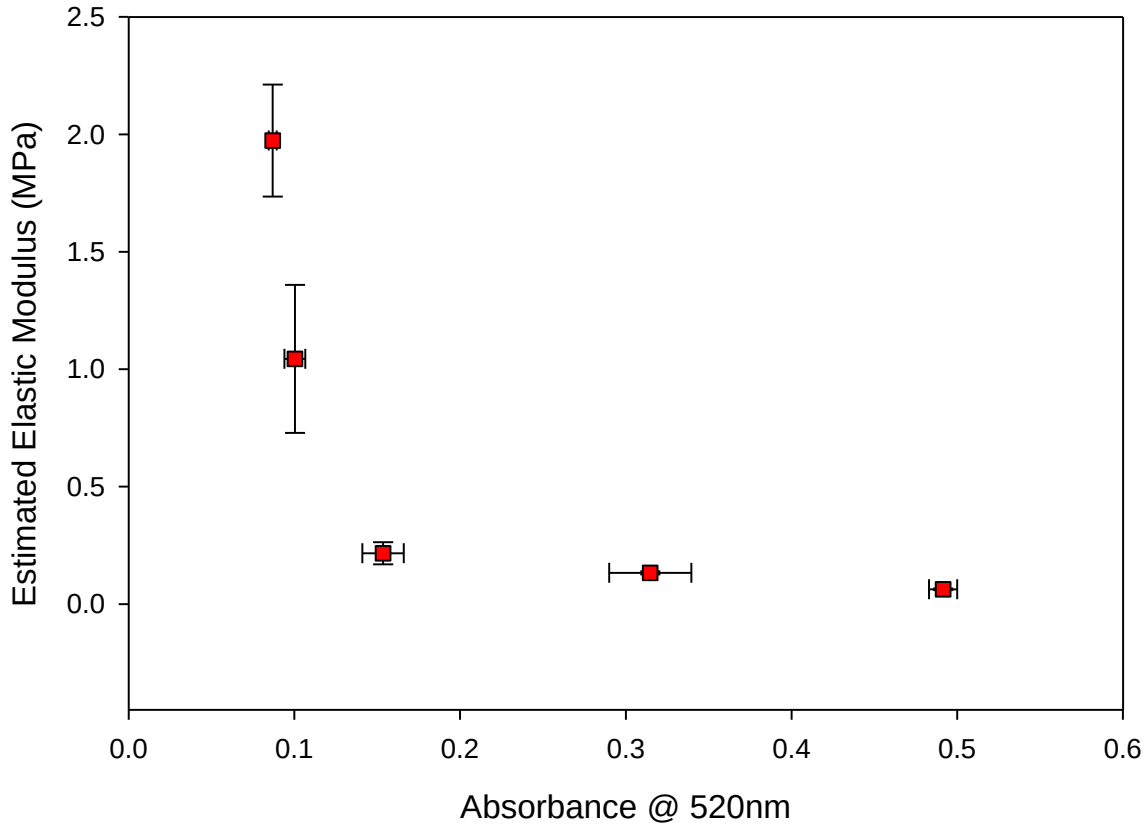

Figure 6.8 Estimated elastic moduli of three mechanical gradients. The moduli were indirectly estimated from absorbance values obtained from spectrophotometric analyses and further calculated from an inverse third order fit of a standard curve.

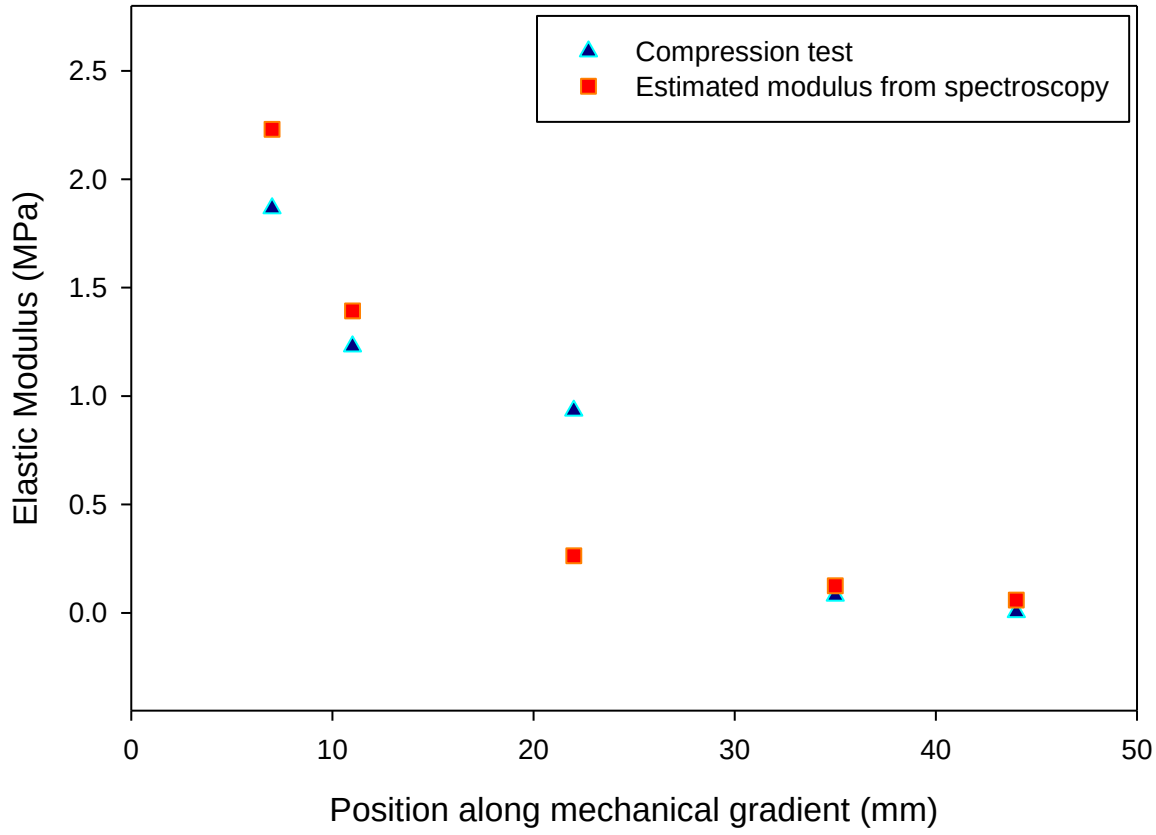

Figure 6.9 Comparison of moduli values measured directly from compression test vs absorbance from spectroscopy on a mechanical gradient.

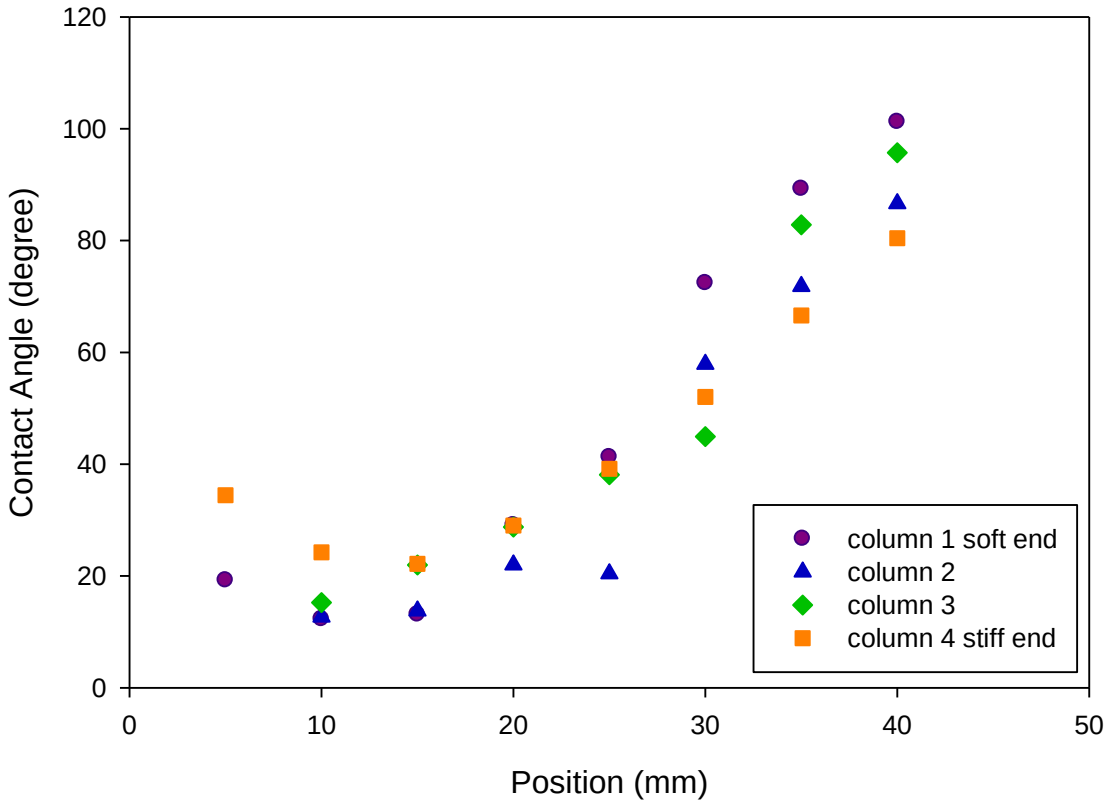

Figure 6.10 Photograph and graph of a 2D gradient surface chemistry gradient running perpendicular to bulk mechanical gradient on 2D combinatorial gradient.

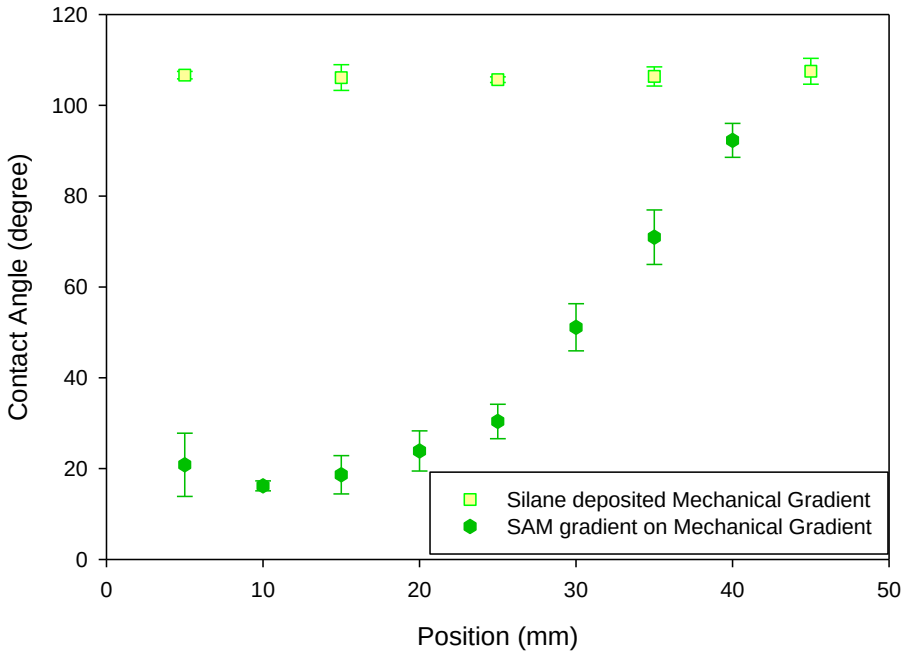

Figure 6.11 Surface chemistry gradients (orthogonal to bulk mechanical gradients) on three 2D combinatorial gradients.

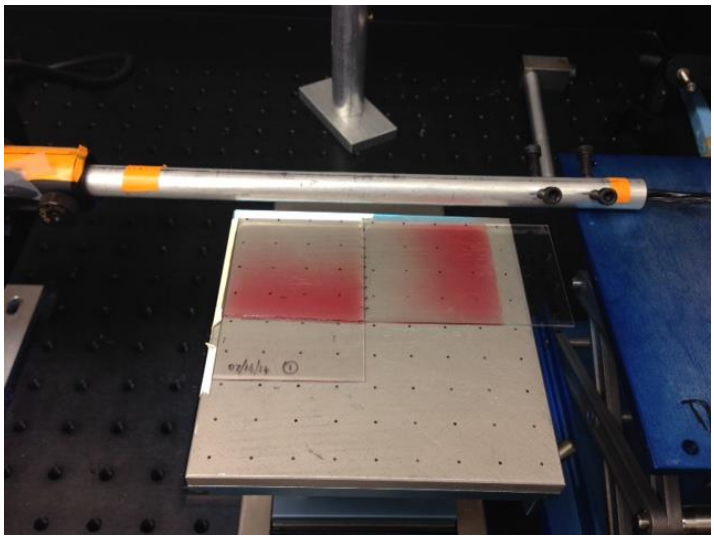

Figure 6.12 Generation of surface chemistry gradients with different directionalities on mechanical gradients.

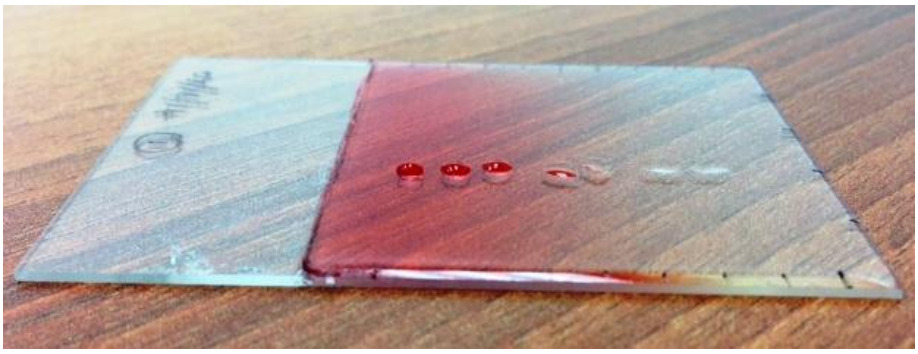

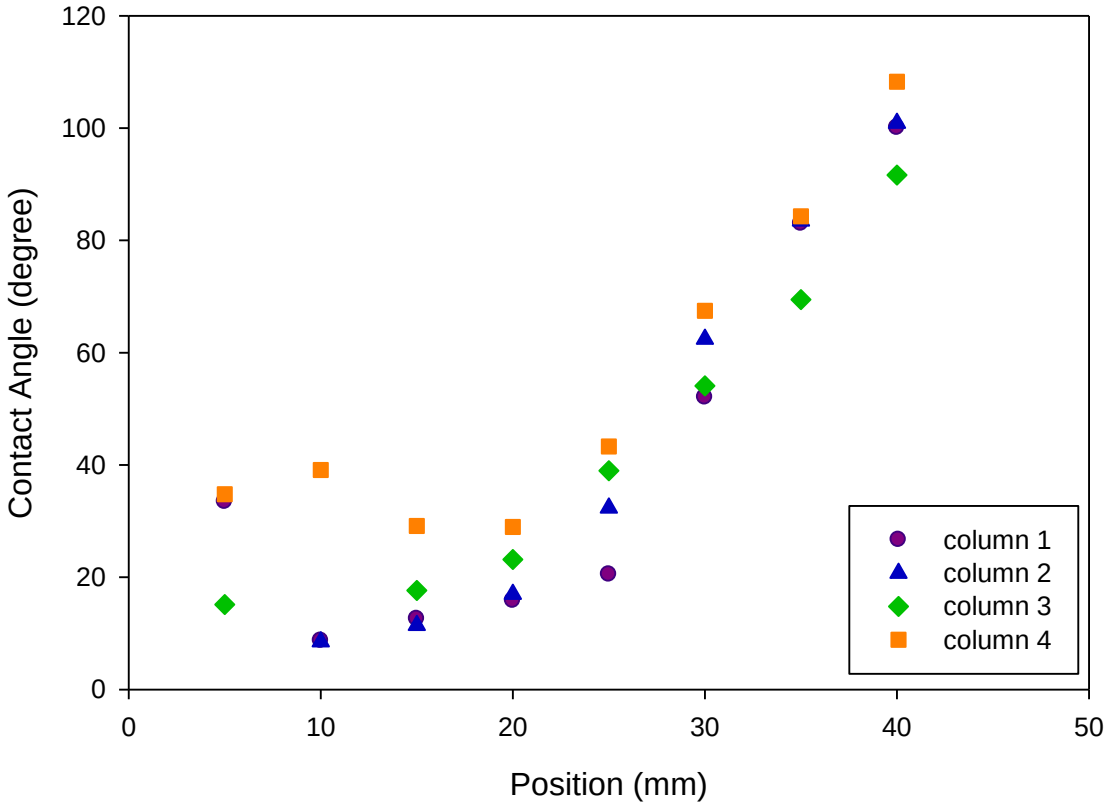

Figure 6.13 Photograph and graph of a 2D gradient with surface chemistry gradient running parallel to bulk mechanical gradient.

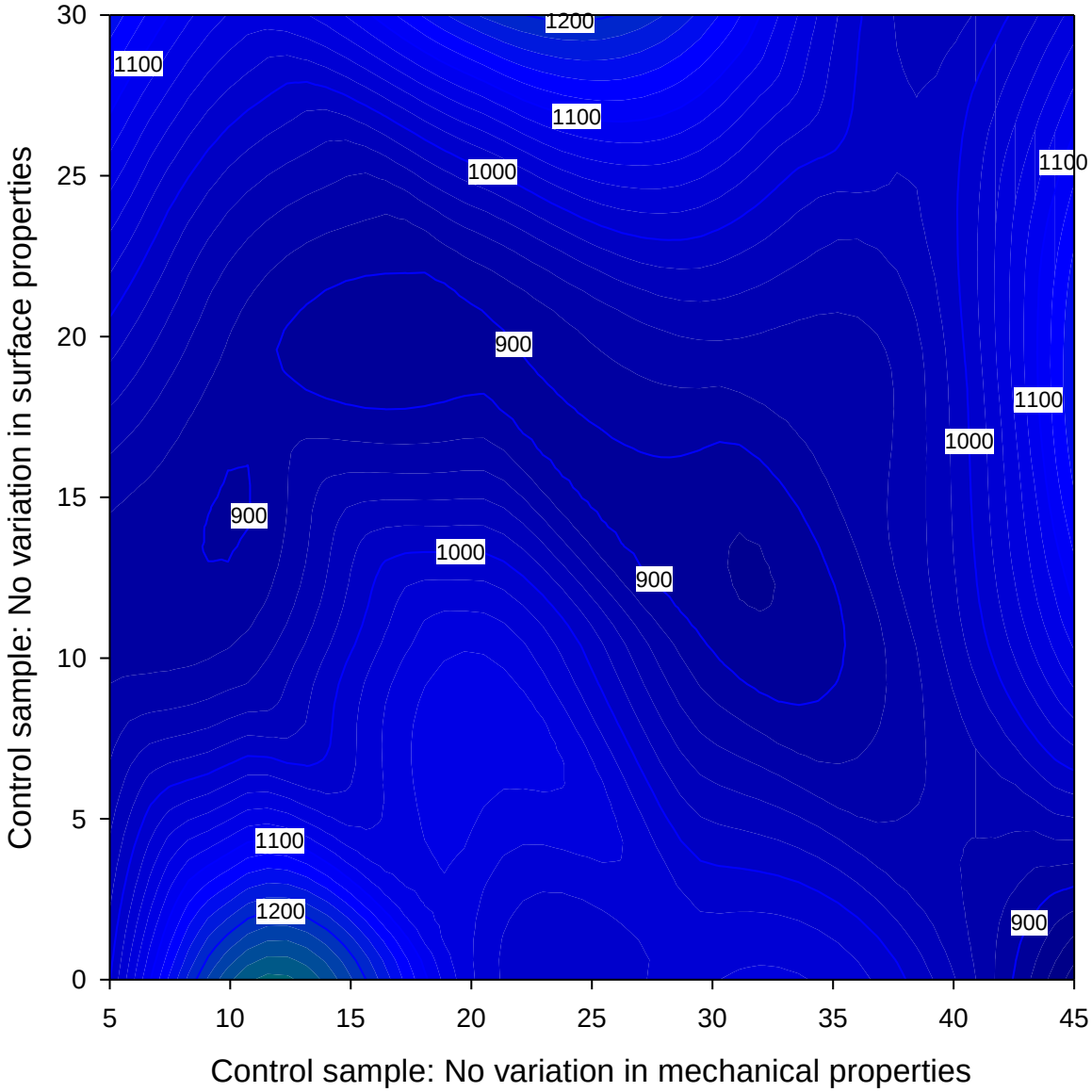

Figure 6.14 Contour plot of cell spreading on a control plain glass sample with uniform material properties.

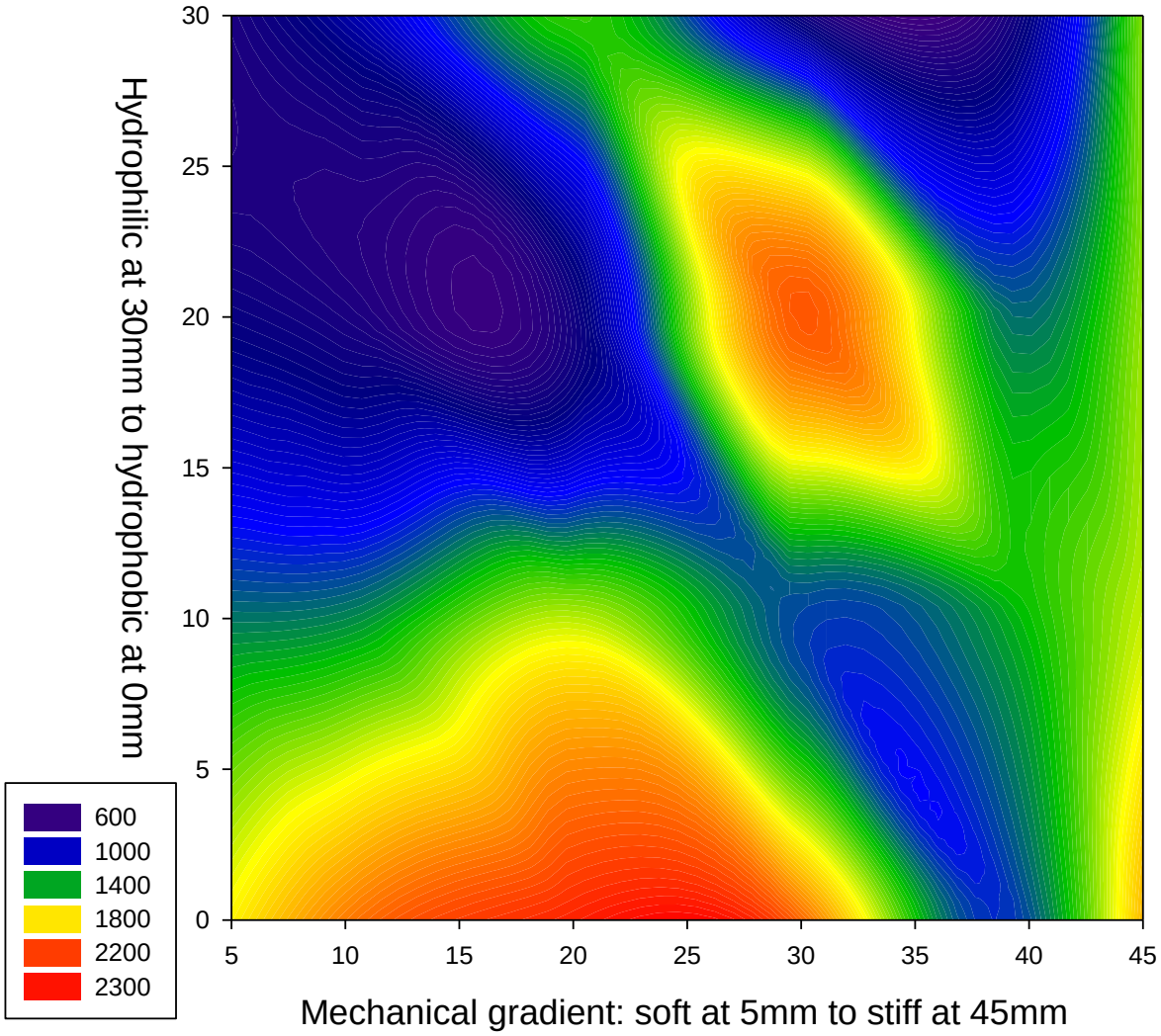

Figure 6.15 Contour plot of cell spreading on 2D combinatorial gradient biomaterials.

6.6 References

Beurer, Eva, Nagaiyanallur V. Venkataraman, Antonella Rossi, Florian Bachmann, Roman Engeli, and Nicholas D. Spencer. 2010. Orthogonal, Three-Component, Alkanethiol-Based Surface-Chemical Gradients on Gold. *Langmuir* 26 (11):8392-8399.

Brown, Xin Q, Keiko Ookawa, and Joyce Y Wong. 2005. Evaluation of polydimethylsiloxane scaffolds with physiologically-relevant elastic moduli: interplay of substrate mechanics and surface chemistry effects on vascular smooth muscle cell response. *Biomaterials* 26 (16):3123-3129.

Di Anibal, Carolina V., Marta Odena, Itziar Ruisánchez, and M. Pilar Callao. 2009. Determining the adulteration of spices with Sudan I-II-II-IV dyes by UV–visible spectroscopy and multivariate classification techniques. *Talanta* 79 (3):887-892.

Gallant, Nathan. Proposal: Combinatorial Biomaterial for Endothelial Cell Mechanobiology.

Garcia, Andrés, and Nathan Gallant. 2003. Stick and grip. *Cell Biochemistry and Biophysics* 39 (1):61-73.

Gray, Darren S., Joe Tien, and Christopher S. Chen. 2003. Repositioning of cells by mechanotaxis on surfaces with micropatterned Young's modulus. *Journal of Biomedical Materials Research Part A* 66A (3):605-614.

Haga, Hisashi, Chikako Irahara, Ryo Kobayashi, Toshiyuki Nakagaki, and Kazushige Kawabata. 2005. Collective Movement of Epithelial Cells on a Collagen Gel Substrate. *Biophysical Journal* 88 (3):2250-2256.

Karageorgiou, Vassilis, and David Kaplan. 2005. Porosity of 3D biomaterial scaffolds and osteogenesis. *Biomaterials* 26 (27):5474-5491.

Krouskop, Thomas A., Thomas M. Wheeler, Faouzi Kallel, Brian S. Garra, and Timothy Hall. 1998. Elastic Moduli of Breast and Prostate Tissues under Compression. *Ultrasonic Imaging* 20 (4):260-274.

Lo, Chun-Min, Hong-Bei Wang, Micah Dembo, and Yu-li Wang. 2000. Cell Movement Is Guided by the Rigidity of the Substrate. *Biophysical journal* 79 (1):144-152.

Mangindaan, Dave, Wei-Hsuan Kuo, and Meng-Jiy Wang. 2013. Two-dimensional amine-functionality gradient by plasma polymerization. *Biochemical Engineering Journal* 78 (0):198-204.

Meredith, J. Carson, Joe- L. Sormana, Benjamin G. Keselowsky, Andrés J. García, Alessandro Tona, Alamgir Karim, and Eric J. Amis. 2003. Combinatorial characterization of cell interactions with polymer surfaces. *Journal of Biomedical Materials Research Part A* 66A (3):483-490.

Palchesko RN, Zhang L, Sun Y, and Feinberg AW. 2012. Development of Polydimethylsiloxane Substrates with Tunable Elastic Modulus to Study Cell Mechanobiology in Muscle and Nerve. *PLoS ONE* 7 ((12): e51499. doi:10.1371/journal.pone.0051499).

Pelham, Robert J, and Yu-li Wang. 1997. Cell locomotion and focal adhesions are regulated by substrate flexibility. *Proceedings of the National Academy of Sciences* 94 (25):13661-13665.

Redd, Michael J., Gavin Kelly, Graham Dunn, Michael Way, and Paul Martin. 2006. Imaging macrophage chemotaxis in vivo: Studies of microtubule function in zebrafish wound inflammation. *Cell Motility and the Cytoskeleton* 63 (7):415-422.

Seidi, Azadeh, Murugan Ramalingam, Imen Elloumi-Hannachi, Serge Ostrovidov, and Ali Khademhosseini. 2011. Gradient biomaterials for soft-to-hard interface tissue engineering. *Acta Biomaterialia* 7 (4):1441-1451.

Simon, Carl G., and Sheng Lin-Gibson. 2011. Combinatorial and High-Throughput Screening of Biomaterials. *Advanced Materials* 23 (3):369-387.

Simon Jr, Carl G., Naomi Eidelman, Scott B. Kennedy, Amit Sehgal, Chetan A. Khatri, and Newell R. Washburn. 2005. Combinatorial screening of cell proliferation on poly(l-lactic acid)/poly(d,l-lactic acid) blends. *Biomaterials* 26 (34):6906-6915.

Singh, Milind, Cory Berkland, and Michael S. Detamore. 2008. Strategies and Applications for Incorporating Physical and Chemical Signal Gradients in Tissue Engineering. *Tissue Engineering. Part B, Reviews* 14 (4):341-366.

Smith Callahan, Laura A., Anna M. Ganios, Erin P. Childers, Scott D. Weiner, and Matthew L. Becker. 2013. Primary human chondrocyte extracellular matrix formation and phenotype maintenance using RGD-derivatized PEGDM hydrogels possessing a continuous Young's modulus gradient. *Acta Biomaterialia* 9 (4):6095-6104.

Smith Callahan, Laura A., Gina M. Policastro, Sharon L. Bernard, Erin P. Childers, Ronna Boettcher, and Matthew L. Becker. 2013. Influence of Discrete and Continuous Culture Conditions on Human Mesenchymal Stem Cell Lineage Choice in RGD Concentration Gradient Hydrogels. *Biomacromolecules* 14 (9):3047-3054.

Venkataraman, Nagaiyanallur V., Clément V. M. Cremmel, Christian Zink, Rebecca P. Huber, and Nicholas D. Spencer. 2014. Chapter 6 - Patterning Gradients. In *Methods in Cell Biology*, edited by P. Matthieu and T. Manuel: Academic Press.

Wang, Peng-Yuan, Lauren R. Clements, Helmut Thissen, Wei-Bor Tsai, and Nicolas H. Voelcker. 2015. Screening rat mesenchymal stem cell attachment and differentiation on surface chemistries using plasma polymer gradients. *Acta Biomaterialia* 11 (0):58-67.

Wang, Peng-Yuan, Wei-Bor Tsai, and Nicolas H. Voelcker. 2012. Screening of rat mesenchymal stem cell behaviour on polydimethylsiloxane stiffness gradients. *Acta Biomaterialia* 8 (2):519-530.

Wong, Joyce Y., Jennie B. Leach, and Xin Q. Brown. 2004. Balance of chemistry, topography, and mechanics at the cell-biomaterial interface: Issues and challenges for assessing the role of substrate mechanics on cell response. *Surface Science* 570 (1-2):119-133.

Wu, Jindan, Zhengwei Mao, Lulu Han, Yizhi Zhao, Jiabin Xi, and Changyou Gao. 2014. A density gradient of basic fibroblast growth factor guides directional migration of vascular smooth muscle cells. *Colloids and Surfaces B: Biointerfaces* 117 (0):290-295.

Wu, Jindan, Zhengwei Mao, Huaping Tan, Lulu Han, Tanchen Ren, and Changyou Gao. 2012. Gradient biomaterials and their influences on cell migration. *Interface Focus* 2 (3):337-355.

CHAPTER 7

CONCLUSIONS AND FUTURE CONSIDERATIONS

The overall objective of this research was to fabricate combinatorial biomaterials with properties that span wide ranges in surface chemistries and mechanical moduli in monotonically varying gradient format for the high throughput screening of cell response to matrix properties. Our central hypothesis was that materials encompassing monotonic gradient properties in both mechanical elastic modulus and surface chemistry could be engineered on a single substrate using PDMS. Additionally, it was expected that using these combinatorial biomaterials for high throughput screening of cell-material interactions would yield patterns in the overall cell response to the increased level of complexity mimicking the extracellular matrix. While some previous work highlighted the use of gradient materials, a vast majority used rigid materials such as glass or very soft polymeric materials such as hydrogels as substrates. The use of biomaterials to manufacture gradients with physiologically relevant ranges of stiffness is very limited. In this study PDMS, a soft silicone elastomeric biomaterial with physiologically relevant stiffness and an easily modified surface, was used to fabricate combinatorial gradient materials.

This research is novel because the fabrication of continuous surface chemistry gradients on PDMS, a soft material and the fabrication of a 2D combinatorial material with gradients in mechanical modulus and surface chemistries using PDMS to conduct high throughput screening of cell response have been illustrated for the first time. Moreover, the combinatorial material approach

also demonstrated the capacity to identify thresholds or patterns in cell response to multiple matrix properties. This implementation of combinatorial gradient biomaterials to conduct research on cell-material interactions is an important milestone for mimicking the extracellular matrix and understanding the complex interplay of multiple simultaneous signals that may direct cell behavior.

The PDMS surface was modified through deposition of a hydrophobic alkylsilane monolayer. A very tightly spatiotemporally regulated ultraviolet ozone oxidation treatment of the alkysilane layer generated a monotonically varying profile of surface chemistries on PDMS. One end of the substrate had a very hydrophilic surface that gradually transitioned over the 40 mm distance to a hydrophobic surface at the other end. This correlated with the extent of oxygenation of the surface whereby the normalized oxygen content declined about 23% from the hydrophilic end to the hydrophobic end. The PDMS surface gradients were prone to hydrophobic recovery and this was circumvented by immersing the gradient substrates in water that preserved the gradient chemistry for more than a week.

Morphological response of two cell types, mouse embryonic fibroblasts and human endothelial cells, were investigated on surface chemistry gradients using automated high throughput imaging and data extraction. Overall, the cell spreading correlated strongly with hydrophobicity of the substrate. This cell response, in turn was mediated by the changes in adsorbed amount and conformational changes in fibronectin to the variations in surface chemistries of gradient substrate. There was a 127% (2.3 fold) increase in cell spreading for fibroblasts on PDMS gradients in contrast to a 76% (1.8 fold) increase on glass gradients. In turn, the HUVECs showed a higher

193% (2.9 fold) increase in spreading area for gradients on PDMS compared to a smaller 42% (1.4 fold) increase on glass gradients. Also, in the case of both cells, spreading on hydrophilic glass was significantly higher than on hydrophilic PDMS. This suggests the importance of the matrix stiffness which presents a different dimension in addition to the surface chemistry gradient. Exploring the dynamics of the protein adhesive layer revealed that while the fibronectin density correlated with increasing hydrophobicity of matrix surface, there existed a biphasic relation for fibronectin conformation with surface chemistry and spreading. The increasing trend of cell spreading with hydrophobicity and a sigmoid curve of cell circularity on the PDMS surface chemistry gradients demonstrated the potential for identifying dominant patterns of cell behavior over wide range of surface properties.

A 2D combinatorial biomaterial was fabricated with PDMS encompassing a gradient in mechanical elastic modulus on one axis and gradient in surface chemistry on the orthogonal axis. Within the combinatorial biomaterial (50mm x 50mm), the mechanical stiffness gradient spanned a difference in two orders of magnitude in the elastic modulus and ranged from very hydrophilic to a hydrophobic surface chemistry gradient along the perpendicular axis. Fibroblasts were cultured on fibronectin coated 2D gradient biomaterials to study the synergistic influence of a range of mechanical and biochemical cue combinations. Automated data extraction from a custom made microscopic imaging macro for the 2D gradient material aided in generating a phase map of cell response based on the position on the 2D gradient. Cells showed a varied response to the presented combination of matrix properties indicating that both mechanics and chemistry influenced in cell morphology; specifically the potential for identifying thresholds of synergy was

confirmed by the observations of maximum spreading on regions that were highly hydrophobic and with intermediate stiffness.

The combinatorial materials platform developed in this project is flexible so that it is easily modified for specific applications. For example, our lab plans to use this technology for cardiovascular applications such as screening mechanotransduction events which could lead to the development of biomaterials for improved endothelialization. Of particular interest is the influence of cell-matrix adhesion on cell-cell adhesion and signaling that occurs within endothelial layers. This could be studied by screening variations in expression of vascular endothelial (VE) cadherin connections between endothelial cells on 2D combinatorial gradient. The independent and synergistic influence of mechanical and chemical cues on cells may also be dissected by conducting experiments separately on 1D and 2D gradients. Another extension of this study could include conducting dynamic endothelial culture assays using a parallel plate chamber.

The roles of wide variations in matrix properties that take place in pathogenesis conditions may also be studied. For example, normal endothelial cells and diseased endothelial cells may be exposed to proinflammatory chemokines and/or anti-inflammatory factors like vasodilators in the culture medium and their respective responses can be investigated as a function of the underlying matrix properties. Similarly, experimental conditions could be adjusted to observe the transition of cancer cells to the more aggressive metastatic state in the so-called epithelial to mesenchymal transition.

From the gradient fabrication point of view, the range of stiffness in a mechanical gradient maybe changed by altering the boundaries. For instance if a 'hot spot' were found at the softer end, new mechanical gradients may be attained with '*stiff*' end having a 2% weight crosslinker and *'soft'* end having a 1.43% weight crosslinker. Gradients in peptides density or growth factors may also be generated by the UVO exposure method instead of the surface chemistry gradients.

In conclusion, we successfully fabricated 1D and 2D gradient biomaterials having a wide range of physiologically relevant mechanical stiffness and/or surface chemistries using PDMS and spatiotemporal surface modification. Cell response on these gradients materials were conducted with a systematic and high throughput approach, with custom macros and automation procedures that were developed to analyze the information rich acquired data. Finally, this approach enabled us to identify variations, patterns and thresholds in cell response that may provide guiding principles for developing biomaterial design criteria for specific biomedical engineering applications.

APPENDIX A: COPYRIGHT PERMISSIONS

A.1 Permission to Use Published Contents in Chapter 4 and Chapter 5

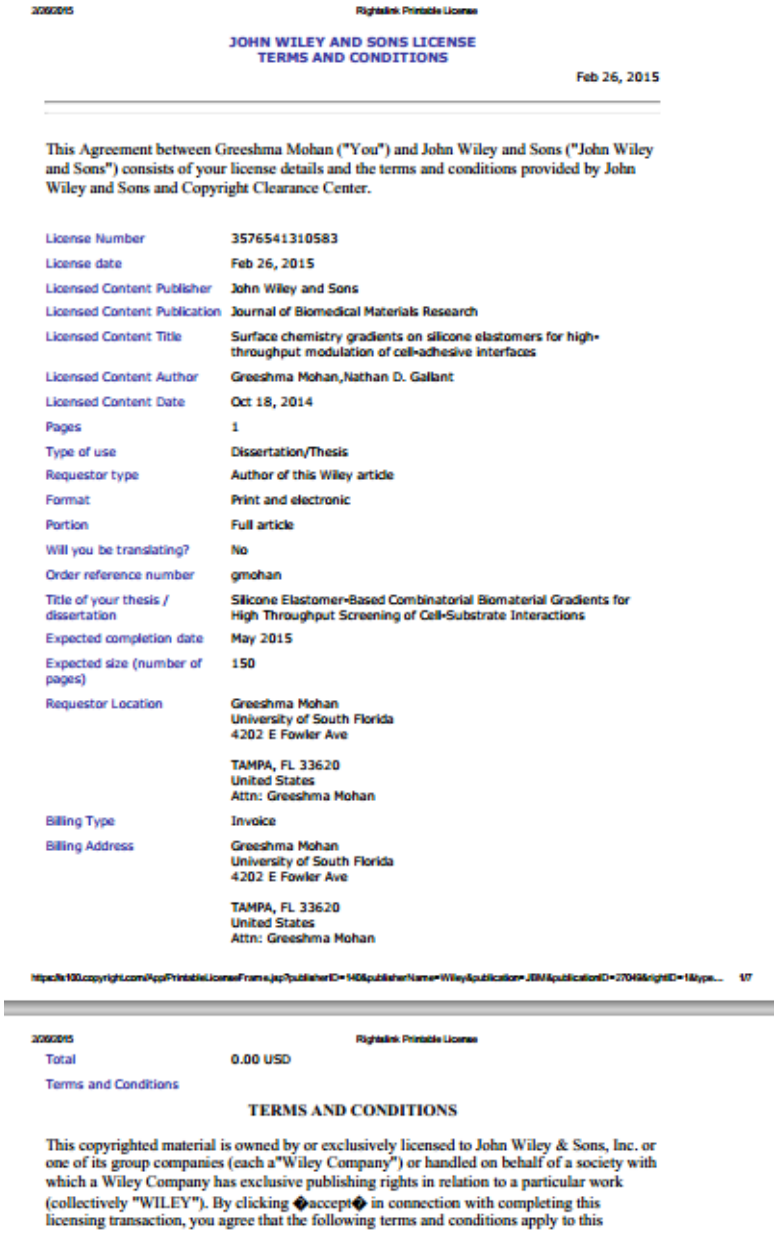

2/26/2015 RightsLink Printable License

JOHN WILEY AND SONS LICENSE TERMS AND CONDITIONS

Feb 26, 2015

This Agreement between Greeshma Mohan ("You") and John Wiley and Sons ("John Wiley and Sons") consists of your license details and the terms and conditions provided by John Wiley and Sons and Copyright Clearance Center.

License Number	3576541310583
License date	Feb 26, 2015
Licensed Content Publisher	John Wiley and Sons
Licensed Content Publication	Journal of Biomedical Materials Research
Licensed Content Title	Surface chemistry gradients on silicone elastomers for high-throughput modulation of cell-adhesive interfaces
Licensed Content Author	Greeshma Mohan,Nathan D. Gallant
Licensed Content Date	Oct 18, 2014
Pages	1
Type of use	Dissertation/Thesis
Requestor type	Author of this Wiley article
Format	Print and electronic
Portion	Full article
Will you be translating?	No
Order reference number	gmohan
Title of your thesis / dissertation	Silicone Elastomer-Based Combinatorial Biomaterial Gradients for High Throughput Screening of Cell-Substrate Interactions
Expected completion date	May 2015
Expected size (number of pages)	150
Requestor Location	Greeshma Mohan University of South Florida 4202 E Fowler Ave TAMPA, FL 33620 United States Attn: Greeshma Mohan
Billing Type	Invoice
Billing Address	Greeshma Mohan University of South Florida 4202 E Fowler Ave TAMPA, FL 33620 United States Attn: Greeshma Mohan

https://s100.copyright.com/AppPrintableLicenseFrame.jsp?publisherID=140&publisherName=Wiley&publication=JBM&publicationID=27049&rightID=18&type... 1/7

2/26/2015 RightsLink Printable License

Total	0.00 USD

Terms and Conditions

TERMS AND CONDITIONS

This copyrighted material is owned by or exclusively licensed to John Wiley & Sons, Inc. or one of its group companies (each a"Wiley Company") or handled on behalf of a society with which a Wiley Company has exclusive publishing rights in relation to a particular work (collectively "WILEY"). By clicking accept in connection with completing this licensing transaction, you agree that the following terms and conditions apply to this